*J. Fluid Mech.* (1994), *vol.* 273, *pp.* 31–82



# Early-period dynamics of an incompressible mixing layer

By Y. BUN AND W. O. CRIMINALE
Department of Applied Mathematics, University of Washington, Seattle, WA 98195, USA

(Received 30 September 1992 and in revised form 11 January 1994)

The evolution of three-dimensional disturbances in an incompressible mixing layer in an inviscid fluid is investigated as an initial-value problem. A Green's function approach is used to obtain a general space–time solution to the problem using a piecewise linear model for the basic flow, thereby making it possible to determine complete and closed-form analytical expressions for the variables with arbitrary input. Structure, kinetic energy, vorticity, and the evolution of material particles can be ascertained in detail. Moreover, these solutions represent the full three-dimensional disturbances that can grow exponentially or algebraically in time. For large time, the behaviour of these disturbances is dominated by the exponentially increasing discrete modes. For the early time, the behaviour is controlled by the algebraic variation due to the continuous spectrum. Contrary to Squire's theorem for normal mode analysis, the early-time behaviour indicates growth at comparable rates for all values of the wavenumbers and the initial growth of these disturbances is shown to rapidly increase. In particular, the disturbance kinetic energy can rise to a level approximately ten times its initial value before the exponentially growing normal mode prevails. As a result, the transient behaviour can trigger the roll-up of the mixing layer and its development into the well-known pattern that has been observed experimentally.

## 1. Introduction

Early transition from laminar to turbulent flow begins with the instability of a flow. To study such an event, the basic flow is superimposed with disturbances where their growth behaviour determines the instability. To analyse the complete transient and asymptotic state of a three-dimensional disturbance, the solution to the initial-value problem that models the temporal evolution of the disturbances must be obtained. In this work, the initial-value problem for an unbounded inviscid incompressible piecewise linear mixing layer (figure 1) is solved using a modification of the analytical method described by Criminale & Drazin (1990) and used by Criminale, Long & Zhu (1991).

The asymptotic behaviour of disturbances in many flows has been studied in great detail by normal mode analysis (Lin 1955; Betchov & Criminale 1967; Drazin & Reid 1981). The classical linear stability theory predicts that a given basic flow is unstable if its corresponding linearized equations have at least one mode (discrete mode) that grows exponentially in time. In contrast to this, recent work has shown that instability of flows can also be due to the transient growth of disturbances (Farrell 1982, 1988; Criminale & Drazin 1990; Criminale *et al.* 1991; Reddy, Schmid & Henningson 1991) and, it will be seen that this omission is critical. The existence of the continuous spectrum in initial-value problems has long been recognized but simply not emphasized and details for any problem are lacking (cf. Drazin & Reid 1981).

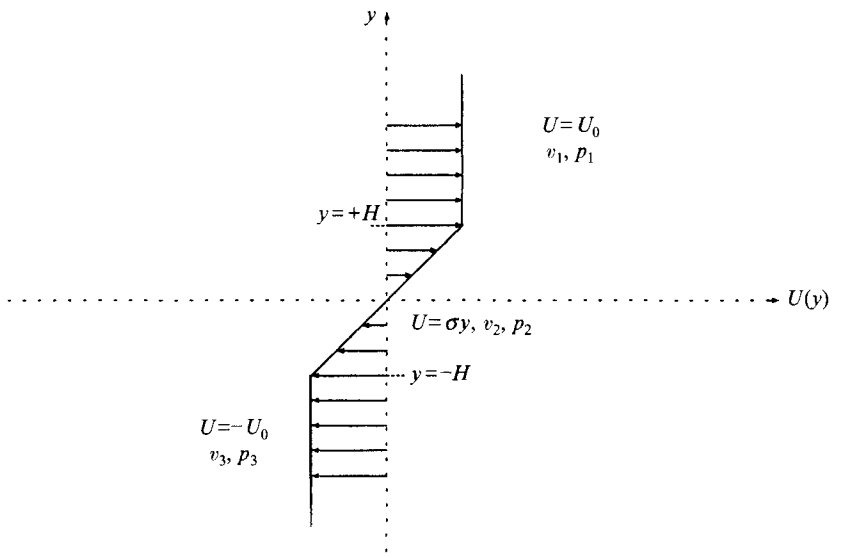


FIGURE 1. Piecewise linear model of mixing layer.

In principle, in the normal mode analysis, a disturbance is expressed as a superposition of modes of various wavelengths where each mode is a travelling wave solution that can grow or decay exponentially in time. This is properly done if the set of normal modes is complete. Unfortunately, all normal modes for the mixing-layer problem do not form a complete discrete spectrum and an arbitrary disturbance cannot be decomposed into such modes alone. To complete the set the continuous spectrum must be added.

For the classical linear stability theory only infinitesimal disturbances are admitted so that the normal mode in the discrete spectrum with the fastest exponential growth rate can be identified to dominate the asymptotic behaviour of the disturbances. However, even here, this theory cannot predict the transient behaviour of the disturbances because it depends on the *decaying* as well as the growing normal modes of the discrete spectrum as well as the *missing continuous spectrum*.

Classical linear stability theory has been used extensively in an attempt to describe the two-dimensional primary instability of the mixing layer but it fails to describe the three-dimensional secondary instability that leads to counter-rotating streamwise vortices that have been observed in experiments (Breidenthal 1981; Bernal & Roshko 1986; Lasheras & Choi 1988) and numerical simulations (Metcalfe *et al.* 1987; Ashurst & Meiburg 1988). The observed secondary coherent structure of streamwise vortices is periodic in the spanwise direction with larger wavenumbers than the range of growing normal modes predicts.

Realistic disturbances in a flow may not arise from the truly infinitesimal amplitude assumed by the classical linear theory; neither do three-dimensional disturbances wait until two-dimensional equilibrium is established before they enter the dynamics (as considered by e.g. Pierrehumbert & Widnall 1982). The possibility that nonlinearity may become significant long before the normal mode components dominate the solution gives special importance to the initial value problem.

For the three-dimensional problem, equations governing the amplitudes of the transverse velocity and vorticity components are considered and are obtained by Fourier transforms. In this case, use of Squire's theorem could be incorrect because the

theorem does not cover the dynamical behaviour in the equation that governs the Fourier amplitude of the transverse vorticity component and is not valid for non-separable normal modes or for the continuous spectrum. Contrary to Squire's theorem, it will be shown that the small-time or transient behaviour for the streamwise–spanwise periodic disturbance grows at a comparable rate for all values of the wavenumber and the initial growth rate of this disturbance rapidly increases.

For initial conditions that are periodic in the streamwise–spanwise plane, the inverse Fourier transform can be made to obtain complete closed-form solutions in the physical coordinate space. With these solutions, the corresponding transient and asymptotic behaviours of the disturbances from the velocity and vorticity fields as well as the kinetic energy are analysed in detail. Interesting findings include the existence of algebraic growth for both transient and asymptotic states (because the fluid is taken as inviscid) when the initial disturbance is independent of the streamwise variable or the initial wavenumber magnitude is equal to an upper bound known as the cut-off value. Exponential growth can exist only if the initial wavenumber magnitude is smaller than the cut-off value. The exponentially growing behaviour is in agreement with the normal modes found from the discrete spectrum. The growth rates of the kinetic energy for all cases (including both algebraic and exponential growth) in the transient period are rapidly changing and amplitudes reach a level approximately ten times their initial values within almost the same time interval.

The evolution of material particles based on the particle path formulation from the Lagrangian viewpoint is investigated as well by integrating directly the velocity obtained in the analysis. The sequence of plots at different times for the particle positions reveal that an algebraically growing disturbance can trigger roll-up of the mixing layer as well as an unstable normal mode. Also, for the initial disturbance with a double mode (streamwise and spanwise dependence), the developed structure of the material particles has undulant surfaces which are periodic in both the streamwise and the spanwise directions and this is compatible with experiments.

The application of the Green's function to the streamwise–spanwise periodic initial disturbance with families of symmetric and asymmetric transverse distributions for the initial transverse velocity component is also given. It is found that the growth rate of the disturbance for the asymmetric case is greater than that for the symmetric one in the transient period and is very sensitive to three-dimensionality.

## 2. The problem

### 2.1. *Experimental observations*

The growth of disturbances in the laminar mixing layer indicates instabilities of the flow and certain disturbances lead to eventual roll-up of the layer. From experimental observations, the roll-up of the layer occurs even if no disturbance is introduced into the flow. Evidently, the roll-up structure is also observed in the turbulent mixing layer, as noted by the large-scale or coherent structure displayed in the revealing shadowgraph taken by Brown & Roshko (1974). This photograph, which also appears in Van Dyke (1982), shows a large-scale two-dimensional roll-up of the layer that exists throughout the mixed fluid region. This two-dimensional roll-up structure is known as the primary structure and is widely accepted to be the result of the Kelvin–Helmholtz instability mechanism that is based on normal mode analysis for the simplest mathematical model of the mixing layer using a zero-thickness vortex sheet.

Another shadowgraph that appears in Van Dyke (1982) was taken by Konrad (1976). This plane view of a mixing layer reveals periodically distributed streamwise

streaks in the braided regions connecting the large-scale rollers of the spanwise vortex tubes. Breidenthal (1981) observed a spanwise sinuous 'wiggle' which was believed to play an important role in introducing streamwise vortices and small-scale motions in the mixing layer. Later Bernal & Roshko (1986) presented evidence of three-dimensional coherent structure in the mixing layer. Here, mushroom-shaped features were found in the perpendicular cross-sectional view of the flow direction at some fixed downstream position. Such mushroom-shaped features, known as the secondary structure, represent the counter-rotating streamwise vortices that are spanwise periodic with wavelengths smaller than that of the streamwise wavelength of the primary structure. It should be noted that this observation cannot be reconciled by classical linear stability theory, which predicts that small wavelength disturbances do not grow.

Ho & Huang (1982) and Oster & Wygnanski (1982) investigated the effects of two-dimensional small-amplitude disturbances generated artificially in the mixing layer behind a splitter plate and concluded that the primary large-scale structure of the mixing layer is very sensitive to small-amplitude periodic disturbances. The frequencies and amplitudes of the disturbances also played important roles in manipulating the spreading rate of the layer.

Artificially generated three-dimensional disturbances in the mixing layer have been further studied in some detail by Lasheras & Choi (1988). Periodic disturbances in the spanwise direction were created by modifying the trailing edge of the splitter plate to give a sinusoidal indentation and it was observed that one origin of the secondary coherent structure was the creation of a transverse vorticity component on the indented splitter plate. As it travels downstream, the transverse vorticity component tilts into the streamwise direction owing to the global shear of the mixing layer and the structure then emerges.

### 2.2. *Numerical simulation*

Direct numerical simulations, such as those of Lin & Corcos (1984), Metcalfe *et al.* (1987), Ashurst & Meiburg (1988) and Rogers & Moser (1989) have been used to study the details of the coherent structure observed experimentally. Instead of simulating the spatial developing mixing layer behind a splitter plate, these approaches assume periodic solutions in the streamwise and spanwise directions of the flow, and the evolution of the flow is traced in time. Periodic inputs such as this also permits dropping of the boundary conditions in the streamwise and spanwise directions, greatly simplifying the numerical scheme.

The results from the numerical simulation of the temporal evolution of the mixing layer confirm that the experimentally observed large-scale structure is dynamically sensitive to small disturbances. For example, on initializing the flow field with the steady-state mean flow (normally a hyperbolic tangent profile) and appropriate streamwise-periodic two-dimensional disturbances, the contour plot of the spanwise vorticity in the mixing layer shows roll-up and a pairing of vortices. This is the primary structure experimentally observed.

On initializing the flow field with the mean flow and three-dimensional periodic disturbances in the streamwise and spanwise directions the mixing layer can evolve into pairs of counter-rotating streamwise vortices. However, the spanwise wavenumber could be large and therefore does not agree with the prediction of the classical linear stability theory in that such a large-wavenumber disturbance does not grow.

### 2.3. *Analytical solutions*

Consider the basic parallel flow in the streamwise $x$-direction with the velocity $U = (U(y), 0, 0)$. A normal mode disturbance is a separable solution and a travelling

wave with an amplitude that depends only on $y$ and is represented as a sum of modes given as

$$\boldsymbol{u}' = \mathrm{Re}\{\hat{\boldsymbol{u}}(y)\,\mathrm{e}^{\mathrm{i}(\alpha x+\gamma z-\omega t)}\}, \tag{2.1}$$

where $\hat{\boldsymbol{u}}(y)$ is a complex vector amplitude function, $\alpha$ is the real wavenumber in the $x$-direction, $\gamma$ is the real wavenumber in the $z$-direction, and $\omega$ is the complex frequency. For instability, the imaginary part of $\omega$ must be positive.

Perhaps the first unbounded flow stability problem was the one posed and solved by Kelvin (1871) where he considered incompressible flow in an inviscid fluid with a discontinuous velocity profile indicating that two streams are separated by a vortex sheet of zero thickness. The instability result found for this model has become known as Kelvin–Helmholtz shear-layer instability. It remains the most popular analytical result used as a theoretical explanation for the primary instability of the mixing layer.

The resultant eigenfrequencies of the normal modes for this flow are

$$\omega = \tfrac{1}{2}\alpha(U_1+U_2) \pm \mathrm{i}\tfrac{1}{2}\alpha(U_1-U_2), \tag{2.2}$$

where $U_2$ is the value for $y > 0$; $U_1$ for $y < 0$. This flow is always unstable because one $\omega_i$ is positive for any $\alpha > 0$ since there is no lengthscale in this simple model. However, for a mixing-layer model with finite thickness, such as the hyperbolic tangent profile, there is a cut-off value of the wavenumber $\alpha$ where the flow is neutrally stable. A growing normal mode exists only if the value of $\alpha$ is smaller than this value (Michalke 1964).

A better model for the basic flow of the mixing layer was proposed by Rayleigh (1894) where the velocity profile was taken as a piecewise linear function of $y$ as shown graphically in figure 1. In non-dimensional variables (detailed non-dimensionalization is given in the next section),

$$U(y) = \begin{cases} 1, & 1 < y \\ y, & -1 < y < 1 \\ -1, & y < -1. \end{cases} \tag{2.3}$$

This is an improvement over the Kelvin–Helmholtz model because (2.3) has a finite thickness and is a close approximation to that computed by Lock (1951) for the continuous $\tanh y$. Also, the normal mode solutions of this model are qualitatively the same as the continuous shear-layer profile with the complex eigenfrequencies being given by

$$\omega = \pm(\alpha/2\tilde{\alpha})[(1-2\tilde{\alpha})^2 - \mathrm{e}^{-4\tilde{\alpha}}]^{1/2} = \pm\tfrac{1}{2}\cos\phi[(1-2\tilde{\alpha})^2 - \mathrm{e}^{-4\tilde{\alpha}}]^{1/2}, \tag{2.4}$$

where $\tilde{\alpha} = (\alpha^2+\gamma^2)^{1/2}$ and $\phi = \tan^{-1}(\gamma/\alpha)$. Thus, there are two normal modes for a given $\tilde{\alpha}$ in the interval $0 < \tilde{\alpha} < \tilde{\alpha}_s \approx 0.64$ corresponding to $\omega_i \gtrless 0$. The flow is unstable, and the growing mode with $\tilde{\alpha} \approx 0.4$ has the largest growth rate. The flow is neutrally stable if $\tilde{\alpha} = \tilde{\alpha}_s$ (the short-wave cut-off) and there is only one eigenfrequency, $\omega = 0$. This result is qualitatively the same as for the $\tanh y$ profile but, unlike the continuous profile result which has no normal mode solutions for $\tilde{\alpha}$ greater than its short-wave cut-off, the piecewise linear profile (2.3) has two neutrally stable normal modes for $\tilde{\alpha} \geqslant \tilde{\alpha}_s$ ($\omega_i = 0$) in this idealization.

Classical linear stability theory based on normal mode analysis provides intuitively sensible results. However, it fails to describe the three-dimensional secondary instability that leads to the counter-rotating streamwise vortices observed in experiments and numerical simulations. The observed secondary coherent structure of streamwise vortices is periodic in the spanwise direction with larger wavenumbers than the range of growing normal modes.

The classical theory predicts that a given basic flow is unstable if its corresponding linearized equations have at least one mode (discrete mode) that grows exponentially in time. But (2.1) requires a knowledge of all modes at time $t = 0$ in order to prescribe an arbitrary disturbance. It turns out that the spectrum of the discrete modes is not complete and thus $u'$ cannot be represented initially as a superposition of discrete modes alone. However, the spectrum of the normal modes can be made complete by including the continuous spectrum of the eigenvalue problem.

Case (1960, 1961) considered the initial value problem for certain parallel flows in inviscid incompressible flow using a Laplace transform in time and a Fourier transform in space. The Laplace integral solution can be decomposed into a sum of the discrete normal modes by the method of residues plus the integral with an integrand that has no poles in the domain of interest. Essentially, this solution combines both the discrete normal and continuous modes. For plane Couette flow, there are no normal modes and the asymptotic behaviour of the continuous mode is $t^{-1}$ as $t \to \infty$ *for an inviscid fluid* (see also Criminale *et al.* 1991).

Lin (1961) reconciled the differences between the method of normal modes and the initial-value presentation of Case. Theoretically, the Laplace integral representation of the solution can be decomposed into an infinite series of normal modes by the method of residues, and the two approaches are essentially equivalent. Any contradiction between the results of the two methods can be avoided by keeping in mind the following facts. A normal mode in the inviscid theory may not be the limit of a normal mode in the viscous theory, and a normal mode in the viscous theory may not have an inviscid limit. In short, a lack of direct correspondence between the inviscid normal modes and the inviscid limit of the viscous one can occur. Also, there are exponentially damped normal modes that may play an important role in the transition process, and the initial value theory has not yet been fully exploited to study this type of disturbance. For example, it has been shown that a superposition of damped normal modes in plane Poiseuille flow could lead to transient growth of the disturbance energy by a factor of approximately 37 (Reddy *et al.* 1991) and is attributed to multiple eigenvalues in such a sensitive system with non-orthogonal eigenfunctions rather than the continuous spectrum.

Although the instability of the mixing layer is essentially that of an inviscid fluid, viscous effects play an important role in the transition to small scales (Ho & Huerre 1984). Esch (1957) and Balsa (1987) studied the viscous effects on the growing disturbances for the basic flow (2.3). It was found that, at large Reynolds numbers, results are virtually identical with the inviscid results. However, for the tanh $y$ profile, the two eigenvalues are complex conjugates of each other for the Orr–Sommerfeld equation with large Reynolds numbers and all wavenumbers. The eigenvalues for the inviscid problem are complex conjugates for wavenumbers that are less than the cut-off value; for wavenumbers greater than the cut-off value, the eigenvalue problem has no solution (cf. Betchov & Criminale 1967). This becomes a moot point because, with viscous effects, the basic flow should be treated as non-parallel. For this work, only the inviscid problem and a parallel basic flow for which the analytical solution is determined is considered.

Realistic disturbances in a flow may not arise from the truly infinitesimal amplitude assumed by the classical linear theory and three-dimensional disturbances may not wait until there is a two-dimensional equilibrium to be established before they enter the dynamics. Although the exponential growth behaviour found from the discrete spectrum dominates the behaviour of disturbances at large time, other behaviour may be relevant at small time. This other behaviour (e.g. algebraic growth) that temporarily

dominates the exponential growth could lead to strong enough nonlinearity to cause the breakdown of the flow in the early period. This suggestion was put forth by Farrell (1982) and Criminale & Drazin (1990). The transient behaviour of disturbances depends on the continuous spectrum as well as the growing and damped normal modes. The possibility that nonlinearity may become significant long before the normal mode components dominate the solution, gives special importance to the initial-value problem.

The main goal here is to find the full and complete solutions of the initial-value problem for the unbounded inviscid incompressible piecewise linear shear flow. Although the result is only approximate for the physical problem, it serves as a good model for a more general continuous shear-layer profile (such as $\tanh y$). Normal modes are successful in approximating the exponential growth rate of the continuous profile where the results here allow for closed-form analytical solutions and completeness. The two-dimensional version of this problem with a vortex dipole initial condition was investigated by Balsa (1988) but only the long-time behaviour of the solution by asymptotic analysis was presented. This problem is three-dimensional and attention is focused on the transient behaviour of the solution as well as its asymptotic fate.

## 3. The initial-value problem

### 3.1. *Linearized equations*

Neglecting any body force, the Euler equations are

$$\nabla \cdot \boldsymbol{u} = 0, \tag{3.1}$$

$$\rho \, \mathrm{D}\boldsymbol{u}/\mathrm{D}t = -\nabla p, \tag{3.2}$$

where the velocity field $\boldsymbol{u} = (u, v, w)$ and the pressure $p$ are the unknowns and functions of $(x, y, z; t)$; $\rho$ is the constant density.

The basic velocity field modelling the mixing layer is considered to be a parallel flow,

$$\boldsymbol{u} = U(y)\boldsymbol{e}_1,$$

where $\boldsymbol{e}_1 = (1, 0, 0)$ and $U(y)$ is as shown in figure 1, or

$$U(y) = \begin{cases} U_0, & H < y \\ \sigma y, & -H < y < H \\ -U_0, & y < -H. \end{cases} \tag{3.3}$$

Non-dimensional variables are defined as

$$\begin{bmatrix} x^* \\ t^* \end{bmatrix} = \begin{bmatrix} x/H \\ \sigma t \end{bmatrix}, \quad \begin{bmatrix} \boldsymbol{u}^* \\ p^* \end{bmatrix} = \begin{bmatrix} \boldsymbol{u}/U_0 \\ p/(\rho U_0^2) \end{bmatrix}.$$

Equations (3.1) and (3.2) become

$$\nabla \cdot \boldsymbol{u} = 0, \tag{3.4}$$

$$\mathrm{D}\boldsymbol{u}/\mathrm{D}t = -\nabla p, \tag{3.5}$$

where the asterisk is dropped from all variables and the basic velocity is as given in (2.3). On introducing a disturbance velocity and pressure, we write the total velocity and pressure as

$$\begin{bmatrix} \boldsymbol{u}(x,y,z;t) \\ p(x,y,z;t) \end{bmatrix} = \begin{bmatrix} U(y)\,\boldsymbol{e}_1 \\ P_0 \end{bmatrix} + \epsilon \begin{bmatrix} \boldsymbol{u}'(x,y,z;t) \\ p'(x,y,z;t) \end{bmatrix},$$

where $\epsilon$ is a small-amplitude parameter. After substituting into the Euler equations and collecting terms of order $\epsilon$ the linearized equations governing inviscid three-dimensional disturbances are obtained. By dropping the prime from all disturbance variables, the linearized equations are

$$\frac{\partial u}{\partial x} + \frac{\partial v}{\partial y} + \frac{\partial w}{\partial z} = 0, \tag{3.6}$$

$$\frac{\partial u}{\partial t} + U\frac{\partial u}{\partial x} + \frac{\mathrm{d}U}{\mathrm{d}y}v = -\frac{\partial p}{\partial x}, \tag{3.7}$$

$$\frac{\partial v}{\partial t} + U\frac{\partial v}{\partial x} = -\frac{\partial p}{\partial y}, \tag{3.8}$$

$$\frac{\partial w}{\partial t} + U\frac{\partial w}{\partial x} = -\frac{\partial p}{\partial z}. \tag{3.9}$$

A convenient form of the governing equations may be obtained by taking the divergence of (3.7)–(3.9) to obtain

$$\nabla^2 p = -2U'\,\partial v/\partial x, \tag{3.10}$$

where $U' = \mathrm{d}U(y)/\mathrm{d}y$ and $\nabla^2$ is the three-dimensional Laplace operator. Then, combining (3.10) with (3.8) the result is

$$(\partial/\partial t)\,\nabla^2 v + U(\partial/\partial x)\,\nabla^2 v = U''\,\partial v/\partial x. \tag{3.11}$$

Equations (3.11), (3.10), (3.7) and (3.9) form a new set of equations. Once the solution for $v$ is found, (3.10) can be used for $p$; (3.7) and (3.9) determine $u$ and $w$ respectively and the problem is complete.

Since the disturbances must be bounded at infinity, $v, u, w$ are bounded as $x, y, z \to \pm\infty$. The linearized equations (3.7), (3.9), (3.10) and (3.11) together with arbitrary initial conditions at $t = 0$ form the initial-value problem.

### 3.2. *Moving coordinates and Fourier transforms*

Further reduction of the governing equations is made by changing the independent variables. Let

$$\xi = x - Ut, \quad \eta = y, \quad \zeta = z, \quad T = t,$$

so that

$$\boldsymbol{u}(\xi,\eta,\zeta;T) = \boldsymbol{u}(x,y,z;t), \quad \text{and} \quad p(\xi,\eta,\zeta;T) = p(x,y,z;t).$$

Under this transformation, the governing equations become

$$(\partial/\partial T)\,\nabla^2 v = 0, \tag{3.12}$$

$$\nabla^2 p = -2U'\,\partial v/\partial \xi, \tag{3.13}$$

$$\partial u/\partial T + U'v = -\partial p/\partial \xi, \tag{3.14}$$

$$\partial w/\partial T = -\partial p/\partial \zeta, \tag{3.15}$$

with the basic flow

$$Y(\eta) = \begin{cases} 1, & 1 < \eta \\ \eta, & -1 < \eta < 1 \\ -1, & \eta < -1. \end{cases} \tag{3.16}$$

The Laplace operator in the moving coordinates is

$$\nabla^2 = \frac{\partial^2}{\partial \xi^2} + \frac{\partial^2}{\partial \eta^2} + \frac{\partial^2}{\partial \zeta^2} - 2U'T\frac{\partial^2}{\partial \xi\, \partial \eta} + U'^2T^2\frac{\partial^2}{\partial \xi^2}.$$

This transformation is known as the convected coordinate transformation and has been used by Kelvin (1887), Orr (1907*a*, *b*) and Tung (1983) in earlier work.

To solve the set of equations (3.12)–(3.15), a two-dimensional Fourier transform, defined by

$$\check{v}(\alpha;\eta;\gamma;T) = \int\int_{-\infty}^{\infty} v(\xi,\eta,\zeta,T)\, e^{i(\alpha\xi+\gamma\zeta)}\, d\xi\, d\zeta$$

is used. The governing equations now become

$$(\partial/\partial T)\,\check{\nabla}^2\check{v} = 0, \tag{3.17}$$

$$\check{\nabla}^2\check{p} = 2i\alpha U'\check{v}, \tag{3.18}$$

$$\partial\check{u}/\partial T + U'\check{v} = i\alpha\check{p}, \tag{3.19}$$

$$\partial\check{w}/\partial T = i\gamma\check{p}, \tag{3.20}$$

with $$\check{\nabla}^2 = \partial^2/\partial\eta^2 + 2i\alpha U'T\partial/\partial\eta - U'^2T^2\alpha^2 - \tilde{\alpha}^2.$$

On introducing polar variables,

$$\tilde{\alpha}^2 = \alpha^2+\gamma^2, \quad \phi = \tan^{-1}(\gamma/\alpha), \tag{3.21}$$

$$\tilde{\alpha}\tilde{u} = \alpha\check{u}+\gamma\check{w}, \quad \tilde{\alpha}\tilde{w} = -\gamma\check{u}+\alpha\check{w}, \tag{3.22}$$

(3.19) and (3.20) become

$$\partial\tilde{u}/\partial T = i\tilde{\alpha}\check{p} - \cos\phi\, U'\check{v}, \tag{3.23}$$

$$\partial\tilde{w}/\partial T = \sin\phi\, U'\check{v}. \tag{3.24}$$

From the continuity equation, it can be shown that $\tilde{u}$ depends on $\check{v}$ alone and, once the solution for $\check{v}$ is found, $\tilde{w}$ is determined from (3.24). Physically, $\tilde{w}$ is proportional to the transverse vorticity component, $\check{\Omega}_y$. The two quantities $\tilde{u}$ and $\tilde{w}$, in terms of $\check{v}$ and $\check{\Omega}_y$, are

$$\tilde{u}(\alpha;\eta;\gamma;T) = -(i/\tilde{\alpha})(\partial/\partial\eta + i\tilde{\alpha}\cos\phi\, U'T)\,\check{v}, \tag{3.25}$$

$$\tilde{w}(\alpha;\eta;\gamma;T) = (i/\tilde{\alpha})\,\check{\Omega}_y, \tag{3.26}$$

where $\check{\Omega}_y = -i\gamma\check{u} + i\alpha\check{w}$ or $\Omega_y = \partial u/\partial\zeta - \partial w/\partial\zeta$ in real space. On solving for $\check{u}$ and $\check{w}$ from (3.22) in terms of $\tilde{u}$ and $\tilde{w}$ and eliminating $\tilde{u}$ using (3.25),

$$\check{u} = -(i/\tilde{\alpha})\{\cos\phi(\partial/\partial\eta - i\tilde{\alpha}\cos\phi\, U'T)\,\check{v} - \sin\phi\check{\Omega}_y\}, \tag{3.27}$$

$$\check{w} = -(i/\tilde{\alpha})\{\sin\phi(\partial/\partial\eta - i\tilde{\alpha}\cos\phi\, U'T)\,\check{v} + \cos\phi\check{\Omega}_y\}. \tag{3.28}$$

The expression for $\check{p}$ in terms of $\check{v}$ may be obtained by eliminating $\check{u}$ and $\check{w}$ in (3.19) and (3.20) using (3.27) and (3.28). This results in

$$-\tilde{\alpha}^2\check{p} = \frac{\partial^2\check{v}}{\partial\eta\,\partial T} + i\alpha\, U'T\frac{\partial\check{v}}{\partial T} + 2i\alpha U'\check{v}. \tag{3.29}$$

With the solutions for $\check{v}$ and $\check{\Omega}_y$ found, (3.27), (3.28) and (3.29) can be used to obtain the three unknowns $\check{u}$, $\check{w}$ and $\check{p}$. Therefore, the problem is reduced to solving the two differential equations that govern $\check{v}$ and $\check{\Omega}_y$,

$$(\partial/\partial T)\,\check{\nabla}^2\check{v} = 0, \tag{3.30}$$

$$\partial\check{\Omega}_y/\partial T = \mathrm{i}\tilde{\alpha}\sin\phi U'\check{v}. \tag{3.31}$$

Classical linear stability theory assumes that $v$ and all other dependent variables are travelling waves and are separable solutions. This means that the Fourier amplitudes are either exponentially growing, decaying, oscillatory or time independent. Based on the travelling wave solution, Squire's theorem can be applied to obtain the solution for a three-dimensional problem from two-dimensional data ($\phi = 0$). However, Squire's theorem does not cover the dynamical behaviour governed by equation (3.31) (nor non-separable solutions) and the interpretation of these results could be totally wrong. For example, if the disturbance is streamwise independent ($\alpha = 0$), then $\check{v}$ is independent of $T$ and, integrating (3.31), the solution for $\check{\Omega}_y$ indicates linear growth in $T$. Thus, for a three-dimensional problem, both (3.30) and (3.31) must be solved completely.

In each layer corresponding to $\eta > 1$, $-1 < \eta < 1$, $\eta < -1$, the governing equation (3.30) for $\check{v}$ can be integrated with respect to $T$ and the result is

$$\check{\nabla}^2\check{v}(\alpha;\eta;\gamma;T) = \check{\nabla}_0^2\check{v}(\alpha;\eta;\gamma;0). \tag{3.32}$$

where $$\check{\nabla}_0^2 = \partial^2/\partial\eta^2 - \tilde{\alpha}^2.$$

### 3.3. *Green's function*

The solution of a Green's function that satisfies

$$\check{\nabla}^2\check{G}(\eta;\eta_0) = \delta(\eta-\eta_0), \tag{3.33}$$

where $$\check{\nabla}^2 = \partial^2/\partial\eta^2 + 2\mathrm{i}\alpha U'T\partial/\partial\eta - U'^2T^2\alpha^2 - \tilde{\alpha}^2$$

and

$$U'(\eta) = \begin{cases} 0, & \eta > 1 \\ 1, & |\eta| < 1 \\ 0, & \eta < -1, \end{cases} \tag{3.34}$$

is sought for the system. This Green's function can then be used to construct the solution to the problem (3.32) by the following integral:

$$\check{v} = \int_{-\infty}^{\infty} \check{v}(\alpha;\eta_0;\gamma;0)\,\check{G}(\eta;\eta_0)\,\mathrm{d}\eta_0.$$

Equation (3.33) for the external layers $|\eta| > 1$ is

$$\{\partial^2/\partial\eta^2 - \tilde{\alpha}^2\}\,\check{G} = \delta(\eta-\eta_0)$$

and, for $\eta \neq \eta_0$, is

$$\{(\partial/\partial\eta + \mathrm{i}\alpha U'T)^2 - \tilde{\alpha}^2\}\,\check{G} = 0.$$

The solutions are

$$\check{G} = \begin{cases} v^+ = \mathrm{e}^{-\mathrm{i}\alpha U'T\eta}(A_1\,\mathrm{e}^{-\tilde{\alpha}\eta} + A_2\,\mathrm{e}^{\tilde{\alpha}\eta}), & \eta > \eta_0, \\ v^- = \mathrm{e}^{-\mathrm{i}\alpha U'T\eta}(B_1\,\mathrm{e}^{-\tilde{\alpha}\eta} + B_2\,\mathrm{e}^{\tilde{\alpha}\eta}), & \eta < \eta_0. \end{cases} \tag{3.35}$$

Applying the two conditions for the Green's problem (3.33),

$$(v_2^+ - v_2^-)\,|_{\eta=\eta_0} = 0, \quad \left(\frac{\partial v_2^+}{\partial\eta} - \frac{\partial v_2^-}{\partial\eta}\right)\Bigg|_{\eta=\eta_0} = 1,$$

with (3.35), results in

$$(A_1-B_1)\,e^{-\tilde{\alpha}\eta_0}+(A_2-B_2)\,e^{\tilde{\alpha}\eta_0}=0,$$
$$-(\tilde{\alpha}+i\alpha U'T)(A_1-B_1)\,e^{-\tilde{\alpha}\eta_0}+(\tilde{\alpha}-i\alpha U'T)(A_2-B_2)\,e^{\tilde{\alpha}\eta_0}=e^{i\alpha U'T\eta}.$$

Then, solving for $A_1-B_1$ and $A_2-B_2$ gives

$$A_1-B_1=-(1/2\tilde{\alpha})\,e^{\tilde{\alpha}\eta_0+i\alpha U'T\eta_0},\quad A_2-B_2=(1/2\tilde{\alpha})\,e^{-\tilde{\alpha}\eta_0+i\alpha U'T\eta_0}.$$

After eliminating $A_1$ and $B_2$ in (3.35),

$$\check{G}=e^{-i\alpha U'T\eta}(B_1\,e^{-\tilde{\alpha}\eta}+A_2\,e^{\tilde{\alpha}\eta})+\begin{cases}-(1/2\tilde{\alpha})\,e^{-\tilde{\alpha}(\eta-\eta_0)-i\alpha U'T(\eta-\eta_0)}, & \eta>\eta_0\\ -(1/2\tilde{\alpha})\,e^{\tilde{\alpha}(\eta-\eta_0)-i\alpha U'T(\eta-\eta_0)}, & \eta<\eta_0.\end{cases}$$

On letting $B_1=Be^{\tilde{\alpha}+i\alpha U'T}$ and $A_2=Ce^{\tilde{\alpha}-i\alpha U'T}$,

$$\check{G}(\eta;\eta_0)=B(T)\,e^{-(\tilde{\alpha}+i\alpha U'T)(\eta-1)}+C(T)\,e^{(\tilde{\alpha}-i\alpha U'T)(\eta+1)}+\check{G}^{(r)},\tag{3.36}$$

where

$$\check{G}^{(r)}=-(1/2\tilde{\alpha})\,e^{-\tilde{\alpha}|\eta-\eta_0|-i\alpha U'T(\eta-\eta_0)}.\tag{3.37}$$

Thus, the general solution for the Green's function that satisfies the conditions at infinity ($\check{G}\to 0$ as $\eta\to\pm\infty$) is the composite form

$$\check{G}(\eta;\eta_0)=\begin{cases}\check{G}_1=A(T)\,e^{-\tilde{\alpha}(\eta-1)}+\check{G}_1^{(r)}, & \eta>1\\ \check{G}_2=B(T)\,e^{-(\tilde{\alpha}+i\alpha T)(\eta-1)}+C(T)\,e^{(\tilde{\alpha}-i\alpha T)(\eta+1)}+\check{G}_2^{(r)}, & |\eta|<1\\ \check{G}_3=D(T)\,e^{\tilde{\alpha}(\eta+1)}+\check{G}_3^{(r)}, & \eta<-1,\end{cases}\tag{3.38}$$

where

$$\left.\begin{aligned}\check{G}_1(r)&=-(1/2\tilde{\alpha})\,e^{-\tilde{\alpha}|\eta-\eta_0|}, && \eta>1,\\ \check{G}_2(r)&=-(1/2\tilde{\alpha})\,e^{-\tilde{\alpha}|\eta-\eta_0|-i\alpha T(\eta-\eta_0)}, && |\eta|<1,\\ \check{G}_3(r)&=-(1/2\tilde{\alpha})\,e^{-\tilde{\alpha}|\eta-\eta_0|}. && \eta<-1.\end{aligned}\right\}\tag{3.39}$$

The general solution (3.38) requires

$$\check{G}^{(r)}|_{T=0}=\check{G}|_{T=0},$$

which implies that, at $T=0$,

$$B(0)=C(0)=0.\tag{3.40}$$

To determine the full forms for $B$ and $C$ for all values of $T$, matching conditions must be used. In general, $A$, $B$, $C$ and $D$ depend on $T$, $\alpha$, and $\gamma$.

### 3.4. *Matching conditions*

Physical conditions require that the displacement of all fluid particles is continuous at the interfaces $\eta=\pm 1$. When linearized, this is tantamount to the transverse velocity component being continuous at the two interfaces. Continuity of the pressure is also required from dynamic considerations. Inspection of the original equation of the linearized set, (3.8), changing to moving coordinates and taking the two-dimensional Fourier transforms gives

$$\partial\check{v}/\partial T=-(\partial/\partial\eta+i\alpha U'T)\check{p}.$$

This equation can be rewritten as

$$(\partial/\partial\eta)(e^{i\alpha UT}\check{p})=-e^{i\alpha UT}\partial\check{v}/\partial T.$$

Integrating in the $\eta$-direction across $\eta_0$ yields

$$e^{i\alpha UT}\check{p}|_{\eta=\eta_0-\epsilon}^{\eta_0+\epsilon}=-\int_{\eta_0-\epsilon}^{\eta_0+\epsilon}e^{i\alpha UT}\frac{\partial\check{v}}{\partial T}d\eta.$$

Thus, if $\check{v}$ and $U$ are continuous at $\eta_0$, then the right-hand side vanishes as $\epsilon \to 0$. As a consequence, $\check{p}$ must be continuous at $\eta_0$.

The four matching conditions that determine $A$, $B$, $C$ and $D$ are

$$(\check{v}_1 - \check{v}_2)|_{\eta=1=0}, \quad (\check{v}_2 - \check{v}_3)|_{\eta=1} = 0, \quad (\check{p}_1 - \check{p}_2)|_{\eta=1} = 0, \quad (\check{p}_2 - \check{p}_3)|_{\eta=1} = 0. \tag{3.41}$$

The expression for $\check{p}$ used for the matching conditions is in terms of $\check{v}$ and is given by (3.29) or

$$\check{p} = -\frac{1}{\tilde{\alpha}^2}\left[\frac{\partial}{\partial T}\left(\frac{\partial \check{v}}{\partial \eta} + i\alpha U' T\check{v}\right) + i\alpha U'\check{v}\right]. \tag{3.42}$$

Substituting the general solution $\check{G}$ (3.38) for $\check{v}$ and (3.42) for the pressure in the matching conditions results in

$$A - B - e^{2(\tilde{\alpha} - i\alpha T)}C = F_1, \tag{3.43}$$

$$e^{2(\tilde{\alpha} + i\alpha T)}B + C - D = F_2, \tag{3.44}$$

$$\dot{A} - \dot{B} + e^{2(\tilde{\alpha} - i\alpha T)}\dot{C} = -(i\alpha/\tilde{\alpha})[B + (1 - 2\tilde{\alpha})\, e^{2(\tilde{\alpha} - i\alpha T)}C] + H_1, \tag{3.45}$$

$$e^{2(\tilde{\alpha} + i\alpha T)}\dot{B} - \dot{C} + \dot{D} = (i\alpha/\tilde{\alpha})[(1 - 2\tilde{\alpha})\, e^{2(\tilde{\alpha} + i\alpha T)}B + C] + H_2, \tag{3.46}$$

where $\dot{}$ denotes the derivative with respect to $T$ and

$$F_1 = \check{G}_2^{(r)}|_{\eta=1}, \qquad H_1 = -\frac{1}{\tilde{\alpha}}\left[\frac{\partial}{\partial T}\left(\frac{\partial}{\partial \eta} + i\alpha T\right) + i\alpha\right]\check{G}_2^{(r)}|_{\eta=1},$$

$$F_2 = -\check{G}_2^{(r)}|_{\eta=-1}, \quad H_2 = \frac{1}{\tilde{\alpha}}\left[\frac{\partial}{\partial T}\left(\frac{\partial}{\partial \eta} + i\alpha T\right) + i\alpha\right]\check{G}_2^{(r)}|_{\eta=-1}.$$

On taking the derivative of (3.43) and (3.44) with respect to $T$, substituting the results into (3.45) and (3.46), a $2 \times 2$ coupled system results, namely

$$\dot{\boldsymbol{x}} = \boldsymbol{R}\boldsymbol{x} + \boldsymbol{f} \tag{3.47}$$

where

$$\boldsymbol{x} = \begin{bmatrix} B \\ C \end{bmatrix}, \quad \boldsymbol{R} = \frac{i\alpha}{2\tilde{\alpha}}\begin{bmatrix} (1 - 4\tilde{\alpha}) & e^{-2(\tilde{\alpha} + i\alpha T)} \\ -e^{-2(\tilde{\alpha} - i\alpha T)} & -(1 - 4\tilde{\alpha}) \end{bmatrix}$$

and

$$\boldsymbol{f} = \frac{1}{2}\begin{bmatrix} (H_2 + \dot{F}_2)\, e^{-2(\tilde{\alpha} + i\alpha T)} \\ (H_1 - \dot{F}_1)\, e^{-2(\tilde{\alpha} - i\alpha T)} \end{bmatrix}. \tag{3.48}$$

This system of ordinary differential equations provides a unique solution for the two coefficients $B$ and $C$ for the general solution (3.38). The other two coefficients $A$ and $D$ are solved using (3.43) and (3.44). Therefore, the problem of finding a unique solution to the initial-value problem rests on finding the solution for the system of equations (3.47).

For the corresponding homogeneous equations (3.47), the first equation is differentiated and, eliminating $C$ and $\dot{C}$, the result is

$$\ddot{B} + i2\alpha\dot{B} + \frac{1}{4\tilde{\alpha}^2}(1 - 4\tilde{\alpha} - e^{-4\tilde{\alpha}})\, B = 0.$$

Since the coefficients of the equation for $B$ are constants, solutions of the form $B = e^{i\omega T}$ follow. After substituting and solving for the eigenfrequencies $\omega_{1,2}$,

$$\omega_{1,2} = -\alpha \pm \frac{\alpha}{2\tilde{\alpha}} r^{1/2}, \quad r = (1 - 2\tilde{\alpha})^2 - e^{-4\tilde{\alpha}}. \tag{3.49}$$

Without the Doppler shift term, $-\alpha$, the resultant eigenfrequencies are the same as those for the normal mode solutions given in (2.4).

A compact form of solution for the system (3.47) can be constructed in terms of a fundamental matrix as follows:

$$x = \boldsymbol{\Phi}(T)\int_0^T \boldsymbol{\Phi}^{-1}(\tau)\boldsymbol{f}(\tau)\,\mathrm{d}\tau. \tag{3.50}$$

The matrix, $\boldsymbol{\Phi}(T)$, satisfies

$$\dot{\boldsymbol{\Phi}} = \boldsymbol{R}\boldsymbol{\Phi}, \quad \boldsymbol{\Phi}(0) = \boldsymbol{I}, \tag{3.51}$$

where $\boldsymbol{R}$ is given by (3.47). The first column of the equations is

$$\begin{bmatrix}\dot{\Phi}_{11}\\ \dot{\Phi}_{21}\end{bmatrix} = \boldsymbol{R}\begin{bmatrix}\Phi_{11}\\ \Phi_{21}\end{bmatrix}, \quad \begin{bmatrix}\Phi_{11}(0)\\ \Phi_{21}(0)\end{bmatrix} = \begin{bmatrix}1\\ 0\end{bmatrix}. \tag{3.52}$$

The solution of $\Phi_{11}$ is

$$\Phi_{11} = \tilde{\omega}_1 \mathrm{e}^{\mathrm{i}\omega_1 T} + (1-\tilde{\omega}_1)\mathrm{e}^{\mathrm{i}\omega_2 T},$$

where $\omega_1, \omega_2$ are given by (3.49) and

$$\tilde{\omega}_1 = \frac{1}{\omega_2-\omega_1}\left\{\omega_2 - \frac{\alpha}{2\tilde{\alpha}}(1-4\tilde{\alpha})\right\} = \frac{1-2\tilde{\alpha}+r^{1/2}}{2r^{1/2}}.$$

After substituting this solution in the first equation of the system (3.52), which is

$$\dot{\Phi}_{11} = \tfrac{1}{2}\mathrm{i}(1-4\tilde{\alpha})\frac{\alpha}{\tilde{\alpha}}\Phi_{11} + \tfrac{1}{2}\mathrm{i}\frac{\alpha}{\tilde{\alpha}}\mathrm{e}^{-2\tilde{\alpha}-\mathrm{i}2\alpha T}\Phi_{21},$$

the solution for $\Phi_{21}$ is found. The solutions for $\Phi_{12}$ and $\Phi_{22}$ are found in a similar way. In matrix form,

$$\boldsymbol{\Phi} = \begin{bmatrix}\tilde{\omega}_1 \mathrm{e}^{\mathrm{i}\omega_1 T} - \tilde{\omega}_2 \mathrm{e}^{\mathrm{i}\omega_2 T} & \tilde{\omega}_3(\mathrm{e}^{\mathrm{i}\omega_1 T} - \mathrm{e}^{\mathrm{i}\omega_2 T})\\ \tilde{\omega}_3(\mathrm{e}^{-\mathrm{i}\omega_1 T} - \mathrm{e}^{-\mathrm{i}\omega_2 T}) & \tilde{\omega}_1 \mathrm{e}^{-\mathrm{i}\omega_1 T} - \tilde{\omega}_2 \mathrm{e}^{-\mathrm{i}\omega_2 T}\end{bmatrix}. \tag{3.53}$$

Its inverse is

$$\boldsymbol{\Phi}^{-1} = \begin{bmatrix}\tilde{\omega}_1 \mathrm{e}^{-\mathrm{i}\omega_1 T} - \tilde{\omega}_2 \mathrm{e}^{-\mathrm{i}\omega_2 T} & \tilde{\omega}_3(\mathrm{e}^{\mathrm{i}\omega_2 T} - \mathrm{e}^{\mathrm{i}\omega_1 T})\\ \tilde{\omega}_3(\mathrm{e}^{-\mathrm{i}\omega_2 T} - \mathrm{e}^{-\mathrm{i}\omega_1 T}) & \tilde{\omega}_1 \mathrm{e}^{\mathrm{i}\omega_1 T} - \tilde{\omega}_2 \mathrm{e}^{\mathrm{i}\omega_2 T}\end{bmatrix}, \tag{3.54}$$

with

$$\tilde{\omega}_{1,2} = \frac{1-2\tilde{\alpha}\pm r^{1/2}}{2r^{1/2}}, \quad \tilde{\omega}_3 = \frac{\mathrm{e}^{-2\tilde{\alpha}}}{2r^{1/2}}.$$

The eigenfrequencies (3.49) depend on both $\alpha$ and $\tilde{\alpha}$. Consequently, as $\tilde{\alpha} \to \tilde{\alpha}_s \approx 0.64$, the two eigenfrequencies coalesce. At this limiting value of $\tilde{\alpha} = \tilde{\alpha}_s$, the matrix solution of system (3.51) is

$$\boldsymbol{\Phi} = \begin{bmatrix}(1-\mathrm{i}qT)\mathrm{e}^{-\mathrm{i}\alpha T} & \mathrm{i}qT\mathrm{e}^{-\mathrm{i}\alpha T}\\ -\mathrm{i}qT\mathrm{e}^{\mathrm{i}\alpha T} & (1+\mathrm{i}qT)\mathrm{e}^{\mathrm{i}\alpha T}\end{bmatrix}, \tag{3.55}$$

and its inverse is

$$\boldsymbol{\Phi}^{-1} = \begin{bmatrix}(1+\mathrm{i}qT)\mathrm{e}^{\mathrm{i}\alpha T} & -\mathrm{i}qT\mathrm{e}^{-\mathrm{i}\alpha T}\\ \mathrm{i}qT\mathrm{e}^{\mathrm{i}\alpha T} & (1-\mathrm{i}qT)\mathrm{e}^{-\mathrm{i}\alpha T}\end{bmatrix}, \tag{3.56}$$

where

$$q = \frac{\alpha}{2\tilde{\alpha}}\mathrm{e}^{-2\tilde{\alpha}}.$$

The solution (3.55) denotes *algebraically growing* behaviour and it is due to the multiple eigenvalues when $\tilde{\alpha}_0 = \tilde{\alpha}_s$.

The inhomogeneous term $f$ (3.48) may be rewritten in terms of $\check{G}^{(r)}$ as

$$f=\frac{e^{-2\tilde{\alpha}}}{2\tilde{\alpha}}\begin{bmatrix} e^{-i2\alpha T}\left\{\frac{\partial}{\partial T}\left[\frac{\partial \check{G}_2^{(r)}}{\partial \eta}+(i\alpha T-\tilde{\alpha})\,\check{G}_2^{(r)}\right]+i\alpha \check{G}_2^{(r)}\right\}_{\eta=-1} \\ -e^{i2\alpha T}\left\{\frac{\partial}{\partial T}\left[\frac{\partial \check{G}_2^{(r)}}{\partial \eta}+(i\alpha T+\tilde{\alpha})\,\check{G}_2^{(r)}\right]+i\alpha \check{G}_2^{(r)}\right\}_{\eta=1}\end{bmatrix}. \tag{3.57}$$

On evaluating (3.57) with $\check{G}_2^{(r)}$ given by (3.37),

$$f=-i\,e^{i\alpha y_0 T}\begin{bmatrix}\bar{f}_1 e^{-i\alpha T} \\ \bar{f}_2 e^{\alpha T}\end{bmatrix}, \tag{3.58}$$

with

$$\bar{f}_1\equiv(\alpha/4\tilde{\alpha}^2)(2\tilde{\alpha}-1)\{\tilde{\alpha}[|1+y_0|-(1+y_0)]+1\}e^{-\tilde{\alpha}|1+y_0|},$$

$$\bar{f}_2\equiv(\alpha/4\tilde{\alpha}^2)(2\tilde{\alpha}-1)\{\tilde{\alpha}[(1-y_0)-|1-y_0|]-1\}e^{-\tilde{\alpha}|1-y_0|}.$$

The solution matrix, (3.50), is used where $\Phi$ and $\Phi^{-1}$ are the matrix and its inverse given by (3.53) and (3.54) respectively. Once (3.50) is integrated, the internal-layer solution $\check{G}_2$ is completed. The solution (3.50) is the core component of the specific solution in the internal layer since

$$\check{G}_2(\eta;\eta_0)=B(T)e^{-(\tilde{\alpha}+i\alpha T)(\eta-1)}+C(T)e^{(\tilde{\alpha}-i\alpha T)(\eta+1)}+\check{G}_2^{(r)}. \tag{3.59}$$

From the matching conditions that require $\check{G}$ to be continuous at the two interfaces, the expressions for the two coefficients of the Green's function in the external layers are

$$A=(\check{G}_2-\check{G}_1^{(r)})|_{\eta=1}\quad\text{and}\quad D=(\check{G}_2-\check{G}_3^{(r)})|_{\eta=-1}.$$

Thus, the Green's function for all layers is

$$\check{G}(\eta;\eta_0)=\begin{cases}\check{G}_1=(\check{G}_2-\check{G}_1^{(r)})|_{\eta=1}e^{-\tilde{\alpha}_0(\eta-1)}+\check{G}_1^{(r)}, & \eta>1\\ \check{G}_2, & |\eta|<1\\ \check{G}_3=(\check{G}_2-\check{G}_3^{(r)})|_{\eta=-1}e^{\tilde{\alpha}_0(\eta+1)}+\check{G}_3^{(r)}, & \eta<-1.\end{cases} \tag{3.60}$$

## 4. Specific disturbance velocities

### 4.1. *Implicit form of v for the initial delta function*

The transverse structure is taken as one initial condition to be the same as the Green's function and satisfies

$$\nabla^2 v(x,y,z,0)=\Omega_0 e^{-i(\alpha_0 x+\gamma_0 z)}\delta(y-y_0), \tag{4.1}$$

where $\alpha_0,\gamma_0$ are the initial wavenumber in the $x$- and $z$-directions, $\Omega_0$ is a constant, and $\delta$ is the Dirac delta function centred at $y=y_0$. In addition, the implicit form of $v$ corresponding to the initial condition (4.1) with the delta function replaced by a top-hat function is evaluated. Although in this work all expressions involve complex numbers, it is their real parts that are taken to represent the corresponding physical quantities.

For each layer corresponding to the piecewise linear basic flow, the governing equation for $\check{v}$ in the Fourier space $(\alpha;\eta;\gamma;T)$ with the initial condition (4.1) is

$$\check{\nabla}^2\check{v}(\alpha;\eta;\gamma;T)=\check{\Omega}_0\,\delta(\bar{\eta}), \tag{4.2}$$

where $\check{\Omega}_0 = (2\pi)^2 \Omega_0 \, \delta(\alpha - \alpha_0)\, \delta(\gamma - \gamma_0), \quad \bar{\eta} = \eta - y_0.$

The solution for $\check{v}$ in terms of the Green's function is

$$\check{v}(\alpha; \eta; \gamma; T) = \int_{-\infty}^{\infty} \check{\Omega}_0 \, \delta(\eta_0 - y_0)\, \check{G}(\eta; \eta_0)\, \mathrm{d}\eta_0.$$

Upon integration,

$$\check{v}(\alpha; \eta; \gamma; T) = \check{\Omega}_0 \, \check{G}(\eta; y_0).$$

Since $\check{\Omega}_0 = (2\pi)^2 \Omega_0 \, \delta(\alpha - \alpha_0)\, \delta(\gamma - \gamma_0)$, the full Fourier inversion to obtain the solution in the moving coordinate space $(\xi, \eta, \zeta; T)$ can be obtained. In terms of the Eulerian coordinates the implicit form for the solution of $v$ in the internal layer will be

$$v_2(x, y, z; t) = \bar{\Omega}_0 \, \mathrm{e}^{\tilde{\alpha}_0}(\bar{B}(T)\, \mathrm{e}^{-\tilde{\alpha}_0 y + \mathrm{i}\alpha_0 T} + \bar{C}(T)\, \mathrm{e}^{\tilde{\alpha}_0 y - \mathrm{i}\alpha_0 T}) + v_2^{(r)}, \tag{4.3}$$

where $\bar{\Omega}_0 = \Omega_0 \, \mathrm{e}^{-\mathrm{i}(\alpha_0 x + \gamma_0 z)},$

$$v_2^{(r)} = -(\bar{\Omega}_0 / 2\tilde{\alpha}_0)\, \mathrm{e}^{-\tilde{\alpha}_0 |y| + \mathrm{i}\alpha_0 y_0 T}, \tag{4.4}$$

$$\begin{bmatrix} \bar{B} \\ \bar{C} \end{bmatrix} = \boldsymbol{\Phi} \int_0^t \boldsymbol{\Phi}^{-1}(\tau) \tilde{\boldsymbol{f}}(\tau)\, \mathrm{d}\tau; \tag{4.5}$$

$\boldsymbol{\Phi}$ and $\boldsymbol{\Phi}^{-1}$ are given by (3.53) and (3.54) respectively with $\alpha, \gamma$ changed to $\alpha_0, \gamma_0$ and

$$\tilde{\boldsymbol{f}}(\tau) = -\mathrm{i}\, \mathrm{e}^{\mathrm{i}\alpha_0 y_0 \tau} \begin{bmatrix} \bar{f}_1 \, \mathrm{e}^{-\mathrm{i}\alpha_0 \tau} \\ \bar{f}_2 \, \mathrm{e}^{\alpha_0 \tau} \end{bmatrix}, \tag{4.6}$$

with $\bar{f}_1 \equiv (\alpha_0 / 4\tilde{\alpha}_0^2)(2\tilde{\alpha}_0 - 1)\{\tilde{\alpha}_0[|1 + y_0| - (1 + y_0)] + 1\}\, \mathrm{e}^{-\tilde{\alpha}_0 |1 + y_0|},$

$\bar{f}_2 \equiv (\alpha_0 / 4\tilde{\alpha}_0^2)(2\tilde{\alpha}_0 - 1)\{\tilde{\alpha}_0[(1 - y_0) - |1 - y_0|] - 1\}\, \mathrm{e}^{-\tilde{\alpha}_0 |1 - y_0|}.$

The solution for all three layers is

$$v(x, y, z; t) = \begin{cases} (v_2 - v_1^{(r)})|_{y=1}\, \mathrm{e}^{-\tilde{\alpha}_0 (y-1)} + v_1^{(r)}, & y > 1 \\ v_2, & |y| < 1 \\ (v_2 - v_3^{(r)})|_{y=-1}\, \mathrm{e}^{\tilde{\alpha}_0 (y+1)} + v_3^{(r)}, & y < -1, \end{cases} \tag{4.7}$$

where $v_{1,3}^{(r)} = -\dfrac{\bar{\Omega}_0}{2\tilde{\alpha}_0} \mathrm{e}^{-\tilde{\alpha}_0 |\bar{y}|}.$

### 4.2. *Implicit form of v for the initial top-hat function*

The problem (4.2) with the delta function replaced by a top-hat function is now considered. The solution is important because the top-hat function can be used to represent any general initial condition at finite discrete points, i.e. finite differencing of the initial condition. Then, the sum of a finite number of these solutions forms an approximate solution to a more general problem. Moreover, unlike the delta function, the top-hat function is non-singular.

The governing equation for $\check{v}$ becomes

$$\check{\nabla}^2 \check{v}(\alpha; \eta; \gamma; T; y_0) = \check{\Omega}_0 \sqcap(\bar{\eta}; \epsilon), \tag{4.8}$$

where $\bar{\eta} = \eta - y_0$ and

$$\sqcap(\bar{\eta}; \epsilon) = \begin{cases} 1/2\epsilon, & |\bar{\eta}| < \epsilon \\ 0, & |\bar{\eta}| > \epsilon, \end{cases} \tag{4.9}$$

with $-1 < y_0 - \epsilon$ and $y_0 + \epsilon < 1$.

The solution for $\check{v}$ in terms of the Green's function is

$$\check{v}(\alpha;\eta;\gamma;T)=\int_{-\infty}^{\infty}\check{\Omega}_0\Pi(\eta_0-y_0;\epsilon)\check{G}(\eta;\eta_0)\,\mathrm{d}\eta_0.$$

Since $\Pi(\eta_0-y_0;\epsilon)$ vanishes for all $|\eta_0-y_0|>\epsilon$, the limits of the integral reduce to $y_0-\epsilon, y_0+\epsilon$, and the integral becomes

$$\check{v}(\alpha;\eta;\gamma;T)=\frac{\check{\Omega}_0}{2\epsilon}\int_{y_0-\epsilon}^{y_0+\epsilon}\check{G}_2(\eta;\eta_0)\,\mathrm{d}\eta_0.$$

Upon substitution for $\check{G}_2$,

$$\check{v}=\frac{\check{\Omega}_0}{2\epsilon}\int_{y_0-\epsilon}^{y_0+\epsilon}\{B(T)\,\mathrm{e}^{-(\tilde{\alpha}+\mathrm{i}\alpha T)(\eta-1)}+C(T)\,\mathrm{e}^{(\tilde{\alpha}-\mathrm{i}\alpha T)(\eta+1)}+\check{G}_2^{(r)}\}\,\mathrm{d}\eta_0, \tag{4.10}$$

where $\boldsymbol{x}=(B,C)$ is given by (3.50) and

$$\check{G}_2^{(r)}=-(1/2\tilde{\alpha})\,\mathrm{e}^{-\tilde{\alpha}|\eta-\eta_0|+\mathrm{i}\alpha_0\eta_0 T}.$$

After integration, the full Fourier inversion can be made to obtain the solution in the moving coordinates and then, in terms of the Eulerian coordinates,

$$v_2(x,y,z;t)=\bar{\Omega}_0\,\mathrm{e}^{\tilde{\alpha}_0}\{\bar{B}(t)\,\mathrm{e}^{-\tilde{\alpha}_0 y+\mathrm{i}\alpha_0 T}+\bar{C}(t)\,\mathrm{e}^{\tilde{\alpha}_0 y-\mathrm{i}\alpha_0 T}\}+v_2^{(r)}, \tag{4.11}$$

where $\bar{\Omega}_0=\Omega_0\,\mathrm{e}^{-\mathrm{i}(\alpha_0 x+\gamma_0 z)}$,

$$v_2^{(r)}=\frac{-\bar{\Omega}_0}{2\tilde{\alpha}_0}\begin{cases}\dfrac{\sin(\epsilon\beta_2)}{\epsilon\beta_2}\,\mathrm{e}^{-\tilde{\alpha}_0\bar{\eta}-\mathrm{i}\alpha_0\bar{\eta}T}, & \bar{\eta}>\epsilon\\[2ex] \dfrac{-\mathrm{i}}{2}\left[\mathrm{e}^{-\mathrm{i}\alpha_0\bar{\eta}T}\left(\dfrac{\mathrm{e}^{\mathrm{i}\epsilon\beta_1}}{\epsilon\beta_1}\mathrm{e}^{\tilde{\alpha}_0\bar{\eta}}-\dfrac{\mathrm{e}^{-\mathrm{i}\epsilon\beta_2}}{\epsilon\beta_2}\mathrm{e}^{-\tilde{\alpha}_0\bar{\eta}}\right)+\dfrac{1}{\epsilon\beta_2}-\dfrac{1}{\epsilon\beta_1}\right], & |\bar{\eta}|<\epsilon\\[2ex] \dfrac{\sin(\epsilon\beta_1)}{\epsilon\beta_1}\,\mathrm{e}^{\tilde{\alpha}_0\bar{\eta}-\mathrm{i}\alpha_0\bar{\eta}T}, & \bar{\eta}<-\epsilon,\end{cases} \tag{4.12}$$

$\beta_{1,2}=\alpha_0 T\pm\mathrm{i}\tilde{\alpha}_0$, and

$$\begin{bmatrix}\bar{B}\\ \bar{C}\end{bmatrix}=\boldsymbol{\Phi}\int_0^T\boldsymbol{\Phi}^{-1}(\tau)\tilde{\boldsymbol{f}}(\tau)\,\mathrm{d}\tau; \tag{4.13}$$

$\boldsymbol{\Phi}$ and $\boldsymbol{\Phi}^{-1}$ are given by (3.53) and (3.54) with $(\alpha,\gamma)$ changed to $(\alpha_0,\gamma_0)$ and

$$\tilde{\boldsymbol{f}}(\tau)=\frac{\mathrm{i}\alpha_0}{4\tilde{\alpha}_0^2}\,\mathrm{e}^{-3\tilde{\alpha}_0+\mathrm{i}\alpha_0 y_0\tau}\begin{bmatrix}\dfrac{\sin(\epsilon\bar{\beta}_1)}{\epsilon\bar{\beta}_1}\,\mathrm{e}^{-(\tilde{\alpha}_0 y_0+\mathrm{i}\alpha_0\tau)}\\[2ex] -\dfrac{\sin(\epsilon\bar{\beta}_2)}{\epsilon\bar{\beta}_2}\,\mathrm{e}^{\tilde{\alpha}_0 y_0+\mathrm{i}\alpha_0\tau}\end{bmatrix}, \tag{4.14}$$

$\bar{\beta}_{1,2}=\alpha_0\tau\pm\mathrm{i}\tilde{\alpha}_0$. The solution for all three layers takes the same form as (4.7).

As $\epsilon\to 0$, the expression for $v^{(r)}$ (4.12) approaches (4.4), and $\tilde{\boldsymbol{f}}$ approaches (4.6) or the top-hat function approaches the delta function.

### 4.3. *Detailed explicit form of v for the initial delta function*

With the initial condition for $v$ satisfying

$$\nabla^2 v_\delta(x,y,z;0)=\Omega_0\,\mathrm{e}^{-\mathrm{i}(\alpha_0 x+\gamma_0 z)}\delta(y-y_0),$$

the explicit form of the solution $v$ in the physical coordinates is

$$v_\delta(x,y,z;t;y_0) = \begin{cases} v_{\delta 1} = (v_{\delta 2} - v_{\delta 1}^{(r)})|_{y=1}\, e^{-\tilde{\alpha}_0(y-1)} + v_{\delta 1}^{(r)}, & y > 1 \\ v_{\delta 2} = (\bar{\Omega}_0/2\tilde{\alpha}_0)(C_1 e^{i\omega_0 T} + C_2 e^{-i\omega_0 T} + C_3 e^{i\alpha_0 y_0 T}), & |y| < 1 \\ v_{\delta 3} = (v_{\delta 2} - v_{\delta 3}^{(r)})|_{y=-1}\, e^{\tilde{\alpha}_0(y+1)} + v_{\delta 3}^{(r)}, & y < -1, \end{cases} \quad (4.15)$$

where

$$\omega_0 = \frac{\alpha_0 r_0^{1/2}}{2\tilde{\alpha}_0}, \quad r_0 \equiv (1-2\tilde{\alpha}_0)^2 - e^{-4\tilde{\alpha}_0},$$

$$C_1 = \frac{e^{-\tilde{\alpha}_0}}{r_0^{1/2}(2\tilde{\alpha}_0 y_0 - r_0^{1/2})}\{(\tilde{\omega}_1 \tilde{f}_1 + \tilde{\omega}_3 \tilde{f}_2)\, e^{-\tilde{\alpha}_0 y} - (\tilde{\omega}_3 \tilde{f}_1 + \tilde{\omega}_2 \tilde{f}_2)\, e^{\tilde{\alpha}_0 y}\},$$

$$C_2 = \frac{e^{-\tilde{\alpha}_0}}{r_0^{1/2}(2\tilde{\alpha}_0 y_0 + r_0^{1/2})}\{(\tilde{\omega}_3 \tilde{f}_1 + \tilde{\omega}_1 \tilde{f}_2)\, e^{\tilde{\alpha}_0 y} - (\tilde{\omega}_2 \tilde{f}_1 + \tilde{\omega}_3 \tilde{f}_2)\, e^{-\tilde{\alpha}_0 y}\},$$

$$C_3 = -e^{-\tilde{\alpha}_0|\bar{y}|} - C_1 - C_2,$$

$$\tilde{\omega}_{1,2} = \frac{1-2\tilde{\alpha}_0 \pm r_0^{1/2}}{2r_0^{1/2}}, \quad \tilde{\omega}_3 = \frac{e^{-2\tilde{\alpha}}}{2r_0^{1/2}},$$

$$\tilde{f}_1 = \{\tilde{\alpha}_0[|1+y_0| - (1+y_0)] + 1\}\, e^{-\tilde{\alpha}_0|1+y_0|},$$

$$\tilde{f}_2 = \{\tilde{\alpha}_0[(1-y_0) - |1-y_0|] - 1\}\, e^{-\tilde{\alpha}_0|1-y_0|},$$

$$\bar{y} \equiv y - y_0, \quad \tilde{\alpha}_0^2 \equiv \alpha_0^2 + \gamma_0^2, \quad \bar{\Omega}_0 \equiv \Omega_0\, e^{-i(\alpha_0 x + \gamma_0 z)},$$

and $$v_{\delta 1,3}^{(r)} = -(\bar{\Omega}_0/2\tilde{\alpha}_0)\, e^{-\tilde{\alpha}_0|y| + i\alpha_0 U(y) T}.$$

$C_1$, $C_2$ and $C_3$ are bounded for all $\tilde{\alpha}_0$, $y$ and $y_0$ except for the following values of $\tilde{\alpha}_0$:

$$\tilde{\alpha}_0 = 0, \quad \tilde{\alpha}_0 = \tilde{\alpha}_s \approx 0.64 \quad \text{with} \quad \omega_0 = 0 \text{ or } \omega_0 = \alpha_0 y_0.$$

In summary, the solution (4.15), depending on the parameter $\tilde{\alpha}_0$, is

(i) $0 < \tilde{\alpha}_0 < \tilde{\alpha}_s \approx 0.64$; $\omega_0$ purely imaginary: The solution has an exponentially growing, an exponentially decaying and an oscillating term in $T$.

(ii) $\tilde{\alpha}_0 = \tilde{\alpha}_s \approx 0.64$; $\omega_0 = 0$ and $y_0 \neq 0$: The solution grows algebraically in $T$ and the eigenvalues coalesce.

(iii) $\tilde{\alpha}_0 = \tilde{\alpha}_s \approx 0.64$; $\omega_0 = 0$ and $y_0 = 0$: The solution grows algebraically in $T$. The two eigenvalues of (3.47) have the same value and the inhomogeneous term $\boldsymbol{f}$ is in resonance with the system.

(iv) $\tilde{\alpha}_0 > \tilde{\alpha}_s \approx 0.64$; $\omega_0$ is real and $\alpha_0 y_0 = \omega_0$: The solution grows algebraically in $T$. The forcing term $\boldsymbol{f}$ in the system (3.47) is in resonance.

(v) $\tilde{\alpha}_0 = 0$: The solution is independent of $T$.

Since the solution (4.15) depends on three parameters, $y_0$, $\alpha_0$, $\gamma_0$, it is prudent to analyse the cases for different values of $\phi = \tan^{-1}(\gamma_0/\alpha_0)$ in addition to the above five cases. Different values of the parameter $\phi$ corresponds to different angles of the initial obliquity for the initial three-dimensional disturbance.

(i) $0 < \tilde{\alpha}_0 < \tilde{\alpha}_s \approx 0.64$; $\omega_0$ *purely imaginary*

Here, the value of $\tilde{\alpha}_0$ is in the interval $0 < \tilde{\alpha}_0 < \tilde{\alpha}_s \approx 0.64$, and the branch of the square root is taken to be positive so that

$$\omega_0 = (i\alpha_0/2\tilde{\alpha}_0)[e^{-4\tilde{\alpha}_0} - (1-2\tilde{\alpha}_0)^2]^{1/2}.$$

The solution (4.15) has one exponentially decaying term as shown with the coefficient $C_1$, one exponentially growing term as shown with the coefficient $C_2$, and one oscillating term as shown with the coefficient $C_3$.

For large $T$, the exponentially growing term dominates the solution. Thus, the solution tends to

$$v(x,y,z;t) \sim (\bar{\Omega}_0/2\tilde{\alpha}_0)\,C_2\,\mathrm{e}^{-\mathrm{i}\omega_0 T} \quad \text{as} \quad T\to\infty \tag{4.16}$$

where $$-\mathrm{i}\omega_0 = \tfrac{1}{2}\cos\phi\,[\mathrm{e}^{-4\tilde{\alpha}_0}-(1-2\tilde{\alpha}_0)^2]^{1/2}, \quad \phi = \tan^{-1}(\gamma_0/\alpha_0).$$

The exponential growth rate $-\mathrm{i}\omega_0$ is exactly the same as that corresponding to the normal mode. For a fixed value of $\tilde{\alpha}_0$, the maximum and minimum growth rates are $\phi = 0$ and $\frac{1}{2}\pi$ respectively. This is the key argument that proves Squire's theorem for normal mode disturbances which states that for any unstable three-dimensional mode, there is a corresponding faster-growing two-dimensional mode. The two-dimensional mode is equivalent to the case $\phi = 0$ and $w = 0$.

Note that Squire's theorem does not cover the dynamical behaviour of the transverse vorticity $\Omega_y$ governed by (3.31) and the solution for $\Omega_y$, together with $v$, directly influences the behaviour of the other two velocity components (3.27) and (3.28). However, the solution to the governing equation for $\Omega_y$ would be an integral with $v$ as the major part of the integrand. So, at large time, the exponential growth rate of all velocity components is the same as that for $v$. Thus, as long as $T$ is large, Squire's theorem is applicable.

For small time, all terms in the solution (4.15) are important to the growth rate of $v$. Also, during the transient time, the growth rate depends on the coefficients $C_1$, $C_2$ and $C_3$. Squire's theorem is not valid for the reasons cited and because the solutions are non-separable. The disturbance kinetic energies for this solution for different angles of obliquity grow at a comparable rate during the transient time, as will be shown in §6.

Other aspects of the $\Omega_y$ equation have been exploited as well and presented most succinctly by Benney & Gustavsson (1981). In this work, it was shown that there could be resonant solutions for $\Omega_y$ with $v$. Interestingly, resonance occurs for damped exponential solutions and the algebraic dependence allows possible transient growth but it is not due to the continuous spectrum.

(ii) $\tilde{\alpha}_0 = \tilde{\alpha}_s \approx 0.64$; $\omega_0 = 0$ *and* $y_0 \neq 0$

When $\omega_0 = 0$, the solution (4.15) has no exponentially growing behaviour. However, by taking the limit of the solution (4.15) as $\tilde{\alpha}_0 \to \tilde{\alpha}_s$ ($\omega_0 \to 0$), a solution linear in $T$ results where

$$v_2(x,y,z;t) = (\bar{\Omega}_0/2\tilde{\alpha}_s)(P_0+\mathrm{i}P_1\alpha_s T+P_2\,\mathrm{e}^{\mathrm{i}\alpha_s y_0 T}), \tag{4.17}$$

with

$$\begin{aligned}
P_1 &= (\mathrm{e}^{-3\tilde{\alpha}_s}/2\tilde{\alpha}_s^2 y_0)\cosh(\tilde{\alpha}_s y)(\tilde{f}_2-\tilde{f}_1),\\
P_0 &= (1/y_0)[P_1+(\mathrm{e}^{-\tilde{\alpha}_s}/2\tilde{\alpha}_s)(\mathrm{e}^{-\tilde{\alpha}_s y}\tilde{f}_1+\mathrm{e}^{\tilde{\alpha}_s y}\tilde{f}_2)],\\
P_2 &= -P_0-\mathrm{e}^{-\tilde{\alpha}_s|y-y_0|},\\
\tilde{f}_1 &\equiv \{\tilde{\alpha}_s[|1+y_0|-(1+y_0)]+1\}\,\mathrm{e}^{-\tilde{\alpha}_s|1+y_0|},\\
\tilde{f}_2 &\equiv \{\tilde{\alpha}_s[(1-y_0)-|1-y_0|]-1\}\,\mathrm{e}^{-\tilde{\alpha}_s|1-y_0|},\\
\tilde{\alpha}_s^2 &\equiv \alpha_s^2+\gamma_s^2, \quad \bar{\Omega}_0 \equiv \Omega_0\,\mathrm{e}^{-\mathrm{i}(\alpha_\sigma x+\gamma_s z)}.
\end{aligned}$$

Note that here $\tilde{\alpha}_s$ implies $\mathrm{e}^{-2\tilde{\alpha}_s} = 2\tilde{\alpha}_s - 1$. Another way of getting the solution (4.17) is by reconsidering (3.47), which governs the two coefficients of $\check{v}_2$. The corresponding homogeneous equation of (3.47) has solutions in the form of $\exp(\mathrm{i}\omega_{1,2}T)$, where $\omega_{1,2}$ are the two eigenvalues of the system. When $\tilde{\alpha}_0 = \tilde{\alpha}_s \approx 0.64$ such that $\omega_0(\tilde{\alpha}_s) = 0$, $\mathrm{i}\omega_{1,2}T = -\mathrm{i}\alpha T$, which gives only one exponential solution for the homogeneous equation. Therefore, the two independent solutions must be in the following form:

$$(\mathrm{e}^{-\mathrm{i}\alpha T}, T\mathrm{e}^{-\mathrm{i}\alpha T}). \tag{4.18}$$

On re-evaluating $(B, C)$ based on the two linear independent solutions (4.18), (4.3) is obtained.

By analysing the growing term of the solution (4.17), $v$ is found to grow linearly in $T$ with the coefficient $iP_1\alpha_s = P_1\tilde{\alpha}_s\cos\phi$. Since $P_1$ depends only on $\tilde{\alpha}_s$, $y$ and $y_0$, this solution is also in agreement with Squire's theorem: $\phi = 0$ and $\frac{1}{2}\pi$ give the maximum and minimum growth rates respectively. However, Squire's theorem does not cover the dynamical behaviour of the transverse vorticity $\Omega_y$ governed by (3.31) and the solution for $\Omega_y$, together with $v$, directly influences the behaviour of the other two velocity components (3.27) and (3.28). In fact, the growth rates for the other velocity components do not depend on $\phi$ as the simple $\cos\phi$ in the solution for $v$.

(iii) $\tilde{\alpha}_0 = \tilde{\alpha}_s \approx 0.64$; $\omega_0 = 0$ *and* $y_0 = 0$

As mentioned in the previous case, when $\tilde{\alpha}_0 = \tilde{\alpha}_s$, there is only one eigenfrequency for the solution of the corresponding homogeneous equation of (3.47). Since the exponential term of the homogeneous solution is the same as one component of the forcing function $f$ when $y_0 = 0$, a resonant solution is generated.

Either way, reconstructing the solution from the solution of the system (3.47), or taking the limit of the solution (4.3) as $y_0 \to 0$, gives

$$v_2(x, y, z; t) = \frac{\bar{\Omega}_0}{2\tilde{\alpha}_s}\left[-e^{-\tilde{\alpha}_s|y|} + i\sinh(\tilde{\alpha}_s y)\frac{\alpha_s}{\tilde{\alpha}_s}e^{-2\tilde{\alpha}_s}T - \cosh(\tilde{\alpha}_s y)\left(\frac{\alpha_s}{\tilde{\alpha}_s}e^{-2\tilde{\alpha}_s}\right)^2\frac{T^2}{2}\right]. \tag{4.19}$$

(iv) $\tilde{\alpha}_0 > \tilde{\alpha}_s \approx 0.64$; $\omega_0$ *real and* $\alpha_0 y_0 = \omega_0$; $|y_0| < 1$

When the initial wavenumber magnitude is greater than the neutral value ($\tilde{\alpha}_0 > \tilde{\alpha}_s$), the solution (4.15) has no exponentially growing behaviour. For $\alpha_0 y_0 \neq \omega_0$, it is purely oscillatory. However, when $\alpha_0 y_0 = \omega_0$, the limit of (4.15), as $\alpha_0 y_0 \to \omega_0$, is required and

$$v_2(x, y, z; t) = (\bar{\Omega}_0/2\tilde{\alpha}_0)(S_0 + iS_1\alpha_0 T - e^{-\tilde{\alpha}_0|\bar{y}| + i\alpha_0 y_0 T}), \tag{4.20}$$

where

$$S_0 = \frac{e^{-2\tilde{\alpha}_0}}{8\tilde{\alpha}_0^2 y_0^2}\{(1-2\tilde{\alpha}_0)\cosh(\tilde{\alpha}_0\bar{y}) + 2\tilde{\alpha}_0 y_0\sinh(\tilde{\alpha}_0\bar{y}) - e^{-2\tilde{\alpha}_0}\cosh(\tilde{\alpha}_0\bar{y})\}, \tag{4.21}$$

$$S_1 = -\frac{e^{-2\tilde{\alpha}_0}}{4\tilde{\alpha}_0^2 y_0}\{(1-2\tilde{\alpha}_0)\cosh(\tilde{\alpha}_0\bar{y}) - 2\tilde{\alpha}_0 y_0\sinh(\tilde{\alpha}_0\bar{y}) - e^{-2\tilde{\alpha}_0}\cosh(\tilde{\alpha}_0\bar{y})\}. \tag{4.22}$$

For large values of $\tilde{\alpha}_0$, $\omega_0$ is real, and $\omega_0 \to 1$ as $\tilde{\alpha}_0 \to \infty$. These real eigenfrequencies are encountered in many other applications of the normal mode analysis for piecewise linear basic flows, when the curvature of the basic profile is concentrated at a discrete set of points (cf. Betchov & Criminale 1967).

(v) $\tilde{\alpha}_0 = 0$

Here the specific solution for the transverse velocity component is independent of time and equals the initial value. This can be shown by starting from the continuity equation where

$$-i\alpha_0 u - i\gamma_0 w + \partial v/\partial y = 0,$$

for which $\alpha_0 = \tilde{\alpha}_0 = \cos\phi = 0$, $\gamma_0 = \tilde{\alpha}_0\sin\phi = 0$ when $\tilde{\alpha}_0 = 0$. Thus, $v = v(\phi, T)$ and independent of $y$. Since $v$ must be continuous at the two interfaces $y = \pm 1$,

$$v(\phi, T) \equiv v_1(\phi, T) = v_2(\phi, T) = v_3(\phi, T)$$

also follows. The momentum equation in the $y$-direction for this case reduces to

$$\partial v/\partial T = -\partial p_j/\partial y,$$

where $j = 1$, 2 or 3 denotes the corresponding layer. Integrating with respect to $y$,

$$p_j = -\frac{\partial v(\phi, T)}{\partial T} y + p_{0,j}(\phi, T).$$

Since the disturbed pressure must be bounded as $y \to \pm\infty$, for the external layers,

$$\partial v(\phi, T)/\partial T = 0.$$

This gives

$$v = v(\phi)$$

only. Thus, when $\tilde{\alpha}_0 = 0$, the specific solution for the transverse velocity component is a steady-state solution. However, this does not mean that the other two components of the disturbance velocity are also constant. In fact, from the momentum equation in the $x$-direction this case simplifies to

$$\partial u/\partial T = -U'v$$

which can immediately be integrated to give

$$u = -U'vT + u_0(x, y, z).$$

So, in the internal layer where $U' = 1$, $u$ can increase linearly in $T$ if $v$ is not identically zero. This suggests that any analysis of the disturbance must include all three components of the velocity field.

### 4.4. *Other velocity components and pressure*

For convenience, three-dimensional solutions are analysed using various values of the initial polar variables $\tilde{\alpha}_0 \equiv (\alpha_0^2 + \gamma_0^2)^{1/2} \neq 0$ and the angle $\phi \equiv \tan^{-1}(\gamma_0/\alpha_0)$ instead of $(\alpha_0, \gamma_0)$. The expressions for the other velocity components and pressure in the two-dimensional Fourier space are given by (3.27), (3.28) and (3.29). In the physical coordinates,

$$u = -\frac{\mathrm{i}}{\tilde{\alpha}_0}\left\{\cos\phi \frac{\partial v}{\partial y} - \sin\phi \Omega_y\right\}, \tag{4.23}$$

$$w = -\frac{\mathrm{i}}{\tilde{\alpha}_0}\left\{\sin\phi \frac{\partial v}{\partial y} + \cos\phi \Omega_y\right\}, \tag{4.24}$$

$$p = \frac{1}{\tilde{\alpha}_0^2}\left(\mathrm{i}\tilde{\alpha}_0 \cos\phi U - \frac{\partial}{\partial t}\right)\frac{\partial v}{\partial y} - \mathrm{i}\frac{\cos\phi}{\tilde{\alpha}_0} U'v, \tag{4.25}$$

where

$$\Omega_y(x, y, z, t) = \mathrm{i}U'(y)\tilde{\alpha}_0 \sin\phi\, \mathrm{e}^{\mathrm{i}\alpha_0 y T} \int_0^T v(x, y, z, \tau)\, \mathrm{e}^{-\mathrm{i}\alpha_0 y \tau}\, \mathrm{d}\tau + \Omega_{y0}(x - Ut, y, z), \tag{4.26}$$

and has the simpler form in the moving coordinates,

$$\Omega_y(\xi, \eta, \zeta, T) = \mathrm{i}U'(\eta)\tilde{\alpha}_0 \sin\phi \int_0^T v(\xi, \eta, \zeta, \tau)\, \mathrm{d}\tau + \Omega_{y0}(\xi, \eta, \zeta).$$

Since $U'(y) = 0$ in the external layers, $\Omega_y$ is conserved for all values of $\tilde{\alpha}_0$ and $\phi$.

In the internal layer, $\phi = 0$ and $\frac{1}{2}\pi$ are the two extreme cases for which the solution depends only on two spatial variables $x, y$ and $y, z$ respectively. $\Omega_y$ for the two extreme cases is

$$\Omega_y(x,y,z,t) = \Omega_{y0}(x-Ut,y,z) + \begin{cases} 0, & \phi = 0 \\ -(\bar{\Omega}_0/2\tilde{\alpha}_0)\,\mathrm{e}^{-\tilde{\alpha}_0|\bar{y}|}T, & \phi = \frac{1}{2}\pi, \end{cases} \tag{4.27}$$

where $\phi = 0$ and $w \equiv 0$, the usual consideration of a two-dimensional initial disturbance that is independent of the spanwise $z$-direction. Since $w \equiv 0$ gives $\Omega_y \equiv 0$, the expression for the streamwise velocity simplifies to

$$u = -(\mathrm{i}/\alpha_0)\,\partial v/\partial y. \tag{4.28}$$

This is two-dimensional planar motion with only one non-zero component of vorticity, $\Omega_z$.

When $\phi = 0$ but $w(x,y,z,0) \neq 0$, the expression for $u$ in terms of $v$ is the same as (4.28). With $w(x,y,z,0) = w_0(x,y,z) \neq 0$, the solution for $w$ is

$$w(x,y,z,t) = w_0(x-Ut,y,z). \tag{4.29}$$

This unsteady solution for $w$ can lead to a growing streamwise vorticity component, $\Omega_x$.

The other extreme is $\phi = \frac{1}{2}\pi$. The resultant transverse and spanwise velocity disturbances $v$, $w$ and pressure are independent of $t$, but $u$ increases linearly in $t$. In fact,

$$\begin{bmatrix} u \\ v \\ w \\ p \end{bmatrix} = -\begin{bmatrix} U'(y)\,vt - u_0 \\ (\bar{\Omega}_0/2\gamma_0)\,\mathrm{e}^{-\gamma_0|\bar{y}|} \\ (\mathrm{i}/\gamma_0)\,\partial v/\partial y \\ 0 \end{bmatrix}, \tag{4.30}$$

where $u_0(y,z;y_0) = \bar{\Omega}_0\,\tilde{u}_0(y,y_0)$, $\bar{\Omega}_0 = \Omega_0\,\mathrm{e}^{-\mathrm{i}\gamma_0 z}$ and $\tilde{u}_0(y,y_0)$ represents an arbitrary vertical structure of the initial velocity disturbance $u_0$.

The above result is similar to the solution found earlier by Ellingsen & Palm (1975) and is a very simple expression that may explain a physical process regarding the origin of the three-dimensional instability in the mixing layer. The initial disturbance for this case is independent of $x$ but periodic in $z$ with initial wavenumber $\gamma_0 = \tilde{\alpha}_0$.

The streamwise velocity $u$ grows linearly in time while the transverse and spanwise velocities, $v, w$ remain constant. Since $u$ is independent of $x$, the growth of $u$ has a distortion effect on the mean flow and such an effect could lead to local breakdown of the laminar flow regime and is a typical of so-called fast transition.

### 4.5. *Three-dimensional initial disturbance as a single oblique mode*

The streamwise-independent initial disturbance ($\phi = \frac{1}{2}\pi$) is a special infinite-wave-train initial disturbance that has a simple structure. However, this structure does not model the initial disturbance that leads to nonlinear roll-up of the spanwise vortices because of the streamwise independence. An infinite-wave-train initial disturbance that could lead to nonlinear roll-up would have to be for $\phi = 0$. This solution has been discussed in the previous section. Here, the solution $\Omega_y$ corresponding to the three-dimensional initial disturbance with an oblique wave $0 < \phi < \frac{1}{2}\pi$ is considered.

(i) $0 < \tilde{\alpha}_0 < \tilde{\alpha}_s \approx 0.64$; *exponential growth and decay*

$$\Omega_y = -\bar{\Omega}_0 \tan\phi\{\tilde{C}_1\,\mathrm{e}^{\mathrm{i}\omega_0 T} + \tilde{C}_2\,\mathrm{e}^{-\mathrm{i}\omega_0 T}\tilde{C}_3\,\mathrm{e}^{\mathrm{i}\tilde{\alpha}_0 y_0 T\cos\phi} + \tilde{C}_4\,\mathrm{e}^{\mathrm{i}\tilde{\alpha}_0 y T\cos\phi}\} + \Omega_{y0}(x-Ut,y,z). \tag{4.31}$$

(ii) $\tilde{\alpha}_0 \approx 0.64$ *and* $y_0 \neq 0$; *algebraic growth and resonance*

$$\Omega_y = -(\bar{\Omega}_0/2\tilde{\alpha}_s)\tan\phi\{\tilde{P}_0 + i\tilde{P}_1 T\cos\phi + \tilde{P}_2 e^{i\tilde{\alpha}_s y_0 T\cos\phi} + \tilde{P}_3 e^{i\tilde{\alpha}_s y T\cos\phi}\} + \Omega_{y0}(x - Ut, y, z). \quad (4.32)$$

(iii) $\tilde{\alpha}_0 = \tilde{\alpha}_s \approx 0.64$ *and* $y_0 = 0$; *algebraic growth*

$$\Omega_y = -(\bar{\Omega}_0/2\tilde{\alpha}_s)\tan\phi\{\tilde{Q}_0(1 - e^{i\tilde{\alpha}_s yT\cos\phi}) + i\tilde{Q}_1 T\cos\phi + \tilde{Q}_2 T^2\cos^2\phi\} + \Omega_{y0}(x - Ut, y, z). \quad (4.33)$$

(iv) $\tilde{\alpha}_0 > \tilde{\alpha}_s \approx 0.64$, $|y_0| < 1$ *and* $\omega_0 = y_0\tilde{\alpha}_0\cos\phi$; *algebraic growth*

$$\Omega_y = -(\bar{\Omega}_0/2\tilde{\alpha}_0)\tan\phi\{\tilde{S}_0 + i\tilde{S}_1 T\cos\phi + \tilde{S}_2 e^{i\tilde{\alpha}_0 y_0 T\cos\phi} + \tilde{S}_3 e^{i\tilde{\alpha}_0 yT\cos\phi}\} + \Omega_{y0}(x - Ut, y, z). \quad (4.34)$$

Except for $\omega_0$, all coefficients in (4.31)–(4.34) listed below depend only on $y, y_0, \tilde{\alpha}_0$:

$$\omega_0 = \tfrac{1}{2}r_0^{1/2}\cos\phi, \quad r_0 = (1 - 2\tilde{\alpha}_0)^2 - e^{-4\tilde{\alpha}_0},$$

$$\tilde{C}_1 = (2\tilde{\alpha}_0 y - r_0^{1/2})^{-1}C_1, \quad \tilde{C}_2 = (2\tilde{\alpha}_0 y + r_0^{1/2})^{-1}C_2,$$

$$\tilde{C}_3 = C_3/(2\tilde{\alpha}_0\bar{y}), \quad \tilde{C}_4 = -(\tilde{C}_1 + \tilde{C}_2 + \tilde{C}_3),$$

$$\tilde{P}_0 = \frac{P_0}{y} + \frac{P_2}{\tilde{\alpha}_0\cos\phi y^2}, \quad \tilde{P}_1 = \frac{P_1}{y}, \quad \tilde{P}_2 = \frac{P_2}{y}, \quad \tilde{P}_3 = -\tilde{P}_0 - \tilde{P}_2,$$

$$\tilde{Q}_0 = \frac{1}{y}\left\{\frac{e^{-2\tilde{\alpha}_s}}{\tilde{\alpha}_s y}\sinh(\tilde{\alpha}_s y) + \frac{e^{-4\tilde{\alpha}_s}}{\tilde{\alpha}_s^2 y^2}\cosh(\tilde{\alpha}_s y) - e^{-\tilde{\alpha}_s|y|}\right\},$$

$$\tilde{Q}_1 = \frac{e^{-2\tilde{\alpha}_s}}{y}\sinh(\tilde{\alpha}_s y) + \frac{e^{-4\tilde{\alpha}_s}}{\tilde{\alpha}_s y^2}\cosh(\tilde{\alpha}_s y), \quad \tilde{Q}_2 = -\frac{e^{-4\tilde{\alpha}_0}}{2y}\cosh(\tilde{\alpha}_s y),$$

$$\tilde{S}_0 = \frac{S_0}{y} + \frac{S_1}{y^2}, \quad \tilde{S}_1 = \frac{S_1}{y}, \quad \tilde{S}_2 = \frac{S_2}{\bar{y}}, \quad \tilde{S}_3 = -(\tilde{S}_0 + \tilde{S}_2).$$

These expressions for $\Omega_y$ together with $v$ given previously represent a complete description for all three components of the disturbance velocity field; the velocities $u$ and $w$ are expressed in terms of $v$ and $\Omega_y$ as shown in (4.23) and (4.24). The spatial structure of all velocity components are periodic in the $(x, z)$-plane with the wave vector $(\cos\phi, \sin\phi)$. Detailed structure in $y$ also depends on the initial value of the transverse vorticity $\Omega_y(x, y, z, 0) = \Omega_{y0}(x, y, z)$ which can be arbitrarily specified.

The single oblique wave disturbance with $0 < \phi < \frac{1}{2}\pi$ grows exponentially or algebraically in time depending on the scalar wavenumber $\tilde{\alpha}_0$. When $\tilde{\alpha}_0 < \tilde{\alpha}_s \approx 0.64$, all components of the disturbance velocity grow exponentially in $T$; when $\tilde{\alpha}_0 = \tilde{\alpha}_s$, growth is algebraic in $T$. For $\tilde{\alpha}_0 < \tilde{\alpha}_s \approx 0.64$ and for large $T$, the exponentially growing term dominates the solution and (4.15) may be rewritten as

$$v(x, y, z; t) \sim (\bar{\Omega}_0/2\tilde{\alpha}_0)C_2 e^{-i\omega_0 T} \quad \text{as} \quad T \to \infty, \quad (4.35)$$

where

$$-i\omega_0 = \frac{\cos\phi}{2\tilde{\alpha}_0}[e^{-4\tilde{\alpha}_0} - (1 - 2\tilde{\alpha}_0)^2]^{1/2}, \quad \phi = \tan^{-1}(\gamma_0/\alpha_0).$$

The exponential growth rate, $-i\omega_0$, is exactly the same as that corresponding to the normal mode. For a fixed value of $\tilde{\alpha}_0$, the maximum and minimum growth rates are at $\phi = 0$ and $\phi = \frac{1}{2}\pi$ respectively. This is the key argument that proves Squire's theorem

for separable normal mode disturbances in inviscid flow where the two-dimensional mode is equivalent to the case $\phi = 0$ and $w = 0$.

During the transient time of the evolution the growth of the disturbance is dominated by the algebraic behaviour. The factor $\tan\phi$ appearing in the expressions for $\Omega_y$ is important for the oblique wave solution. When $\phi$ is near zero, the growth rate of $\Omega_y$ is small compared to $v$. The reverse occurs when $\phi$ is near $\frac{1}{2}\pi$. When $\tilde{\alpha}_0 = \tilde{\alpha}_s \approx 0.64$ and $y \neq 0$, the growth rate of $v$ has a factor $\cos\phi$ but the growth rate of $\Omega_y$ has a factor $\sin\phi$.

For the case $\tilde{\alpha}_0 < \tilde{\alpha}_s$, the exponential may be expanded in a power series in $T$ and, for small $T$, the growth rate of $v$ has a factor $\cos\phi$ and the growth rate of $\Omega_y$ has a factor $\sin\phi$. These results together with (4.23) and (4.24) reveal that the growth behaviours of $u$ and $w$ do not agree with Squire's theorem. This observation is not a conflict since it should be noted that these solutions are, unlike normal modes, non-separable. Thus, the theorem could not be applicable. However, it is not clear from the expressions for $v, \Omega_y$ and $u, w$ what value of $\phi$ corresponds to the fastest growth rate during the transient time.

## 5. Vorticity

### 5.1. *Streamwise–spanwise periodic disturbance*

Mathematically, the velocity field and pressure are the primitive variables representing the basic elements of a flow. However, in many instances, it is advantageous to interpret the events in a flow in terms of the vorticity dynamics. For example, the physical mechanism of Kelvin–Helmholtz instability has been conveniently described in terms of the vorticity dynamics (Batchelor 1967).

With vanishing second derivative of the basic velocity $U''(y) = 0$, the linearized equations that govern the vorticity disturbance may be written as

$$\frac{\partial \boldsymbol{\Omega}}{\partial t} + U\frac{\partial \boldsymbol{\Omega}}{\partial x} + U'\left(\frac{\partial \boldsymbol{u}}{\partial z} - \Omega_y \boldsymbol{e}_1\right) = 0, \tag{5.1}$$

where $\boldsymbol{e}_1 \equiv (1,0,0)$ and $\boldsymbol{\Omega}$ is the perturbation vorticity.

For the $x$–$z$ periodic disturbance, (5.1) simplifies to

$$\frac{\partial \boldsymbol{\Omega}}{\partial t} - \mathrm{i}\alpha_0 U\boldsymbol{\Omega} - U'(\mathrm{i}\gamma_0 \boldsymbol{u} + \Omega_y \boldsymbol{e}_1) = 0, \tag{5.2}$$

where

$$\begin{bmatrix} \boldsymbol{u} \\ \boldsymbol{\Omega} \end{bmatrix} = \begin{bmatrix} \bar{\boldsymbol{u}}(y;t) \\ \bar{\boldsymbol{\Omega}}(y;t) \end{bmatrix} \mathrm{e}^{-\mathrm{i}(\alpha_0 x + \gamma_0 z)}.$$

On changing to the moving coordinates, the linear equations governing the disturbance vorticity (5.2) become

$$\frac{\partial \boldsymbol{\Omega}}{\partial T} - U'(\mathrm{i}\gamma_0 \boldsymbol{u} + \Omega_y \boldsymbol{e}_1) = 0. \tag{5.3}$$

For the method of solution (§3), a systematic procedure to solve for the transverse velocity component $v$ was provided. Thus, when $v$ is found, the $\eta$-component of (5.3) can be immediately integrated to give

$$\Omega_y(\xi,\eta,\zeta,T) = \mathrm{i}\gamma_0 U' \int_0^T v(\xi,\eta,\zeta,\tau)\,\mathrm{d}\tau + \Omega_{y0}(\xi,\eta,\zeta). \tag{5.4}$$

The kinematic relations for the other two vorticity components in terms of the velocity field are

$$\Omega_x = (\partial/\partial\eta + i\alpha_0 U'T)\, w + i\gamma_0 v,$$
$$\Omega_z = -(\partial/\partial\eta + i\alpha_0 U'T)\, u - i\alpha_0 v.$$

By defining the polar variables such that

$$\Omega_{\tilde{\alpha}_0} = \cos\phi\Omega_x + \sin\phi\Omega_z,$$
$$\Omega_\phi = -\sin\phi\Omega_x + \cos\phi\Omega_z,$$

then
$$\Omega_{\tilde{\alpha}_0}(\xi,\eta,\zeta,T) = (\partial/\partial\eta + i\tilde{\alpha}_0\cos\phi U'T)\,\tilde{w}(\xi,\eta,\zeta,T), \tag{5.5}$$
$$\Omega_\phi(\xi,\eta,\zeta,T) = -(\partial/\partial\eta + i\tilde{\alpha}_0\cos\phi U'T)\,\tilde{u} - i\tilde{\alpha}_0 v. \tag{5.6}$$

From the continuity equation and the relation of $\tilde{w}$ in terms of $\Omega_y$,

$$\tilde{u}(\alpha;\eta;\gamma;T) = -(i/\tilde{\alpha})(\partial/\partial\eta + i\tilde{\alpha}\cos\phi U'T)\,\check{v},$$
$$\tilde{w}(\alpha;\eta;\gamma;T) = (i/\tilde{\alpha})\,\check{\Omega}_y.$$

Upon substitution for $\tilde{u}, \tilde{w}$ into (5.5) and (5.6),

$$\Omega_{\tilde{\alpha}_0}(\xi,\eta,\zeta,T) = (-i/\tilde{\alpha}_0)(\partial/\partial\eta + i\tilde{\alpha}_0\cos\phi U'T)\,\Omega_y(\xi,\eta,\zeta,T), \tag{5.7}$$
$$\Omega_\phi(\xi,\eta,\zeta,T) = (i/\tilde{\alpha}_0)\{(\partial/\partial\eta + i\tilde{\alpha}_0\cos\phi U'T)^2 - \tilde{\alpha}_0^2\}\,v. \tag{5.8}$$

From the governing equation (3.32) for $v$, the expression for $\Omega_\phi$ reduces to

$$\Omega_\phi(\xi,\eta,\zeta,T) = (i/\tilde{\alpha}_0)\{\partial^2/\partial\eta^2 - \tilde{\alpha}_0^2\}\,v_0(\xi,\eta,\zeta) \equiv \Omega_{\phi 0}(\xi,\eta,\zeta), \tag{5.9}$$

where $\Omega_{\phi 0}$ is the initial condition that is proportional to the Laplacian of $v_0$ in the Eulerian coordinates, i.e.

$$\nabla^2 v_0(x,y,z) = -i\tilde{\alpha}_0\,\Omega_{\phi 0}(x,y,z).$$

All components of the vorticity field are obtained by simple substitution and, in the moving coordinates,

$$\boldsymbol{\Omega}(\xi,\eta,\zeta,T) = \begin{bmatrix} -i\dfrac{\cos\phi}{\tilde{\alpha}_0}\left(\dfrac{\partial}{\partial\eta} + i\tilde{\alpha}_0\cos\phi U'T\right)\Omega_y - \sin\phi\Omega_\phi \\ \Omega_y \\ -i\dfrac{\sin\phi}{\tilde{\alpha}_0}\left(\dfrac{\partial}{\partial\eta} + i\tilde{\alpha}_0\cos\phi U'T\right)\Omega_y + \cos\phi\Omega_\phi \end{bmatrix}. \tag{5.10}$$

Then, transforming (5.10) to Eulerian coordinates,

$$\boldsymbol{\Omega}(x,y,z,t) = \begin{bmatrix} -i\dfrac{\cos\phi}{\tilde{\alpha}_0}\dfrac{\partial\Omega_y}{\partial y} - \sin\phi\Omega_\phi \\ \Omega_y \\ -i\dfrac{\sin\phi}{\tilde{\alpha}_0}\dfrac{\partial\Omega_y}{\partial y} + \cos\phi\Omega_\phi \end{bmatrix}, \tag{5.11}$$

where

$$\Omega_y(x,y,z,t) = iU'(y)\,\tilde{\alpha}_0\sin\phi\, e^{i\tilde{\alpha}_0\cos\phi yT}\int_0^T v(x,y,z,\tau)\, e^{-i\tilde{\alpha}_0\cos\phi y\tau}\,d\tau + \Omega_{y0}(x-Ut,y,z), \tag{5.12}$$

$$\Omega_\phi(x, y, z, t) = \Omega_{\phi 0}(x - Ut, y, z). \tag{5.13}$$

From the solution (5.11), (5.12) and (5.13), it can be concluded that a unique vorticity field solution is determined once the initial conditions $\Omega_{\phi 0}$ and $\Omega_{y0}$ are known.

### 5.2. *Spanwise-independent disturbance*

In the special case for which the solution is assumed to be independent of the spanwise variable $z$, the vorticity equations (5.2) reduce to

$$\frac{\partial \boldsymbol{\Omega}}{\partial t} + U\frac{\partial \boldsymbol{\Omega}}{\partial x} - U'\Omega_y \boldsymbol{e}_1 = 0 \tag{5.14}$$

subject to the initial conditions

$$\boldsymbol{\Omega}(x, y, 0) = \begin{bmatrix} (\partial/\partial y)\, w_0(x, y) \\ -(\partial/\partial x)\, w_0(x, y) \\ \Omega_{z0}(x, y) \end{bmatrix}, \tag{5.15}$$

where $w_0$ and $\Omega_{z0}$ are the initial velocity and vorticity components in the spanwise direction and are arbitrary functions of $x, y$. Streamwise-periodic functions for $w_0$ and $\Omega_{z0}$ will be considered below. Note that it is not assumed that $w_0 = 0$ which oversimplifies the problem to planar motion. Non-zero $w_0$ and no $z$-dependence is three-dimensional.

On transforming to the moving coordinates, the problem (5.14) and the initial condition (5.15) become

$$\frac{\partial \boldsymbol{\Omega}}{\partial T} - U'\Omega_y \boldsymbol{e}_1 = 0, \tag{5.16}$$

$$\boldsymbol{\Omega}(\xi, \eta, 0) = \begin{bmatrix} (\partial/\partial \eta)\, w_0(\xi, \eta) \\ -(\partial/\partial \xi)\, w_0(\xi, \eta) \\ \Omega_{z0}(\xi, \eta) \end{bmatrix}. \tag{5.17}$$

The $\eta$- and $\zeta$-components of (5.16) implies that $\Omega_y$ and $\Omega_\zeta$ are constant in time. $\Omega_y$ being constant allows an integration of the $\xi$-component (5.16) and the result is

$$\boldsymbol{\Omega}(\xi, \eta, T) = \begin{bmatrix} (\partial/\partial \eta - U'T\partial/\partial \xi)\, w_0(\xi, \eta) \\ -(\partial/\partial \xi)\, w_0(\xi, \eta) \\ \Omega_{z0}(\xi, \eta) \end{bmatrix}. \tag{5.18}$$

In Eulerian coordinates,

$$\boldsymbol{\Omega}(x, y, t) = \begin{bmatrix} (\partial/\partial y)\, w(x, y, t) \\ -(\partial/\partial x)\, w(x, y, t) \\ \Omega_{z0}(x - Ut, y) \end{bmatrix}, \tag{5.19}$$

where

$$w(x, y, t) = w_0(x - Ut, y). \tag{5.20}$$

As an illustration, if the initial disturbance is periodic in the $x$-direction with wavenumber $\alpha_0$ such as

$$\begin{bmatrix} w_0(x, y) \\ \Omega_{z0}(x, y) \end{bmatrix} = \mathrm{e}^{-\mathrm{i}\alpha_0 x} \begin{bmatrix} \bar{w}_0(y) \\ \bar{\Omega}_{z0}(y) \end{bmatrix}, \tag{5.21}$$

then, by substituting (5.21) into (5.19), the vorticity solution is

$$\boldsymbol{\Omega}(x,y,t) = \mathrm{e}^{-\mathrm{i}\alpha_0(x-Ut)} \begin{bmatrix} (\partial/\partial y + \mathrm{i}\alpha_0 U't)\,\bar{w}_0(y) \\ \mathrm{i}\alpha_0\,\bar{w}_0(y) \\ \bar{\Omega}_{z0}(y) \end{bmatrix}. \tag{5.22}$$

The case for which the disturbance is assumed to be independent of $z$ with the initial condition (5.21) has the general solution (5.19). If $w_0$ vanishes, planar motion for which the vorticity in all directions is conserved, results. However, when $w_0$ is not zero, the vorticity in the streamwise $x$ direction, $\Omega_x$, is not conserved, as for an example, the streamwise-periodic initial disturbance (5.21) leads to the solution (5.22) for which $\Omega_x$ grows linearly in time.

### 5.3. *Streamwise-independent disturbance*

For the special case for which the solution is independent of the streamwise variable $x$, the vorticity equations (5.1) in the fixed coordinates reduce to

$$\frac{\partial \boldsymbol{\Omega}}{\partial t} + U'\frac{\partial}{\partial z}\begin{bmatrix} 0 \\ v \\ w \end{bmatrix} = 0. \tag{5.23}$$

From the governing equation for $v$ and the continuity equation, the solutions for $v$ and $w$ are independent of time. All component equations of (5.23) can be immediately integrated to give

$$\boldsymbol{\Omega}(y,z,t) = -U't\frac{\partial}{\partial z}\begin{bmatrix} 0 \\ v(y,z) \\ w(y,z) \end{bmatrix} + \boldsymbol{\Omega}_0(y,z). \tag{5.24}$$

The solution (5.24) with non-zero initial velocity $v$ and $w$ has vorticity in the transverse and spanwise directions that increases linearly in time.

### 5.4. *Vorticity field corresponding to the initial delta function*

In all previous sections, an $x$–$z$ periodic disturbance vorticity field with arbitrary $y$ dependence was discussed. The vorticity field corresponding to the initial delta function solution is found by taking the curl of the velocity field. The result, in the same form as (5.11) with $v$ being the solution corresponding to the initial delta function given in §4, is

$$\boldsymbol{\Omega}(x,y,z,t) = \begin{bmatrix} -\mathrm{i}\dfrac{\cos\phi}{\tilde{\alpha}_0}\dfrac{\partial \Omega_y}{\partial y} - \sin\phi\,\Omega_\phi \\ \Omega_y \\ -\mathrm{i}\dfrac{\sin\phi}{\tilde{\alpha}_0}\dfrac{\partial \Omega_y}{\partial y} + \cos\phi\,\Omega_\phi \end{bmatrix}, \tag{5.25}$$

where

$$\Omega_y(x,y,z,t) = \mathrm{i}U'(y)\tilde{\alpha}_0\sin\phi\,\mathrm{e}^{\mathrm{i}\tilde{\alpha}_0\cos\phi yT}\int_0^T v(x,y,z,\tau)\,\mathrm{e}^{-\mathrm{i}\tilde{\alpha}_0\cos\phi y\tau}\,\mathrm{d}\tau + \Omega_{y0}(x-Ut,y,z), \tag{5.26}$$

$$\Omega_\phi(x,y,z,t) = \Omega_{\phi 0}(x-Ut,y,z). \tag{5.27}$$

All three components of the vorticity field are expressed in terms of only two quantities, $\Omega_\phi$ and $\Omega_y$, where $\Omega_\phi$ is a conserved quantity in all layers. Thus, a unique vorticity-field solution corresponding to the initial delta function is determined once the initial value of the transverse vorticity $\Omega_y(x,y,z,0) = \Omega_{y0}$ is specified.

In the external layers $|y| > 1$, the basic velocity $U$ is constant, and its derivative vanishes. Thus, $\Omega_y(x,y,z,t) = \Omega_{y0}(x-Ut,y,z)$ and, from (5.11), all components of the vorticity field are conserved.

In the internal layer $|y| < 1$, the basic velocity $U = y$, and its derivative is constant. The growth of the disturbance vorticity in time depends on both $\tilde{\alpha}_0$ and $\phi$. For the cases $\phi = 0$ and $\frac{1}{2}\pi$,

$$\Omega_{y2}(x,y,z,t) = \Omega_{y0}(x-Ut,y,z) + \begin{cases} 0, & \phi = 0 \\ \mathrm{i}\frac{1}{2}\bar{\Omega}_0\, \mathrm{e}^{-\tilde{\alpha}_0|\bar{y}|}T, & \phi = \frac{1}{2}\pi. \end{cases} \tag{5.28}$$

When $\phi = 0$ and $w \equiv 0$, all components of the disturbance vorticity are conserved. When $\phi = 0$ but $w \neq 0$, $\Omega_x$ grows linearly in $T$ and the other two components are conserved as given by (5.22).

When $\phi = \frac{1}{2}\pi$ with arbitrary $u_0$, $\Omega_x$ is conserved but the other two components grow linearly in $T$ or

$$\begin{bmatrix} \Omega_x \\ \Omega_y \\ \Omega_z \end{bmatrix} = \tfrac{1}{2}\bar{\Omega}_0\, \mathrm{e}^{-\gamma_0|\bar{y}|} \begin{bmatrix} 0 \\ \mathrm{i}T \\ -\operatorname{sign}(\bar{y})\, T \end{bmatrix} + \begin{bmatrix} -\mathrm{i}(\bar{\Omega}_0/\gamma_0)\,\delta(\bar{y}) \\ \Omega_{y0} \\ -(\mathrm{i}/\gamma_0)\,\partial\Omega_{y0}/\partial y \end{bmatrix}, \tag{5.29}$$

where

$$\Omega_{y0}(y,z;y_0) = -(\mathrm{i}/\tilde{\alpha}_0)\,\bar{\Omega}_0\,\tilde{u}_0(y,y_0), \quad \bar{\Omega}_0 = \Omega_0\,\mathrm{e}^{-\mathrm{i}\gamma_0 z}$$

and $\tilde{u}_0(y,y_0)$ represents an arbitrary vertical structure of the initial velocity disturbance $u_0$. Although the streamwise disturbance vorticity stays constant for all time, the transverse and spanwise vorticity disturbances grow linearly. Thus, when nonlinearity becomes significant, the transverse vorticity disturbance may have tilted into the streamwise direction because of shearing in the basic flow. This is a possible origin of the existent streamwise vorticity disturbance suggested by the experimental study of Lasheras & Choi (1988) and the numerical study of Ashurst & Meiburg (1988). The stretching effect due to the basic shear velocity will intensify any non-zero streamwise vorticity when viscous effects are small. 'Vortex stretching is a physical mechanism for entrainment and production in all turbulent flow' (Hussain 1986).

When $0 < \phi < \frac{1}{2}\pi$, all three components of $\boldsymbol{\Omega}$ grow exponentially and/or algebraically in time depending on the value of $\tilde{\alpha}_0$ because $\Omega_y$ is the integral with $v$ as part of its integrand (5.26). The explicit expressions for $\Omega_y$ for various $\tilde{\alpha}_0$ are given by (4.31)–(4.34). For $\tilde{\alpha}_0 < \tilde{\alpha}_s \approx 0.64$ and $\Omega_y(x,y,z,0) \equiv 0$, all components of $\boldsymbol{\Omega}$ grow exponentially; for $\tilde{\alpha}_0 = \tilde{\alpha}_s$, all components of $\boldsymbol{\Omega}$ grow algebraically. When $\tilde{\alpha}_0 < \tilde{\alpha}_s$, $\Omega_y(x,y,z,0) \neq 0$ and is periodic in the $(x,z)$-plane, the expressions for $\Omega_x$ and $\Omega_z$ have terms that are linear and exponential in $T$.

The growing behaviour of the disturbance vorticity field depends on the wavenumber as well as the initial transverse vorticity component $\Omega_{y0}$. For the case of spanwise independence, all components are conserved when $\Omega_{y0} = w_0 = 0$ but the streamwise vorticity component grows algebraically in time when $\Omega_{y0} \neq 0$. This is different from the growth behaviour of the transverse velocity component, which is not affected by $\Omega_{y0}$ but grows either exponentially or algebraically in time depending on the streamwise wavenumber.

Figures 2–4 show comparison plots of the vorticity magnitudes as a function of time

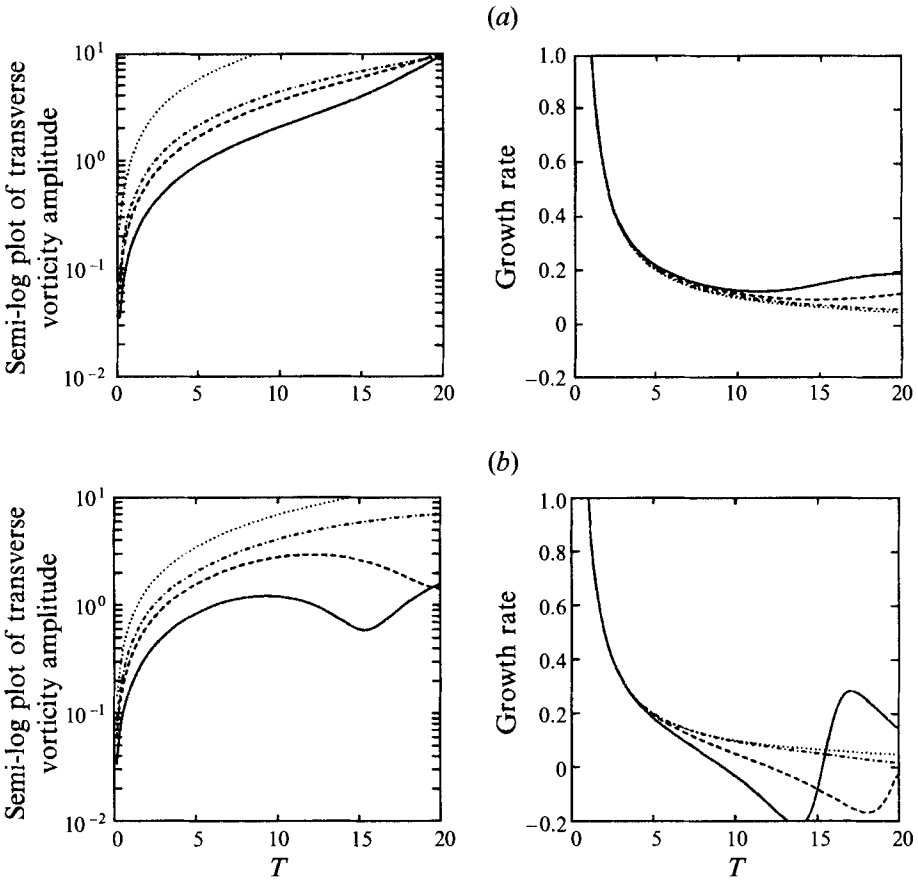


FIGURE 2. (*a*) $|\Omega_y|$ with $\tilde{\alpha}_0 = 0.4$ and $y_0 = 0.8$; (*b*) $|\Omega_y|$ with $\tilde{\alpha}_0 = \tilde{\alpha}_s$ and $y_0 = 0.8$. ——, $\phi = \frac{1}{8}\pi$; – – – –, $\phi = \frac{1}{4}\pi$; –·–·–·–, $\phi = \frac{3}{8}\pi$; ....., $\phi = \frac{1}{2}\pi$.

in semi-log graphs with growth rates defined as $\mathrm{d}\ln(|\Omega|)/\mathrm{d}T$, where $\Omega = \Omega_x$, $\Omega_y$ or $\Omega_z$. The vorticity field is calculated from (5.25), and in all cases $\Omega_{y0} = 0$ is fixed and $y = 1$. For a small value of the oblique angle with wavenumber magnitude less than the cut-off value and $\Omega_{y0} = 0$, all components of the vorticity field grow exponentially in time with the same exponential growth rate as the transverse velocity component but multiplied by small constants. As the oblique angle increases from zero, the transverse vorticity component also grows exponentially in time with the same exponential growth rate as the transverse velocity component but with increasing multiplicative constants; the other two vorticity components have the same exponential growth rate but with different multiplicative constants. As the oblique angle increases to $\frac{1}{2}\pi$, the exponential growth rate of the transverse velocity component and all components of the vorticity field tend to zero.

When the oblique angle equals $\frac{1}{2}\pi$, the transverse and spanwise vorticity components grow algebraically in time and the streamwise velocity component is conserved.

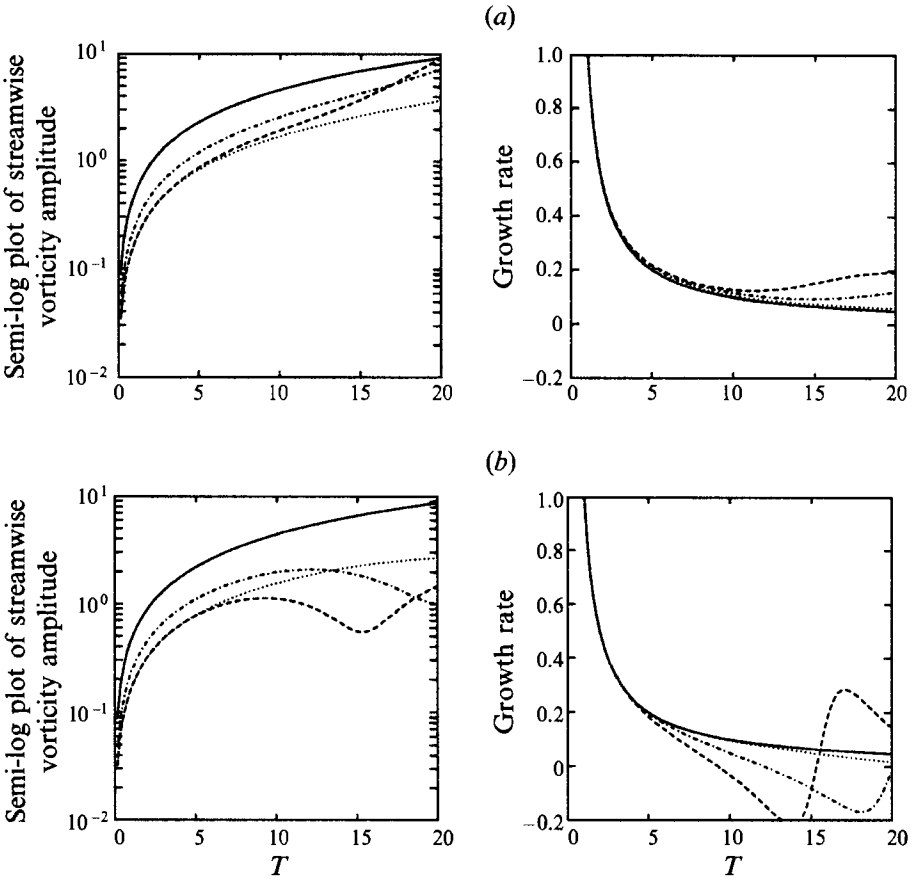


FIGURE 3. (*a*) $|\Omega_x|$ with $\tilde{\alpha}_0 = 0.4$ and $y_0 = 0.8$; (*b*) $|\Omega_x|$ with $\tilde{\alpha}_0 = \tilde{\alpha}_s$ and $y_0 = 0.8$. ——, $\phi = 0$ in (*b*), $\pi$ in (*a*); – – – –, $\phi = \frac{1}{8}\pi$; –·–·–·–, $\phi = \frac{1}{4}\pi$; ....., $\phi = \frac{3}{8}\pi$.

## 6. Evolution of disturbance energy

### 6.1. *Definition*

The kinetic energy for the disturbances as a volume integral over a finite domain in the $(x, z)$-plane and the infinite interval in the $y$-direction is defined as

$$E_K(T) = \frac{\alpha_0 \gamma_0}{2(2\pi)^2} \int_{-\infty}^{+\infty} \int_0^{2\pi/\alpha_0} \int_0^{2\pi/\gamma_0} (u^2 + v^2 + w^2)\, \mathrm{d}z\, \mathrm{d}x\, \mathrm{d}y, \tag{6.1}$$

where $\alpha_0$ and $\gamma_0$ are the wavenumbers of the periodic initial disturbance in the $x$- and $z$-directions respectively. Note that, when $v$ is periodic in the $(x, z)$-plane, it can be written as

$$v(x, y, z, t) = \mathrm{Re}\{\bar{v}(y, T)\, \mathrm{e}^{-\mathrm{i}\tilde{\alpha}_0(\cos\phi x + \sin\phi z)}\}.$$

Since the velocity field must satisfy the continuity equation, $u$ and $w$ must also be periodic in $x$ and $z$. The energy integral (6.1) can then be integrated with respect to the $x$ and $z$ variables leaving

$$E_K(T) = \frac{1}{2} \int_{-\infty}^{+\infty} (|\bar{u}|^2 + |\bar{v}|^2 + |\bar{w}|^2)\, \mathrm{d}y. \tag{6.2}$$

Solutions for the other two velocity components, $u$ and $w$, together with the initial

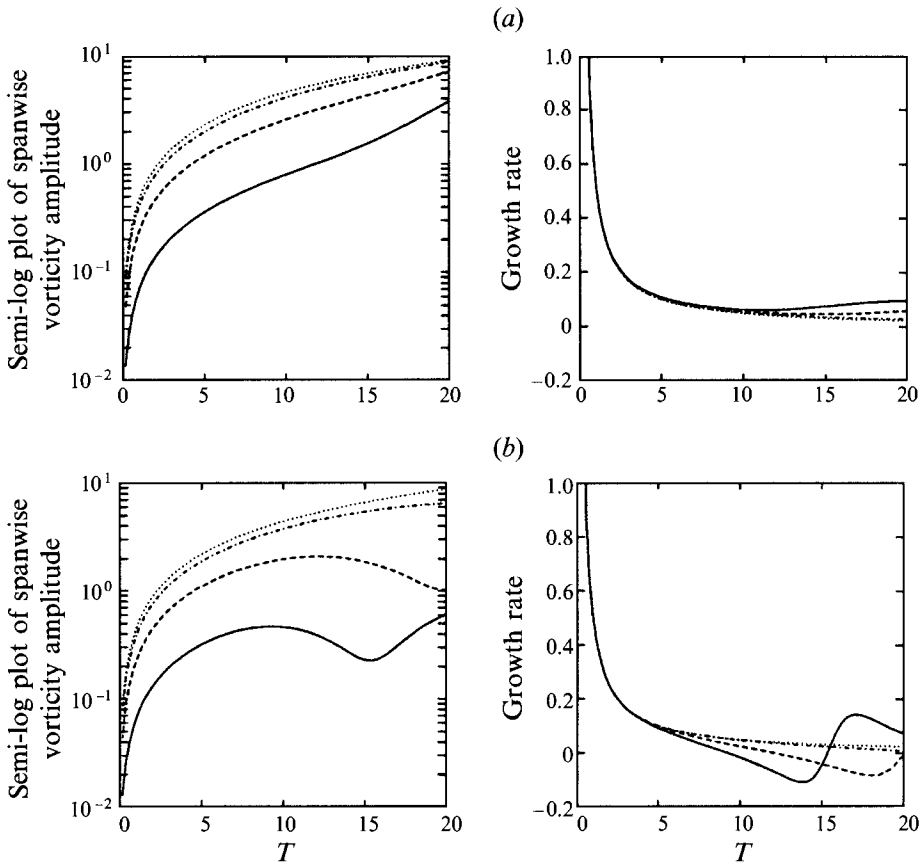


FIGURE 4. (a) $|\Omega_z|$ with $\tilde{\alpha}_0 = 0.4$ and $y_0 = 0.8$; (b) $|\Omega_z|$ with $\tilde{\alpha}_0 = \tilde{\alpha}_s$ and $y_0 = 0.8$. ——, $\phi = \frac{1}{8}\pi$; – – – – –, $\phi = \frac{1}{4}\pi$; – · – · – · –, $\phi = \frac{3}{8}\pi$; . . . . . , $\phi = \frac{1}{2}\pi$.

conditions must be specified in addition to $v$. However, it is more convenient mathematically to consider the initial specification of the transverse vorticity component $\Omega_y$ which is a combination of $u$ and $w$.

Since the velocity components $u$ and $w$ are expressed in terms of $v$ and $\Omega_y$, a unique velocity field solution is found by specifying $\Omega_{y0}(x, y, z)$ in addition to $v$. On using the expressions for $u$ and $w$ shown in (4.23) and (4.24),

$$E_K(T) = \frac{1}{2\tilde{\alpha}_0^2}\int_{-\infty}^{+\infty}\left(\tilde{\alpha}_0^2|v|^2 + \left|\frac{\partial v}{\partial y}\right|^2 + |\Omega_y|^2\right)\mathrm{d}y, \tag{6.3}$$

where the overbar has been dropped from all dependent variables. After integrating the second term of the integrand by parts in the external layers,

$$E_K(T) = \frac{1}{2\tilde{\alpha}_0^2}\left\{v_1^*\frac{\partial v_1}{\partial_y}\bigg|_{y=1}^{\infty} + v_3^*\frac{\partial v_3}{\partial y}\bigg|_{y=-\infty}^{-1} + \int_{-1}^{+1}\left(\tilde{\alpha}_0^2|v|^2 + \left|\frac{\partial v}{\partial y}\right|^2\right)\mathrm{d}y + \int_{-\infty}^{+\infty}|\Omega_y|^2\,\mathrm{d}y\right\}.$$

The solutions for $v$ in the external layers, $v_1$ and $v_3$, are expressed in terms of the solutions for $v$ in the internal layer, $v_2$, or

$$v_1(x, y, z, t) = v_2(x, y, z, t)|_{y=1}\,\mathrm{e}^{-\tilde{\alpha}_0(y-1)},$$
$$v_3(x, y, z, t) = v_2(x, y, z, t)_{y=-1}\,\mathrm{e}^{\tilde{\alpha}_0(y+1)},$$

and, since $v \to 0$ as $y \to \pm\infty$, the expression simplifies to

$$E_K(T) = \frac{1}{2\tilde{\alpha}_0^2}\left\{\operatorname{sign}(y)\,\tilde{\alpha}_0 v_2^* v_2|_{y=-1}^{1} + \int_{-1}^{+1}\left(\tilde{\alpha}_0^2|v|^2 + \left|\frac{\partial v}{\partial y}\right|^2\right)\mathrm{d}y + \int_{-\infty}^{+\infty}|\Omega_y|^2\,\mathrm{d}y\right\}. \quad (6.4)$$

Recall from (4.26) that

$$\Omega_y(x,y,z,t) = \mathrm{i}U'(y)\,\tilde{\alpha}_0 \sin\phi\, \mathrm{e}^{\mathrm{i}\alpha_0 y_T T}\int_0^T v(x,y,z,\tau)\,\mathrm{e}^{-\mathrm{i}\alpha_0 y_T}\,\mathrm{d}\tau + \Omega_{y0}(x-Ut,y,z). \quad (6.5)$$

Thus, with the $x$–$z$ periodic solution, the kinetic energy can be expressed in terms of $v_2$ and $\Omega_{y0}$ as shown in (6.4) and (6.5). This implies that the asymptotic behaviour of the kinetic energy is dominated by the asymptotic behaviour of $v_2$. However, the transient behaviour depends on both $v_2$ and $\Omega_{y0}$ as well as the initial wavenumber and angle of obliquity and the structure of the initial values in the $y$-direction.

### 6.2. *Two-dimensional planar motion*

In the special case for which the oblique angle of the initial wavenumber and the spanwise velocity component are zero, two-dimensional planar motion results. Since $\phi = 0$, $\Omega_y = \mathrm{i}\alpha_0 w$, and so $\Omega_y = 0$. From the initial delta-function solution (4.7) for $v$, the integrand (6.4) of the kinetic energy integral has only one finite discontinuity at $y = y_0$. On integrating by parts,

$$E_K(T) = \frac{1}{2\alpha_0^2}\left\{v_2^*\left(\frac{\partial v_2}{\partial y} + \operatorname{sign}(y)\,\alpha_0 v_2\right)\Big|_{y=-1}^{1} + \int_{-1}^{+1} v^*\left(\alpha_0^2 v - \frac{\partial^2 v}{\partial^2 y}\right)\mathrm{d}y\right\}. \quad (6.6)$$

From the initial delta-function solution for $v$,

$$\alpha_0^2 v - \partial^2 v/\partial^2 y = 2\alpha_0\,\delta(\bar{y})\,v^{(r)}.$$

After employing this expression and integrating,

$$E_K(T) = \frac{v_2^*}{2\alpha_0^2}\left(\frac{\partial v_2}{\partial y} + \operatorname{sign}(y)\,\alpha_0 v_2\right)\Big|_{y=-1}^{1} + \frac{1}{\alpha_s}v_2^*(y=y_0)\,v_2^{(r)}(y=y_0). \quad (6.7)$$

With the implicit expression for the Green's function, solution (4.3) for $v_2$,

$$E_K(T) = (\Omega_0^2/4\alpha_0^3) + \alpha_0\,\mathrm{e}^{4\alpha_0}(|\bar{B}|^2 + |\bar{C}|^2) + 2\alpha_0\,\mathrm{Re}\,[\tilde{B}\tilde{C}^*\,\mathrm{e}^{2\alpha_0} + \bar{V}_0^*\,\mathrm{e}^{\alpha_0 - \mathrm{i}\alpha_0 y_0 t}(\tilde{B}\,\mathrm{e}^{-\alpha_0 y_0} + \tilde{C}\,\mathrm{e}^{\alpha_0 y_0})]. \quad (6.8)$$

The kinetic energy expression for the solution corresponding to the initial top-hat function is

$$E_K(T) = \alpha_0\,\mathrm{e}^{4\alpha_0}(|\bar{B}|^2 + |\bar{C}|^2) + 2\alpha_0\,\mathrm{Re}\left\{\tilde{B}\tilde{C}^*\,\mathrm{e}^{2\alpha_0} + \bar{V}_0^*\,\mathrm{e}^{\alpha_0 - \mathrm{i}\alpha_0 y_0 t}\left(\tilde{B}\frac{\sin(\epsilon\beta_1)}{\epsilon\beta_1}\mathrm{e}^{-\alpha_0 y_0} + \tilde{C}\frac{\sin(\epsilon\beta_2)}{\epsilon\beta_2}\mathrm{e}^{\alpha_0 y_0}\right)\right\} + \frac{\Omega_0^2}{4^2\alpha_0^3\epsilon^2\beta_1^2\beta_2^2}[4\alpha_0\epsilon\beta_1\beta_2 + \beta_1^2(1-\mathrm{e}^{-\mathrm{i}2\epsilon\beta_2}) + \beta_2^2(1-\mathrm{e}^{\mathrm{i}2\epsilon\beta_1})], \quad (6.9)$$

where $\bar{B}, \bar{C}$ for the delta-function solution and the top-hat function solution are given by (4.5) and (4.13) respectively; $\tilde{B} = \bar{B}\mathrm{e}^{\mathrm{i}\alpha_0 t}$, $\tilde{C} = \bar{C}\mathrm{e}^{-\mathrm{i}\alpha_0 t}$, $\bar{V}_0^* = (\Omega_0/2\alpha_0)\,\mathrm{e}^{\mathrm{i}(\alpha_0 x + \gamma_0 z)}$ and $\beta_{1,2} \equiv \alpha_0(T \pm \mathrm{i})$.

By taking the limit of (6.9) as $\epsilon \to 0$, the same expression for $E_K(T)$ as (6.8) results. Closed-form expressions for $\bar{B}$ and $\bar{C}$ for the solution corresponding to the initial delta

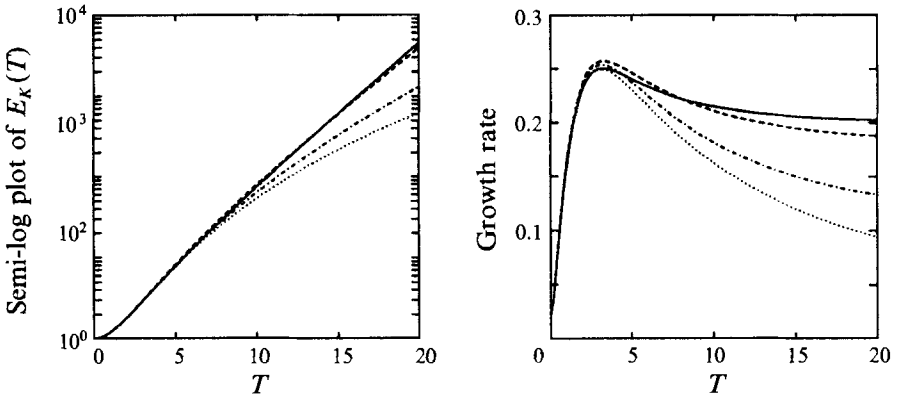


FIGURE 5. $E_K$ for the initial delta function: $\phi = 0$, $\Omega_{y0} \equiv 0$ and $y_0 = 0$. ——, $\tilde{\alpha}_0 = 0.4$; – – – – –, $\tilde{\alpha}_0 = 0.5$; –·–·–·–·–, $\tilde{\alpha}_0 = 0.6$; ....., $\tilde{\alpha}_0 = \tilde{\alpha}_s$.

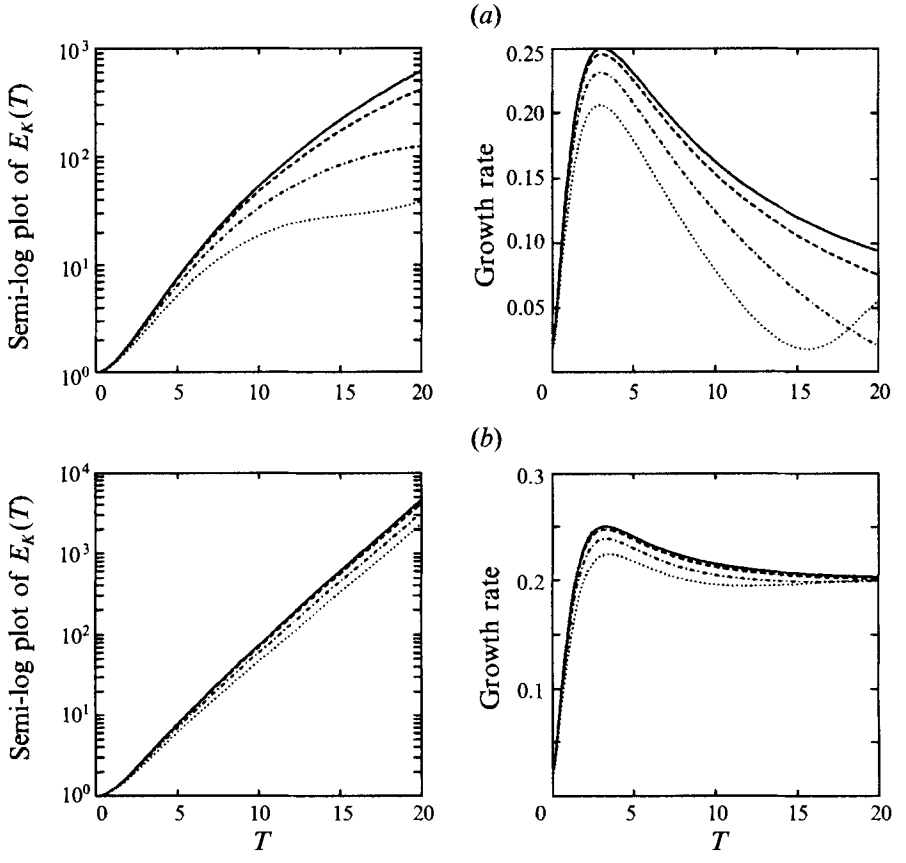


FIGURE 6. $E_K$ for the initial delta function: $\phi = 0$, $\Omega_{y0} \equiv 0$ and (*a*) $\tilde{\alpha}_0 = \tilde{\alpha}_s \approx 0.64$ and (*b*) $\tilde{\alpha}_0 = 0.4$. ——, $y_0 = 0$; – – – – –, $y_0 = 0.2$; –·–·–·–·–, $y_0 = 0.4$; ....., $y_0 = 0.6$.

function are available. However, numerical integration techniques have been used to compute the solution corresponding to the initial top-hat function.

The kinetic energy for both the initial delta function and the top-hat function solutions depends on $T$ and the two parameters $y_0$ and $\alpha_0$. The energy for the top-hat

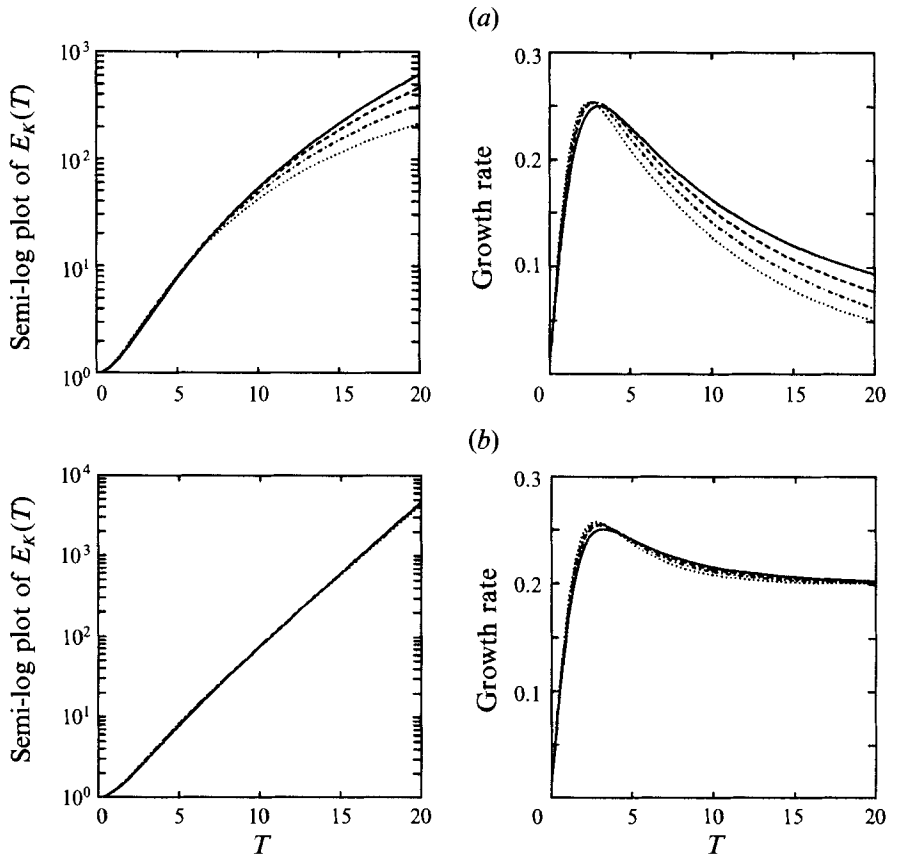


FIGURE 7. $E_K$ for the initial delta and top-hat functions at $y_0 = 0$: (*a*) $\alpha_0 = \alpha_s$; (*b*) $\alpha_0 = 0.4$. ——, initial delta function; – – – – –, initial top-hat function with $\epsilon = 0.2$; –·–·–·–·–, initial top-hat function with $\epsilon = 0.3$; ....., initial top-hat function with $\epsilon = 0.4$.

function contains the additional parameter $\epsilon$. The following discussion is based on plots of $E_K(T)$ normalized by $E_K(0)$ versus $T$ in the semi-log graph and their growth rates as defined by $\frac{1}{2}(\mathrm{d}/\mathrm{d}T)\log\{E_K(T)\}$; the kinetic energies are calculated from the analytical expressions (6.8) and (6.9).

Comparison plots of $E_K$ corresponding to the initial delta function for various $\alpha_0$ and $y_0 = 0$ are shown in figure 5. As can be seen, the growth rates of these disturbances approach the asymptotic behaviour that is the normal mode at large $T$ except when $\alpha_0 = \alpha_s$, where the energy increases algebraically.

Comparison plots of $E_K$ corresponding to the initial delta function for various $y_0$ are shown in figure 6 for two fixed initial wavenumbers: $\alpha_0 = \alpha_s \approx 0.64$ and $\alpha_0 = 0.4$. The largest magnitude of the energy occurs when $y_0 = 0$.

Comparison plots of $E_K$ for the initial delta function and the initial top-hat function solutions that grow algebraically ($\alpha_0 = \alpha_s \approx 0.64$) are shown in figure 7(*a*). This figure illustrates that, as $\epsilon \to 0$, the energy for the top-hat function solution approaches that for the initial delta function. Also, as seen from the graphs, when $y_0$ moves away from zero, the $E_K$ for the initial delta function grows at a slower rate than that for the top-hat function. Although $y_0 = 0$ is nothing special physically, it is special for the initial delta function because it is the location of the singularity.

For $\alpha_0 = 0.4$, the results are shown in figure 7(*b*). The growth of the energy for the

solutions corresponding to the initial top-hat function are almost the same as that for the initial delta function, regardless of the value of $\epsilon$.

The growth rates of the energy for all cases rapidly increase in the early period of its evolution. For the energy corresponding to the solution with purely exponentially growing behaviour, the growth rate rapidly rises above its asymptotic exponential growth rate, then rapidly decreases toward this asymptotic value. During this transient time, for which the growth rate is rapidly changed, its energy, as well as the energy for all other cases, reach a level approximately ten times their initial values.

### 6.3. *Three-dimensional disturbance as a single oblique mode*

From the initial delta-function solution (4.7), the expression for the kinetic energy corresponding to the full three-dimensional solution is

$$E_K(T) = \frac{v_2^*}{2\tilde{\alpha}_0^2}\left(\frac{\partial v_2}{\partial y} + \operatorname{sign}(y)\,\tilde{\alpha}_0 v_2\right)\Big|_{y=-1}^{1} + \frac{1}{\tilde{\alpha}_s} v_2^*(y = y_0)\, v_2(y = y_0) + \frac{1}{2\tilde{\alpha}_0^2}\int_{-\infty}^{+\infty} |\Omega_y|^2 \,\mathrm{d}y. \tag{6.10}$$

The initial value of the energy is

$$E_K(0) = \frac{\Omega_0^2}{4\tilde{\alpha}_0^3} + \frac{1}{2\tilde{\alpha}_0^2}\int_{-\infty}^{+\infty} |\Omega_{y0}(x, y, z)|^2 \,\mathrm{d}y. \tag{6.11}$$

For large $T$ and $\tilde{\alpha}_0 < \tilde{\alpha}_s$, the solution (4.15) for $v$ is dominated by the exponential term,

$$v(x, y, z, t) \sim (\bar{\Omega}_0/2\tilde{\alpha}_0)\, C_2\, \mathrm{e}^{-\mathrm{i}\omega_0 T} \quad \text{as} \quad T \to \infty, \tag{6.12}$$

where

$$-\mathrm{i}\omega_0 = \tfrac{1}{2}\cos\phi[\mathrm{e}^{-4\tilde{\alpha}_0} - (1 - 2\tilde{\alpha}_0)^2]^{1/2}. \tag{6.13}$$

By using the kinetic energy expression (6.10) together with the solution for $\Omega_y$ that depends on $v$ and (6.12), the asymptotic behaviour of the energy for the oblique wave solution approaches the exponentially growing behaviour predicted by the normal mode solution when $\tilde{\alpha}_0 < \tilde{\alpha}_s$. By examining the dependency of the solution in terms of the oblique angle $\phi$, it is found that the growth rate (6.13) has a factor $\cos\phi$ and is maximum at $\phi = 0$. The factor $\cos\phi$ of the exponential growth rate is the key argument that proves the Squire's theorem: $\phi = 0$ and $\frac{1}{2}\pi$ are the maximum and minimum growth rates respectively.

For the case $\phi = 0$ and $y_0 = 0$, $\Omega_{y0}(x, y) = \operatorname{Re}\{\mathrm{i}\alpha_0 w_0(x, y)\} = \operatorname{Re}\{\mathrm{i}\alpha_0 \mathrm{e}^{-\mathrm{i}\alpha_0 x}\bar{w}_0(y)\}$ where $\bar{w}_0$ is an arbitrary function of $y$. The kinetic energy for this case is

$$E_K(T) = \frac{\Omega_0^2}{4\alpha_0^3}\{1 + (\mathrm{e}^{-4\alpha_0} + \mathrm{e}^{-3\alpha_0}\sinh\alpha_0)\, T^2 + \mathrm{e}^{-7\alpha_0}\cosh\alpha_0 \tfrac{1}{4}T^4\} + \frac{1}{2}\int_{-\infty}^{+\infty} |w|^2 \,\mathrm{d}y, \tag{6.14}$$

where $w(x, y, t) = w_0(x - Ut, y)$. Since $w_0$ is periodic in the $x$-direction and of the form $w_0(x, y) = \operatorname{Re}\{\mathrm{e}^{-\mathrm{i}\alpha_0 x}\bar{w}_0(y)\}$, $|w|^2 = |\bar{w}_0(y)|^2$. Therefore, the last term in (6.14) is constant in $T$ and the growth of the kinetic energy is the same for any choice of the streamwise-periodic initial condition, $\Omega_{y0}(x, y)$.

For the case,

$$\phi = \tfrac{1}{2}\pi, \Omega_{y0}(x, y) = \operatorname{Re}\{-\mathrm{i}\gamma_0 u_0(y, z)\} = \operatorname{Re}\{-\mathrm{i}\gamma_0 \mathrm{e}^{-\mathrm{i}\gamma_0 z}\bar{u}_0(y)\},$$

where $\bar{u}_0$ is an arbitrary function of $y$. The kinetic energy for this case is

$$E_K(T) = \frac{\Omega_0^2}{4\gamma_0^3}\{1 + \tfrac{1}{2}(1 - \mathrm{e}^{-2\gamma_0}\cosh(2\gamma_0 y_0))\, T^2\} + \int_{-1}^{+1} \bar{u}_0 v^* T \,\mathrm{d}y + \frac{1}{2}\int_{-\infty}^{+\infty} |\bar{u}_0|^2 \,\mathrm{d}y. \tag{6.15}$$

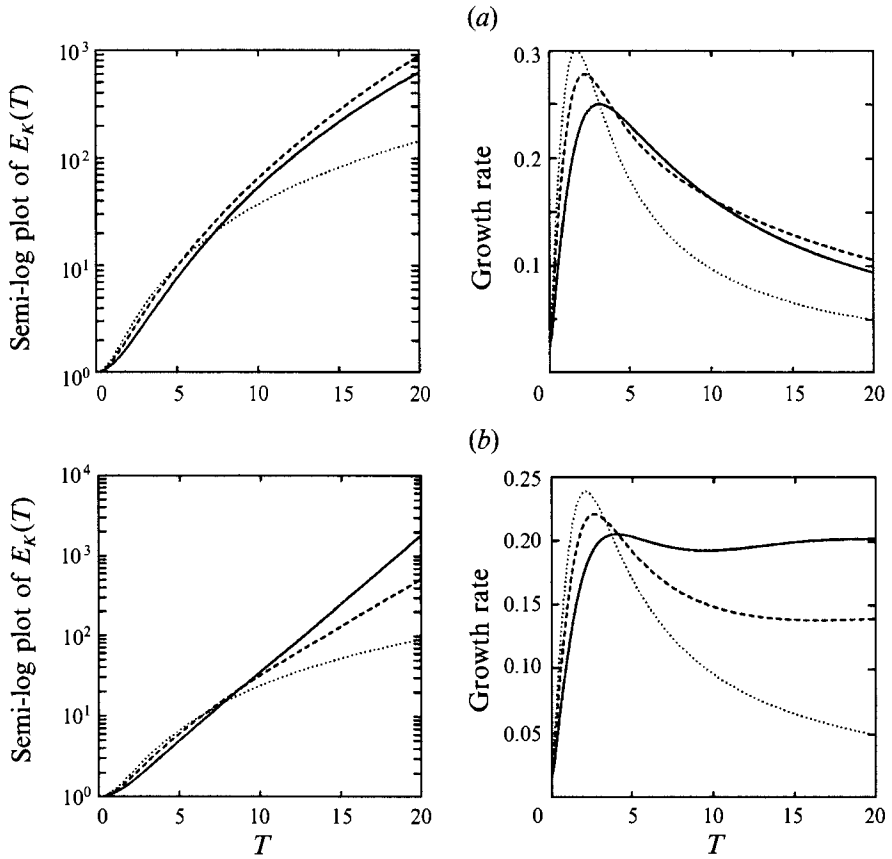


FIGURE 8. $E_K$ for the initial delta function at $\Omega_{y0} \equiv 0$ and $y_0 = 0$: (*a*) $\tilde{\alpha}_0 = \tilde{\alpha}_s$; (*b*) $\Omega_{y0} \equiv 0$. ——, $\phi = 0$; – – – – –, $\phi = \frac{1}{4}\pi$; . . . . . , $\phi = \frac{1}{2}\pi$.

From the first integral of (6.15), which is of order $T$, the structure of $u_0$ affects the transient behaviour of the disturbance kinetic energy but not the asymptotics.

In the transient period, for the case of $\Omega_{y0} = 0$, the growth rate of the energy corresponding to $\phi = 0$ is smaller than that corresponding to $\phi = \frac{1}{2}\pi$, as seen from the kinetic energy expressions (6.14) and (6.15) for the case $\tilde{\alpha}_0 = \tilde{\alpha}_s$ and $y_0 = 0$. As $\phi$ increases from 0 to $\frac{1}{2}\pi$, the growth rate of the disturbance energy increases because the growth of $\Omega_y$ increases. This is in contrast to Squire's theorem. The same comparison results also hold for the case $0 < \tilde{\alpha}_0 < \tilde{\alpha}_s$, as a power series expansion for small $T$ reveals.

The comparison plot of the kinetic energy for the initial delta function corresponding to the solution that grows algebraically in $T$ is shown in figure 8(*a*). The initial wavenumber is $\alpha_0 = \alpha_s$, $\Omega_{y0} = 0$ and the initial pulse is placed at $y_0 = 0$. Various values of the oblique angle illustrate that, in the transient period as $\phi$ increases from 0 to $\frac{1}{2}\pi$, the growth rate of the disturbance energy increases. Similar results are shown for the case where the solution grows exponentially in $T$ (figure 8*b*); the initial wavenumber is $\alpha_0 = 0.4$, $\Omega_{y0} = 0$. Figure 8(*b*) also illustrates that the asymptotic behaviour of the energy approaches the purely exponentially growing behaviour predicted by the normal mode analysis and, as $\phi$ decreases from $\frac{1}{2}\pi$ to 0, the growth rate increases.

Three-dimensional plots of the energy versus wavenumber magnitude, $\tilde{\alpha}_0$, and oblique angle, $\phi$, at some fixed time, $T$, are shown in figure 9. In the early period of the

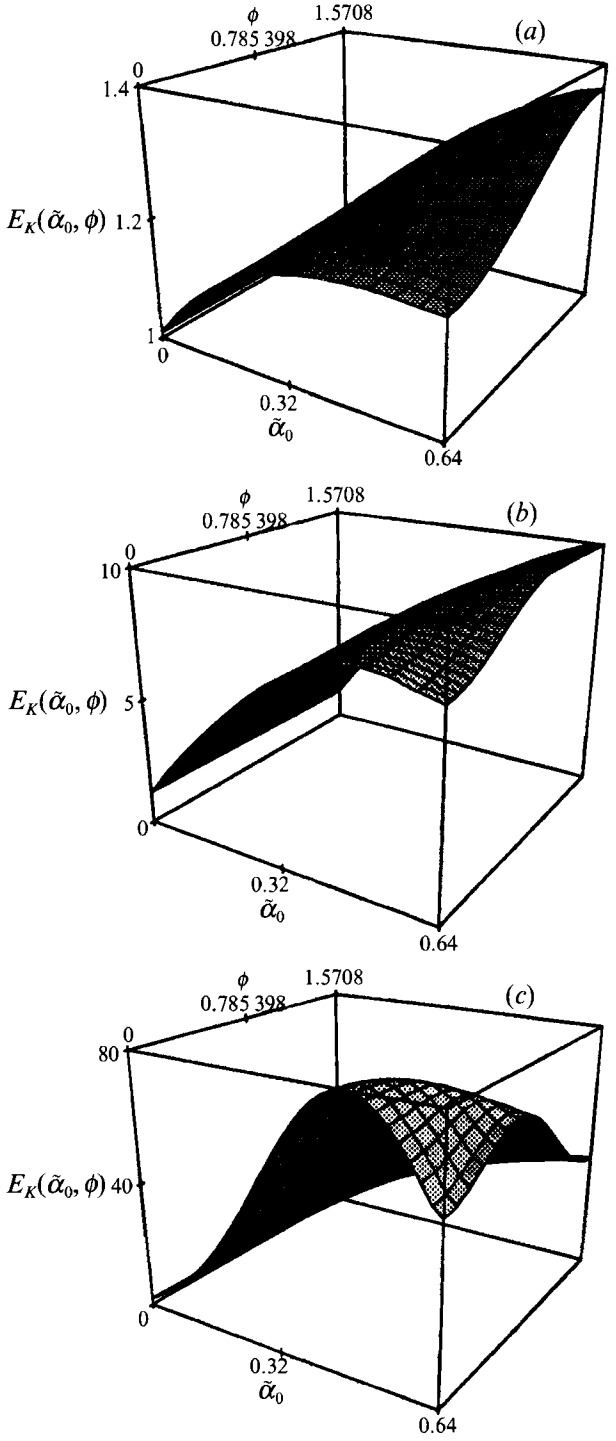


FIGURE 9. $E_K$ versus $\tilde{\alpha}_0$ and $\phi$ for various $t$: (*a*) $t = 1$, (*b*) $t = 5$ and (*c*) $t = 10$.

evolution, $T = 1$, as $\phi$ increases, the energy also increases for all $\tilde{\alpha}_0 > 0$. For later time, such as $T = 5$, the energy level is approximately the same for all values of $\phi$ and $\tilde{\alpha}_0$ except for larger values of $\tilde{\alpha}_0$ when the energy still increases as $\phi$ changes. When $T = 10$, the exponentially growing behaviour becomes strong, and the plot shows that the highest level of the energy occurs at $\tilde{\alpha}$ approximately equal to 0.4 and $\phi = 0$.

In summary, the asymptotic behaviour of the streamwise–spanwise-periodic disturbance can be either exponential or algebraic in time, depending on the value of the wavenumber $\tilde{\alpha}_0$ and the oblique angle $\phi$. The exponentially growing asymptotic behaviour is dominated by the normal mode for which the Squire's theorem is applicable where $\phi = 0$ and $\frac{1}{2}\pi$ give the maximum and minimum growth rates respectively. Contrary to Squire's theorem, in the early period, the maximum and minimum growth rates are at $\phi = \frac{1}{2}\pi$ and $\phi = 0$ and the growth rate changes rapidly. For the disturbance energy corresponding to exponential behaviour, the growth rate rapidly increases and rises above, and then rapidly decreases to, the asymptotic value. During this transient time for which the growth rate is rapidly changing, its energy as well as the energy for all other cases reach the level of about ten times their initial values. Thus, during this transient time, the disturbances may grow to large enough amplitudes and nonlinearity can become significant and the normal modes become moot.

## 7. Evolution of material particles

### 7.1. *Particle path formulation*

One of the natural extensions of particle mechanics is the Lagrangian viewpoint in fluid mechanics. Each particle, as it moves through the flow, is labelled by its original position $\boldsymbol{x}_0$ and the particle path is governed by

$$\mathrm{d}\boldsymbol{x}(t)/\mathrm{d}t = \boldsymbol{u}(\boldsymbol{x}, t), \tag{7.1}$$

$$\boldsymbol{x}(0) = \boldsymbol{x}_0, \tag{7.2}$$

where $\boldsymbol{x}(t)$ is the position of the particle; $\boldsymbol{u}(\boldsymbol{x}, t)$ is the velocity field that includes both the basic flow and the disturbance or

$$\boldsymbol{u}(x, y, z, t) = U(y)\,\boldsymbol{e}_1 + \boldsymbol{u}'(x, y, z, t). \tag{7.3}$$

In all cases, the initial disturbance that corresponds to the delta function with vanishing initial transverse vorticity ($\Omega_{y0} = 0$) is used. Thus, the initial disturbance with a single mode is

$$\nabla_0^2 v'(x, y, z, 0) = \Omega_0\,\delta(y)\,\mathrm{e}^{-\mathrm{i}\tilde{\alpha}_0(\cos\phi x + \sin\phi z)} \quad \text{and} \quad \Omega_y'(x, y, z, 0) = 0.$$

With an analytical solution for the velocity field known for all time and given the initial position of a particle, (7.1) can be integrated to find the new position of the particle at later time. Since the velocity of the particles depends on both particle positions and time, a system of nonlinear non-autonomous first-order differential equations results, making an analytical solution virtually impossible to find. On the other hand, numerical integration of (7.1) with any given initial condition (7.2) is straightforward. A simple Runge–Kutta fourth-order method is used to approximate the solution of the system for several thousand particles initially placed in the mixing layer.

### 7.2. *Two-dimensional planar motion of the mixing layer*

The two-dimensional planar motion of the mixing layer is known to roll up if the wavelength of a streamwise periodic disturbance is much larger than the layer thickness. In the case of temporal evolution of the mixing layer, a normal mode

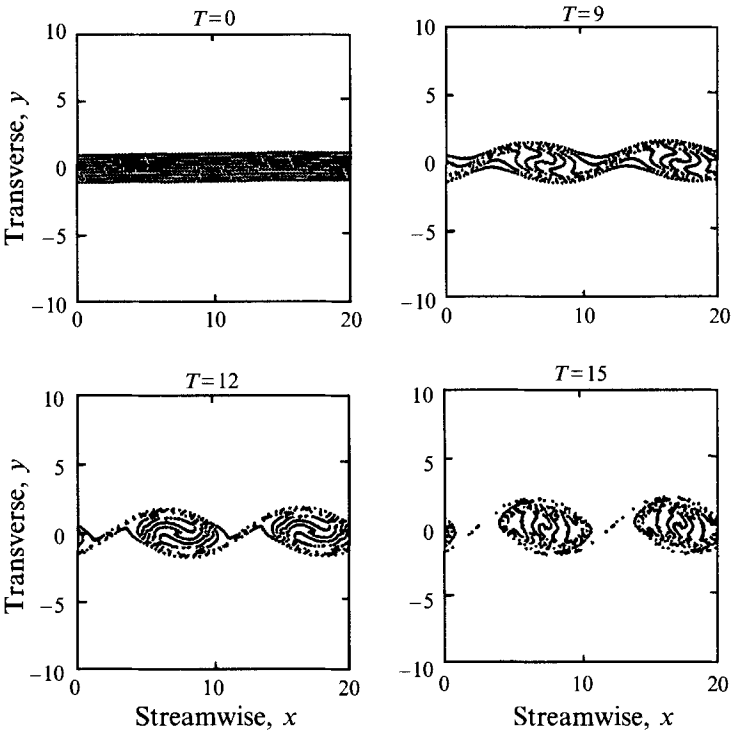


FIGURE 10. Material particles, $\phi = 0$, $E_K(0) = 0.01$ and $\tilde{\alpha}_0 = \tilde{\alpha}_s \approx 0.64$.

disturbance that is streamwise periodic would grow and lead to the layer roll up in the nonlinear regime of the flow evolution. The streamwise wavenumber $\alpha_0$ of the normal mode for which the disturbance grows at a maximum rate exponentially in time is in the range $0 < \alpha_0 < \alpha_s$. The particle path technique described above was used by Michalke (1965) to illustrate the initial roll-up of the mixing layer due to the growth of the normal mode disturbances. The basic velocity profile was taken to be $\tanh y$ and the velocity field was computed numerically. However, with the neutral wavenumber $\alpha_0 = \alpha_s$, such a disturbance does not grow and it was concluded that roll-up of the mixing layer could occur only if the initial wavenumber was in the range of amplification.

It can be recalled that the solution having a streamwise periodic non-normal mode disturbance with wavenumber equal to the neutral wavenumber of the normal mode the disturbance grows algebraically in time. It will be seen that the evolution of the mixing layer using the particle path formulation with algebraic growth and $\alpha_0 = \alpha_s$ also leads to roll-up of the layer (figure 10). The initial disturbance kinetic energy is set to $E_K(0) = 0.01$. The value was chosen to expedite the process in the same manner as done by direct numerical simulations. A smaller initial value for $E_K(0)$ gives in the same result but is slower in evolution.

With the initial wavenumber corresponding to the fastest exponential growth, the initial roll-up of the mixing layer is illustrated in figure 11. The plots do not show the round shape characteristic of concentrated lumps of particles at $T = 15$ as seen in the case of a larger wavenumber (figure 10). This suggests that a nonlinear model of the system with the analytical velocity field is not fully correct at large times because the velocity field solution is based on an assumption of small disturbances. To see this the velocity field is shown in figures 12 and 13. Clearly, disturbance amplitudes are larger

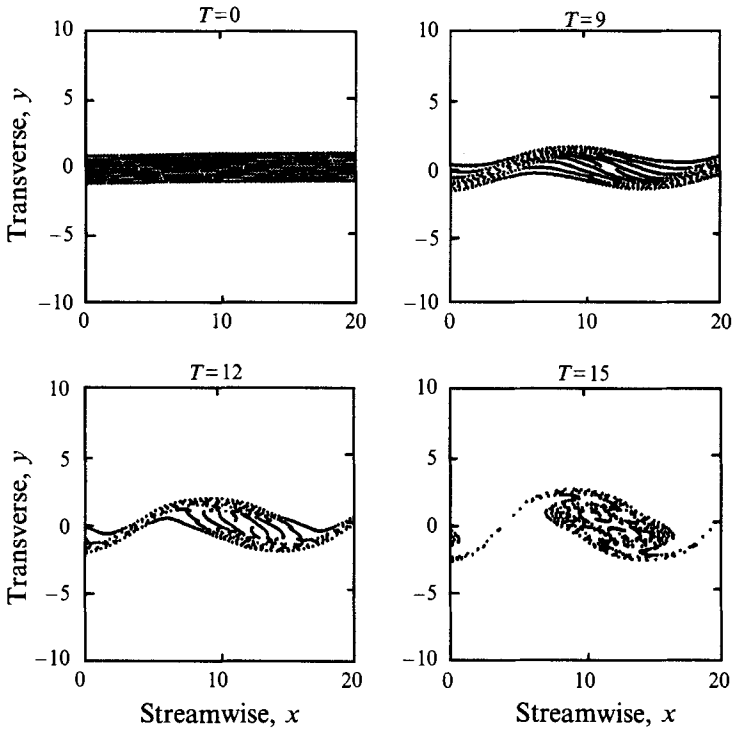


FIGURE 11. Material particles, $\phi = 0$, $E_K(0) = 0.01$ and $\tilde{\alpha}_0 = 0.4$.

than the mean flow at large time ($T = 15$), violating the small-amplitude assumption. Nevertheless, the implications are strong.

Although at large time the model equations are not valid because of the small-amplitude assumption of the velocity field, the sequence of plots at different times for particle positions do show the motion of the evolution of the mixing layer that is valid at small time. The periodic disturbance (larger wavenumber than the normal mode) that grows algebraically in time has also been demonstrated to trigger the roll-up of the mixing layer and is just as efficient as the strongest growing normal mode.

### 7.3. *Three-dimensional disturbance with oblique modes*

The evolution of particles initially placed at the two interfaces of the piecewise linear profile are traced together with the material lines going through all the material particles with the same initial positions in $x$ and $y$ and are shown in the top rows of figures 14, 15 and 16. The particles are initially placed at the two surfaces $y = 1$ and $y = -1$ in the domain $-10 < x < 30$ and $-5 < z < 25$. However, at all $T$, only the particles and lines that are in the box $0 < x < 20$, $-5 < y < 5$ and $0 < z < 20$ are actually plotted.

In all cases, the initial disturbance that grows algebraically in time ($\tilde{\alpha}_0 = \tilde{\alpha}_s$) is taken. Figure 14(*a–c*) shows the evolution of the particles for the case of $\phi = 0$. The particles evolve in the two-dimensional planar motion, but are plotted in three dimensions. The developed structures are elliptical cylinders with the perpendicular cross-section in the $(x, z)$-plane. These cylinders reveal the spanwise vortices that have no variation in the $z$-direction. The material lines are always straight and parallel to the axes of the cylinders for all $T$.

The evolution of the particles for the case of $\phi = \frac{1}{2}\pi$ is shown by figure 14(*d–f*). As

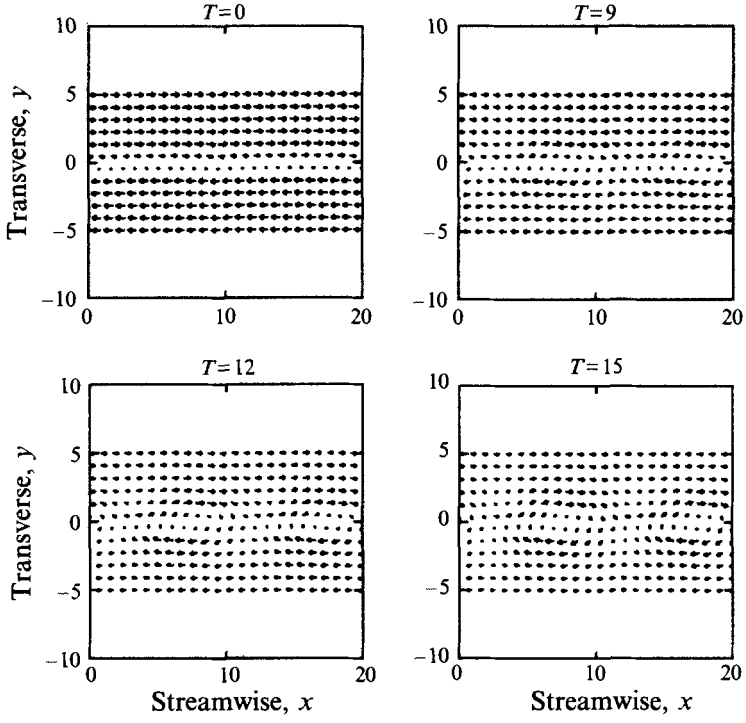


FIGURE 12. Velocity field, $\phi = 0$, $E_K(0) = 0.01$ and $\tilde{\alpha}_0 = \tilde{\alpha}_s \approx 0.64$.

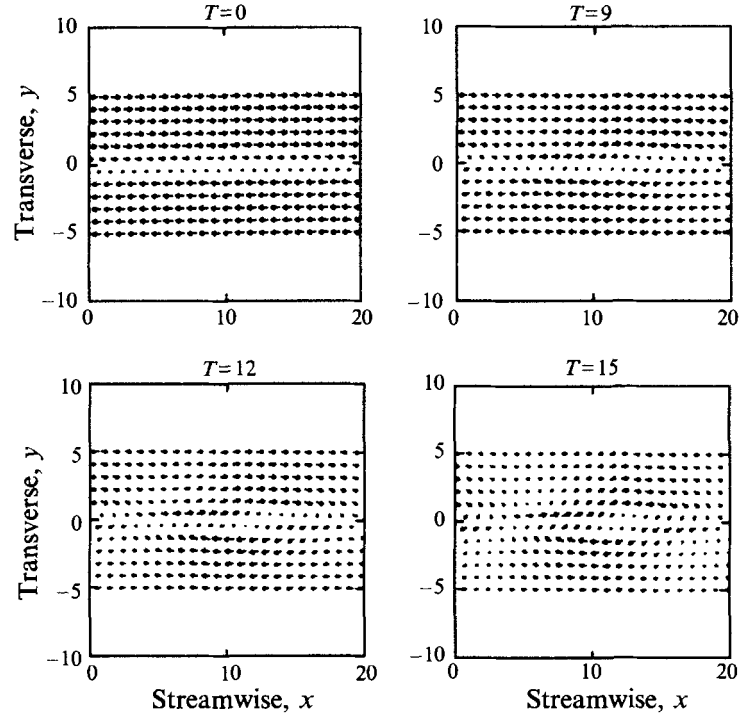


FIGURE 13. Velocity field, $\phi = 0$, $E_K(0) = 0.01$ and $\tilde{\alpha}_0 = 0.4$.

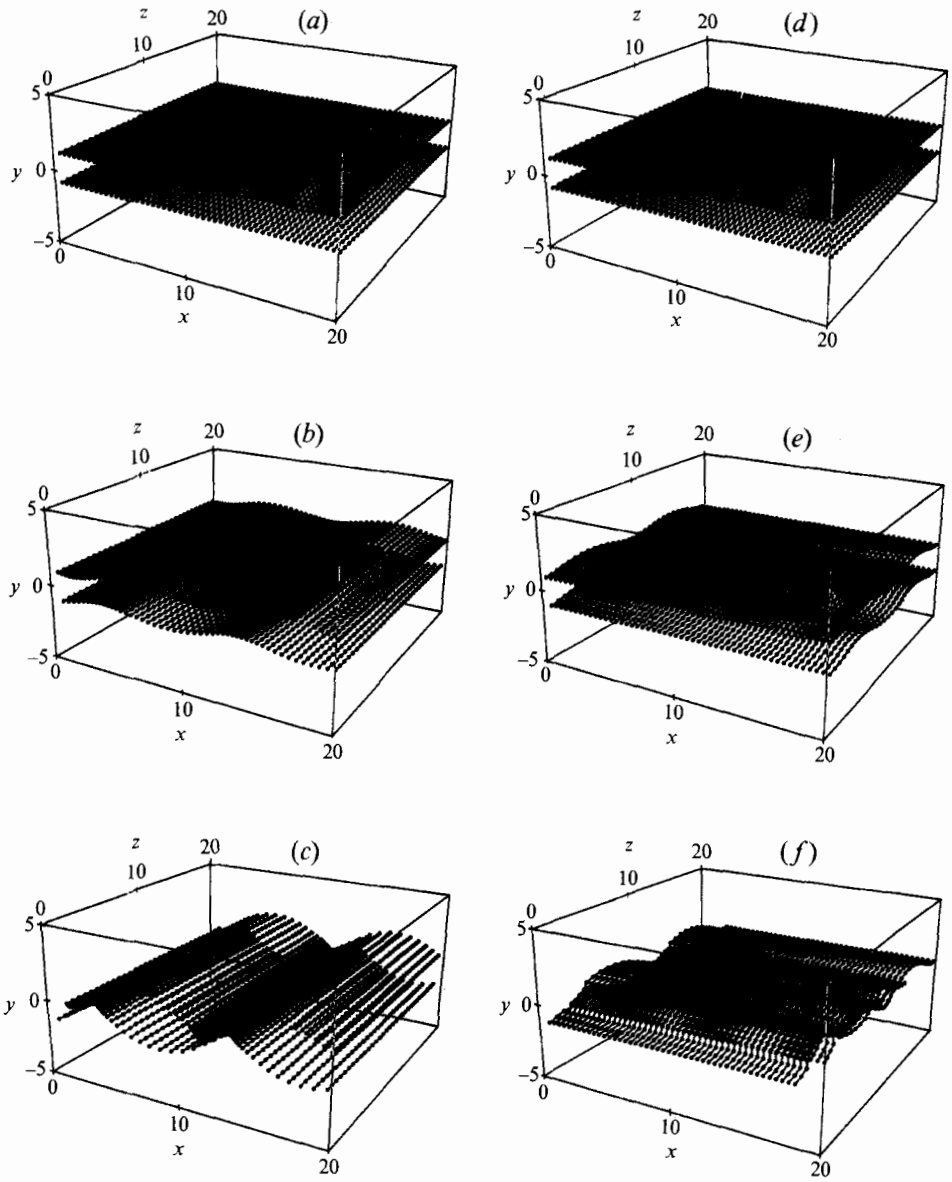


FIGURE 14. Three-dimensional graphs of the particles, single mode, $E_K(0) = 0.01$. ($\tilde{\alpha}_0 = \tilde{\alpha}_s, \phi = 0$): (*a*) $t = 0$, (*b*) $t = 6$ and (*c*) $t = 12$; ($\tilde{\alpha}_0 = \tilde{\alpha}_s, \phi = \frac{1}{2}\pi$): (*d*) $t = 0$, (*e*) $t = 6$ and (*f*) $t = 12$.

seen in the graph, none of the material lines at all $T$ has virtually any variation in the $x$-direction. Thus, the particles with the same initial position in $x$ and $y$ moved at almost the same speed in the $x$-direction. This result may be explained as follows. The initial disturbance, as well as the velocity field at all time, are independent of the streamwise direction. Only the streamwise velocity component grows linearly in $T$; the other two components are independent of $T$. The growth rate of $u$ is proportional to the magnitude of the transverse velocity component $v$ which attains its maximum value at the transverse position $y = 0$ and decays exponentially in the $y$-direction. Consider the particles that are initially connected by one of the initial material lines. As some of these move in the transverse direction away from one of the interfaces into the internal

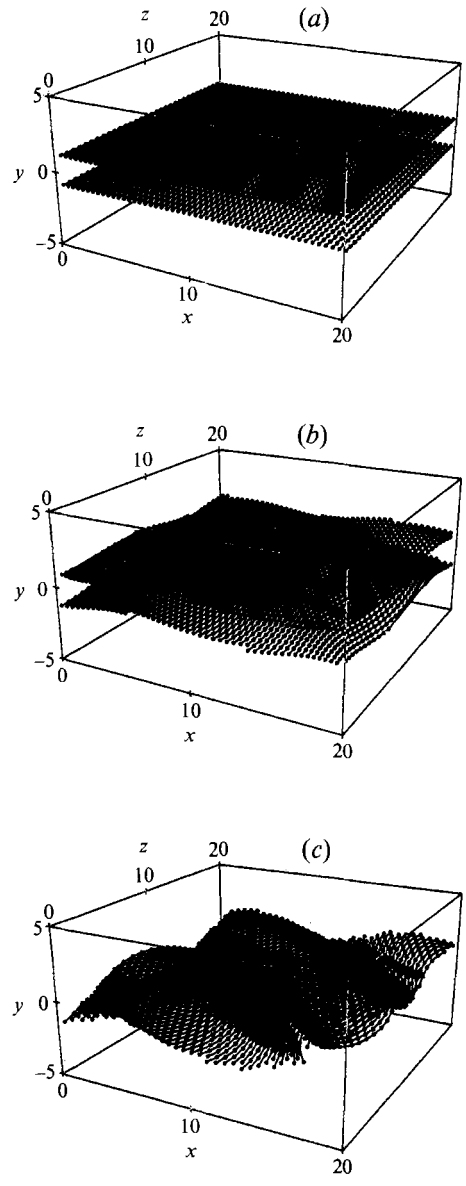


FIGURE 15. Three-dimensional graphs of the particles, single mode, $E_K(0) = 0.01$. ($\tilde{\alpha}_0 = \tilde{\alpha}_s, \phi = \frac{1}{4}\pi$): (*a*) $t = 0$, (*b*) $t = 6$ and (*c*) $t = 12$.

layer the magnitude of the basic flow decreases but the magnitude of the disturbance velocity grows in the same direction as the basic flow. The total streamwise velocity component at the new positions in the internal layer is almost the same as that that is near the interfaces and those particles that move into one of the external layers because the basic flow in the external layers is constant, and $u$ grows slower as the particles move away vertically from $y = 0$.

Figure 15(*a–c*) shows the evolution of the material particles and lines for the case of $\phi = \frac{1}{4}\pi$. The three-dimensional graphs show that the initial two flat surfaces of the material particles evolve into cylindrical structures with the axes in the $(x, z)$-plane in the direction 45° off the $x$-axis. Unlike the case of the two-dimensional planar motion

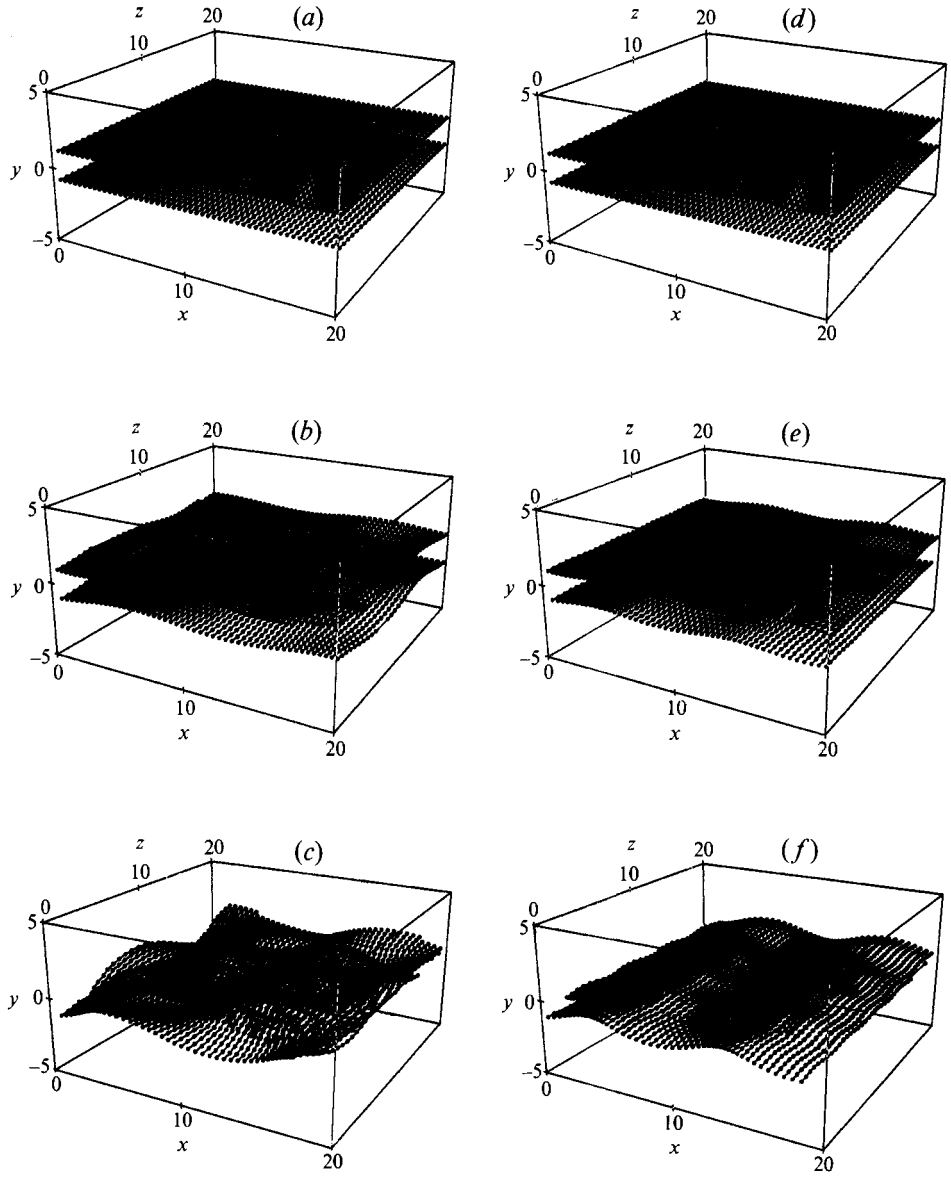


FIGURE 16. Three-dimensional graphs of the particles, two modes, $E_K(0) = 0.01$. ($\tilde{\alpha}_0 = \tilde{\alpha}_s, \phi = \frac{1}{4}\pi$) and ($\tilde{\alpha}_0 = \tilde{\alpha}_s, \phi = -\frac{1}{4}\pi$): (*a*) $t = 0$, (*b*) $t = 6$ and (*c*) $t = 12$; ($\tilde{\alpha}_0 = \tilde{\alpha}_s, \phi = 0$) and ($\tilde{\alpha}_0 = 2\tilde{\alpha}_s, \phi = \frac{1}{2}\pi$): (*d*) $t = 0$, (*e*) $t = 6$ and (*f*) $t = 12$.

$\phi = 0$ where the material lines are always straight and parallel to the axes of the cylindrical vortices, no material lines in this case lie in any one plane. The evolution is affected by the three-dimensionality of the velocity field.

The developed structure arising from a single mode of the periodic disturbance is a row of single oblique vortices. The developed structure arising from two equal and opposite oblique modes is more complex. Figure 16(*a–c*) shows the evolution of the material particles for the case of $\phi = \frac{1}{4}\pi$ for which the initial condition is

$$\nabla_0^2 v'(x, y, z, 0) = \Omega_0 \delta(y)\{e^{-i\tilde{\alpha}_0(\cos\phi x + \sin\phi z)} + e^{-i\tilde{\alpha}_0(\cos\phi x - \sin\phi z)}\}$$

and

$$\Omega_y'(x, y, z, 0) = 0.$$

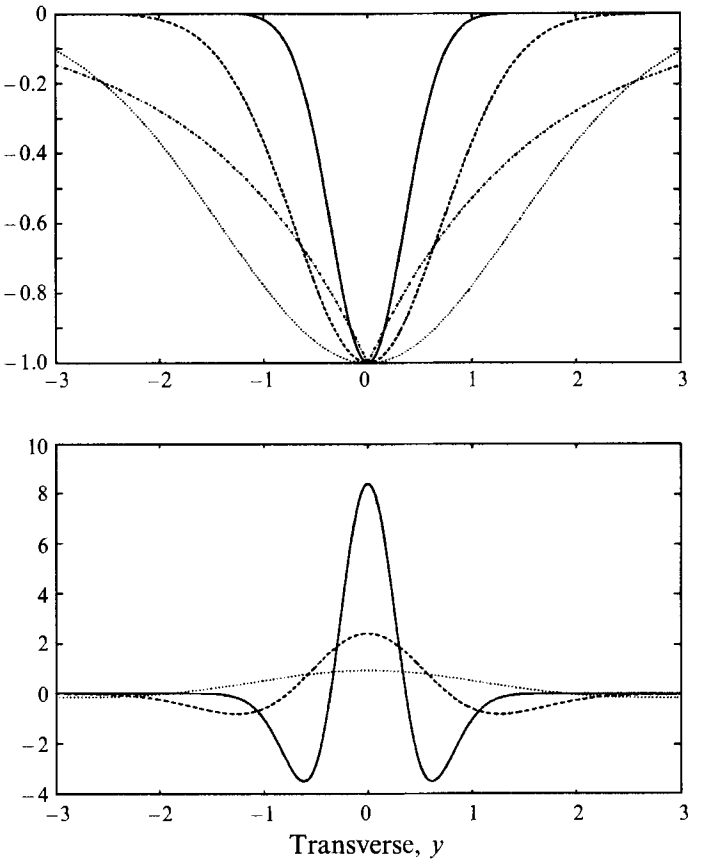


FIGURE 17. Symmetric $v_0(y)$, $\phi = 0$, $\tilde{\alpha}_0 = \tilde{\alpha}_s$, $x = z = 0$, $v_0 = -e^{-y^2/\lambda}$ with various $\lambda$: ——, $\lambda = 0.25$; – – – – –, $\lambda = 1$; . . . . . , $\lambda = 4$; –·–·–·–·–, $v_0 = e^{-\tilde{\alpha}_s|y|}$ or $\nabla^2 v_0 = 2\tilde{\alpha}_s \delta(y)$.

The developed structures are peak–valley surfaces with peaks and valleys alternating. The peaks and the valleys are loci of constant $z$, a distance $\pi/\tilde{\alpha}_0$ apart.

Figure 16(*d–f*) shows the evolution of the material particles and lines for the cases when the initial disturbance is the sum of two modes: $\tilde{\alpha}_0 = \tilde{\alpha}_s$, $\phi = 0$ and $\tilde{\alpha}_0 = 2\tilde{\alpha}_s$, $\phi = \frac{1}{2}\pi$. The initial disturbance satisfies

$$\nabla_0^2 v'(x, y, z, 0) = \Omega_0 \delta(y)(e^{-i\alpha_0 x} + e^{-i\gamma_0 z}) \quad \text{and} \quad \Omega_y'(x, y, z, 0) = 0.$$

The amplitudes of the two modes in the initial disturbance are equal, but the wavenumbers for the $x$-independent mode are twice that of the $z$-independent mode, i.e. $\gamma_0 = 2\alpha_0$. The developed structure is two undulant surfaces which are periodic in the $x$- and $z$-directions with wavenumbers $\tilde{\alpha}_s$ and $2\tilde{\alpha}_s$ respectively. The two surfaces have a tendency to evolve into elliptical cylinders with perpendicular cross-sections in the $(x, y)$-plane that wiggle in the $z$-axis.

## 8. Symmetric and asymmetric initial conditions

### 8.1. *Solutions in terms of the Green's function*

In Fourier space, the solution with the general initial condition is expressed as

$$\check{v} = \Omega_0 \delta(\alpha - \alpha_0) \delta(\gamma - \gamma_0) \int_{\infty}^{-\infty} \check{G}(\eta; y_0; \alpha; \gamma; T) f(y_0) \, dy_0, \tag{8.1}$$

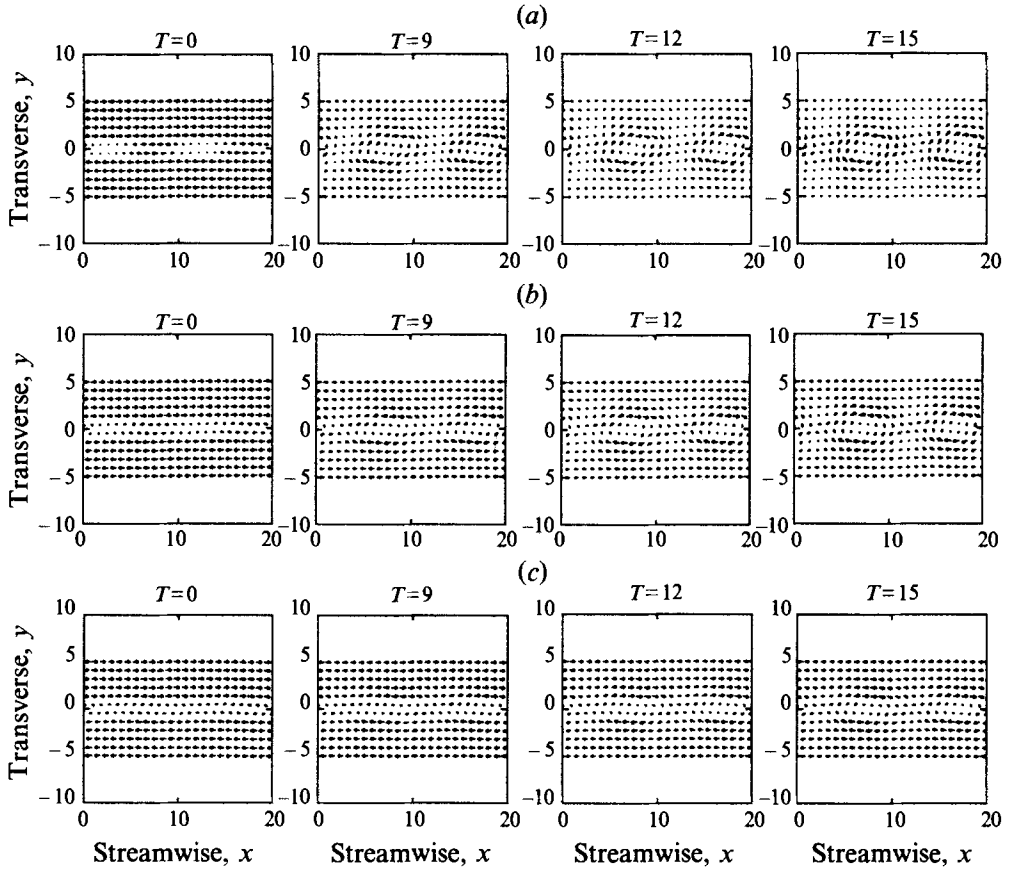


FIGURE 18. Velocity field for symmetric $v_0(y)$: (*a*) $\lambda = 0.25$, (*b*) $\lambda = 1$, (*c*) $\lambda = 4$.

where $f(y_0)$ is a more general variation and $\check{G}$ is the Green's function. After performing the full Fourier inversion, the solution will be

$$v(x,y,z,t) = \int_{\infty}^{-\infty} v_\delta(x,y,z,t;y_0) f(y_0)\,\mathrm{d}y_0, \tag{8.2}$$

where $v_\delta$ is given by (4.15) or the solution to the initial-value problem with the initial condition satisfying

$$\nabla^2 v_\delta(x,y,z,0) = \bar{\Omega}_0\,\delta(y-y_0). \tag{8.3}$$

Similarly, the transverse vorticity component is expressed as

$$\Omega_y(x,y,z,t) = \Omega_{y0}(x-Ut,y,z) + \int_{\infty}^{-\infty} \Omega_{\delta y}(x,y,z,t;y_0) f(y_0)\,\mathrm{d}y_0, \tag{8.4}$$

where $\Omega_{\delta y}$ is the transverse vorticity solution to the initial-value problem with the initial condition satisfying (8.3) and arbitrary initial condition $\Omega_y(x,y,z,0) = \Omega_{y0}(x,y,z)$.

The streamwise and spanwise velocity components which are expressed in terms of $v$ and $\Omega_y$ become

$$u = -\frac{\mathrm{i}}{\tilde{\alpha}_0}\left\{\cos\phi \int_{\infty}^{-\infty} \frac{\partial v_\delta(x,y,z,t;y_0)}{\partial y} f(y_0)\,\mathrm{d}y_0 - \sin\phi\,\Omega_y\right\}, \tag{8.5}$$

$$w = -\frac{\mathrm{i}}{\tilde{\alpha}_0}\left\{\sin\phi \int_{\infty}^{-\infty} \frac{\partial v_\delta(x,y,z,t;y_0)}{\partial y} f(y_0)\,\mathrm{d}y_0 + \cos\phi\,\Omega_y\right\}. \tag{8.6}$$

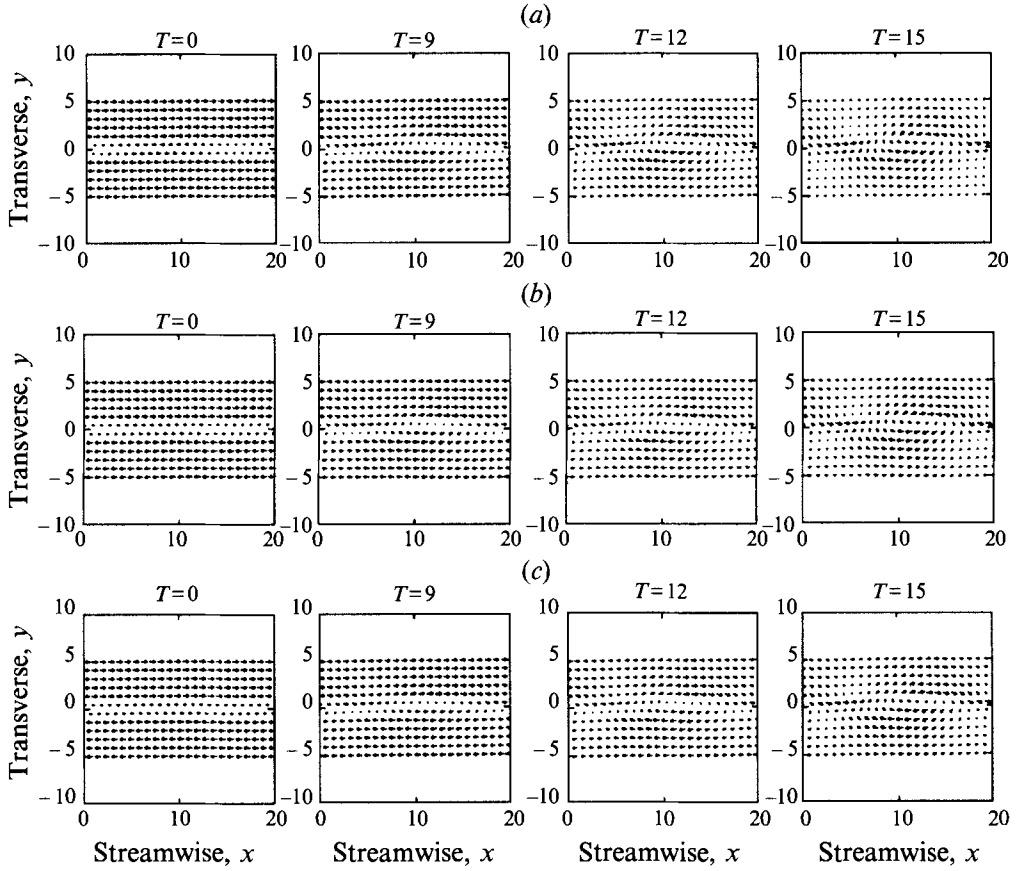


FIGURE 19. Velocity field for symmetric $v_0(y)$: (*a*) $\lambda = 0.25$, (*b*) $\lambda = 1$, (*c*) $\lambda = 4$.

In all cases, the maximum value of $v_0$ is taken to be 0.1 and equals 10% of the basic flow magnitude in the external layers; such a value is taken to expedite the temporal development and a smaller value ultimately evolves in the same way as this choice. For all calculations of the velocity field, the solutions (8.2) and (8.4) are numerically evaluated. Since the integrands are smooth and have a single scale, the simplest numerical integration method can be used, namely the extended trapezoidal rule. The limits of the integration are taken to be $\pm 3$ as an approximation to $\pm\infty$ since the function $f(y)$ that was used is approximately zero at $|y| \geqslant 3$.

### 8.2. *Symmetric transverse structure in* $v_0$

The implicit form of $v$ corresponding to the initial condition (4.1) with $f(y)$ being a top-hat function was shown in §4. Here, a family of the symmetric transverse structure for the initial value of $v$ is chosen to be a Gaussian centred at $y = 0$, namely

$$v_0 \equiv v(x, y, z, 0) = \bar{\Omega}_0 \, \mathrm{e}^{-y^2/\lambda}. \tag{8.7}$$

The plots of (8.7) in the domain of $-3 < y < 3$ for fixed values of $\Omega_0$, $\tilde{\alpha}_0$, $x$ and $z$ for various value of $\lambda$ are shown in figure 17. In this figure the corresponding function $f(y)$ or the transverse variation of $\nabla^2 v_0$ is also depicted.

The evolution of the velocity field for two-dimensional planar motion is shown in figure 18(*a–c*) for the wavenumber $\alpha_0 = \alpha_s$ and, in figure 19(*a–c*), for the wavenumber $\alpha_0 = 0.4$.

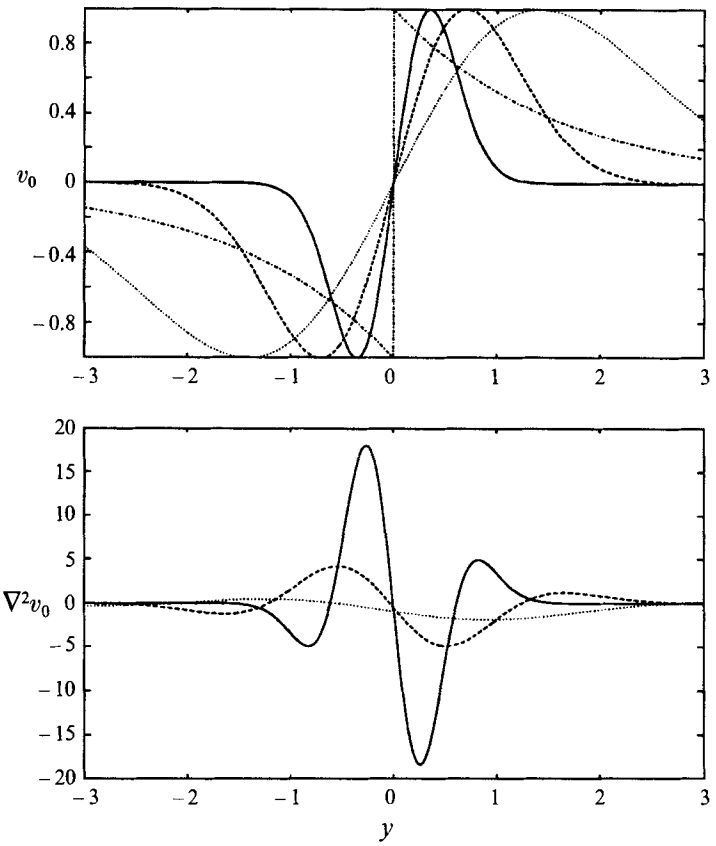


FIGURE 20. Asymmetric, $\phi = 0$, $\tilde{\alpha}_0 = \tilde{\alpha}_s$, $x = z = 0$, $v_0 = -e^{-y^2/\lambda}$ with various $\lambda$: ——, $\lambda = 0.25$; – – – – –, $\lambda = 1$; ......, $\lambda = 4$; –·–·–·–·–, $v_0 = e^{-\tilde{\alpha}_s|y|}$ or $\nabla^2 v_0 = 2\tilde{\alpha}_s \delta(y)$.

On comparing these fields, it can be seen that the formation of the vortices begins sooner for smaller standard deviation, $\lambda$, for the case $\alpha_0 = \alpha_s$. However, in the case $\alpha_0 = 0.4$, the time for the formation of the vortices is insensitive to the variation of $\lambda$.

### 8.3. *Asymmetric transverse structure in* $v_0$

A family of the asymmetric transverse structure for the initial value of $v$ is

$$v_0 \equiv v(x, y, z, 0) = \bar{\Omega}_0 (2e/\lambda)^{1/2} y \, e^{-y^2/\lambda}. \tag{8.8}$$

The plots of $v_0$ for the fixed values of $\Omega_0$, $\alpha_0$, $x$ and $z$ and the corresponding function $f(y)$ for various values of $\lambda$ are shown in figure 20.

The evolution of the velocity field for the two-dimensional planar motion is shown in figure 21(*a–c*) for the wavenumber $\alpha_0 = \alpha_s$ and figure 22(*a–c*) for wavenumber $\alpha_0 = 0.4$. Similar results to those in the previous section are apparent. The formation of the vortices begins sooner for smaller $\lambda$ for the case $\alpha_0 = \alpha_s$. In the case $\alpha_0 = 0.4$, the time for the formation of the vortices is still insensitive to the variation of $\lambda$.

From the continuity equation, the asymmetric transverse structure of $v_0$ implies a symmetric transverse structure of $u_0$. Conversely, the symmetric transverse structure of $v_0$ in the previous section implies an asymmetric transverse structure of $u_0$. It can be seen from the two sets of results for which the initial amplitude of $v_0$ has the same maximum value and the same $\lambda$, that the roll-up of the mixing layer for the asymmetric

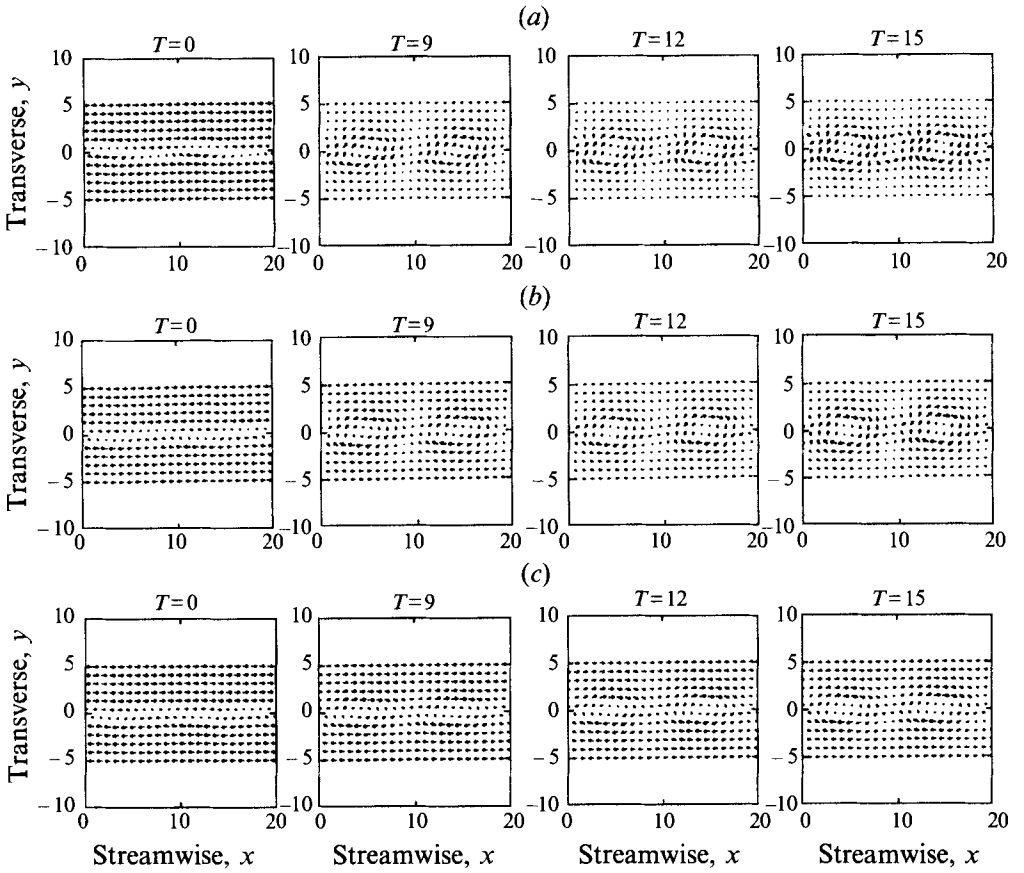


FIGURE 21. Velocity field for asymmetric $v_0(y)$: (*a*) $\lambda = 0.25$, (*b*) $\lambda = 1$, (*c*) $\lambda = 4$.

$v_0$ occurs sooner than that of the symmetric one because the growth rate of the disturbance for the asymmetric case is greater in the transient period.

## 9. Conclusions

The complete three-dimensional solution to the initial-value problem that combines both the discrete and continuous spectra has been obtained for disturbances in a mixing layer. These solutions, which are periodic in the streamwise–spanwise plane, represent descriptions of three-dimensional disturbances that contain both exponential and algebraic dependence on time. While the asymptotic behaviour of these disturbances is dominated by the exponentially growing normal mode, the transient is controlled by algebraic growth. In the transient period, the growth rates are comparable for all wavenumbers and such growth can lead to strong nonlinearity that can cause the breakdown of the flow before normal mode domination.

Without any assumption on the travelling wave solution, it was shown that the application of Squire's theorem to obtain the solution for a three-dimensional problem from its corresponding two-dimensional one could be incorrect because the theorem does not cover the dynamical behaviour governed by the $y$-component of the vorticity, equation (3.31). For example, if the disturbance is streamwise independent, then $\check{v}$ is independent of time and integrating (3.31) for the solution for $\hat{\Omega}_y$ indicates linear

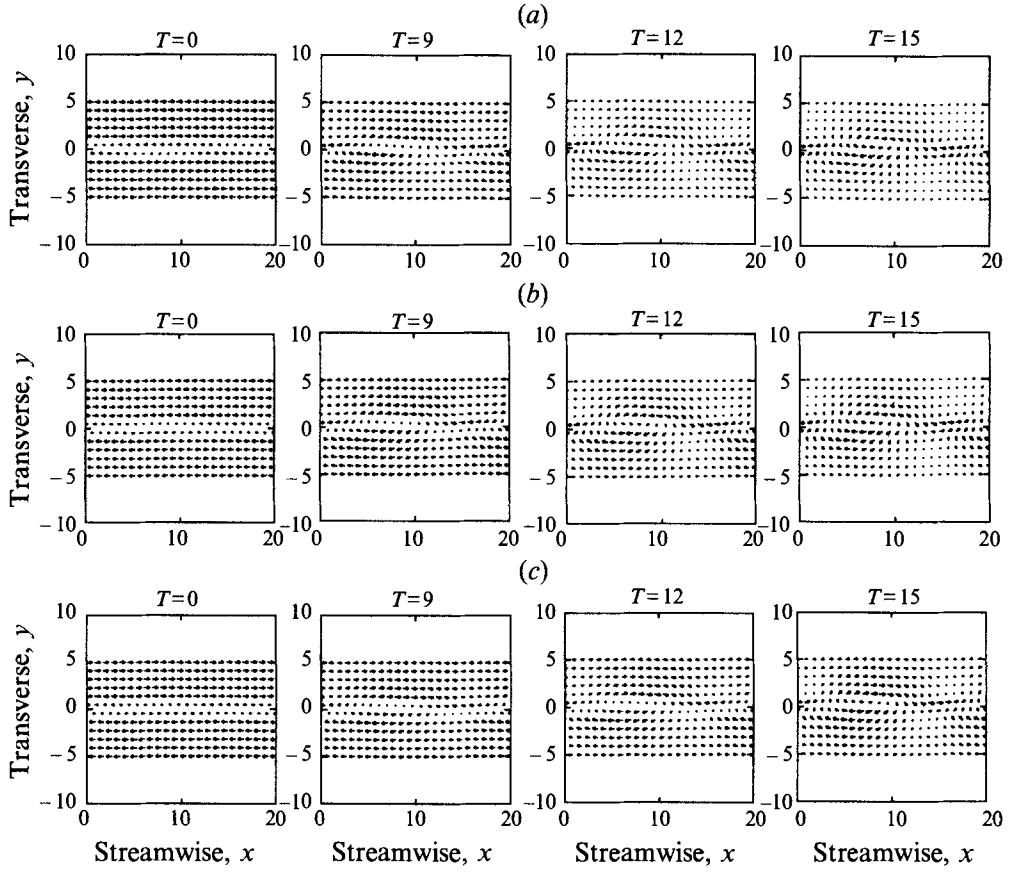


FIGURE 22. Velocity field for asymmetric $v_0(y)$: (*a*) $\lambda = 0.25$, (*b*) $\lambda = 1$, (*c*) $\lambda = 4$.

growth in time. Thus, for a three-dimensional problem, both (3.30) and (3.31) must be considered. Moreover, the theorem is not valid for non-separable disturbances such as these.

From the closed-form solution of the transverse velocity component, the exponentially growing normal mode dominates the long-time behaviour. Consequently, Squire's theorem is applicable in the limit and, with a fixed wavenumber magnitude, the oblique angle at values 0 and $\frac{1}{2}\pi$ gives the maximum and minimum growth rates respectively. However, the expressions for the streamwise and spanwise velocity components of the periodic disturbances are in terms of the transverse velocity and vorticity components as shown in (4.23) and (4.24). The disturbance kinetic energy is an integral with integrand that combines both the transverse velocity and vorticity components. As the oblique angle increases with a fixed wavenumber magnitude, the growth rate of the transverse velocity amplitude decreases but the growth rate of the transverse vorticity amplitude increases in the early period of the evolution. Thus, in the transient period, the growth rates of the streamwise and spanwise velocity amplitudes and the kinetic energy do not have the maximum value when the oblique angle equals zero.

Contrary to Squire's theorem, the energies corresponding to different wavenumbers of the periodic disturbance grow at comparable rates in the transient period. In fact, in the early period as the oblique angle increases from 0 to $\frac{1}{2}\pi$, the growth rate increases

(figures 8 and 9). The growth rate of the energy corresponding to the exponentially growing mode rapidly increases initially, then rapidly decreases asymptotically to a constant value that is equal to the growth rate of the corresponding normal mode. For a fixed wavenumber magnitude and oblique angle and during this transient time for which the growth rate is rapidly changing, the energy of this disturbance rises to a level approximately ten times its initial value.

The complete closed-form solution given in §4 is purely algebraic when the initial disturbance is independent of the streamwise variable (the streamwise velocity component is linear in $T$), which is in agreement with the result of Ellingsen & Palm (1975). This solution is also purely algebraic when the initial wavenumber magnitude is equal to the cut-off value; exponential growth can exist only if the wavenumber magnitude is smaller than the cut-off value. For the two-dimensional problem (independent of $z$) with planar motion ($w = 0$), the streamwise and transverse disturbance vorticities are conserved but, for the problem that is only independent of $z$ with $\Omega_{y0} \neq 0$, the streamwise disturbance vorticity grows linearly in time.

The sequence of plots at different times for the particle positions reveals that an algebraic growth disturbance can also result in the mixing layer evolving to roll up in the transient time and is as effective as a growing normal mode. The roll-up of the mixing layer occurs for all oblique angles less than $\frac{1}{2}\pi$. Although, when the amplitude of the disturbance becomes large, the model equations for a particle path are not strictly valid, the implications are pronounced. The sequence of plots at different times for the particle positions does show the motion of the evolution of the mixing layer which is valid at small time.

When the initial disturbance is a double mode (streamwise independent and spanwise independent), the developed structure of the material particles has undulant surfaces which are periodic in both the streamwise and the spanwise directions. For this case, the two modes grow independently in the linear regime. While the spanwise-independent mode triggers the roll-up, the streamwise-independent mode creates the wiggling surface in the spanwise direction. This structure is similar to the observations of Lasheras & Choi (1988). In particular, the wiggling surface in the spanwise direction depends on the wavenumber of the initial disturbance, and the wiggling interface of the mixing layer in the experiment depends on the wavenumber of the indented periodic trailing edge of the splitter plate.

Comparing the two sets of results for the symmetric transverse structure of the initial condition $v_0$ with the corresponding asymmetric one, the roll-up of the mixing layer for the asymmetric $v_0$ occurs sooner than for the symmetric one. This happens because the growth rate of the disturbance for the asymmetric case is greater in the transient period as shown in figures 18–22. It is also very sensitive to three-dimensionality.

As was suggested by Metcalfe *et al.* (1987), the transition from laminar to turbulent flow in the mixing layer depends significantly on the relative amplitudes of all competing disturbances. If a real disturbance has an initial infinitesimal amplitude and it can be decomposed into normal modes, then the normal mode with the fastest exponential growth rate will dominate the behaviour of the disturbance at large time given by classical linear stability theory. On the other hand, if the initial small amplitude of the disturbance is finite for which the nonlinear terms are small, then nonlinearity can become rapidly significant in the transient time. This nonlinearity may cause the laminar–turbulent transition of the flow with all finite-amplitude modes responsible for the instability because they all grow rapidly at comparable rates in the transient period. The transient growth remains important even with viscosity because viscosity has little effect in the early period. The asymptotically growing behaviour of

the viscous solution for this flow is virtually identical with the inviscid results (Esch 1957; Balsa 1987).

A general solution expressed in terms of the Green's function found in §3 has advantages over the normal mode method including: (*a*) arbitrary initial disturbances can be treated; (*b*) complete behaviour of a three-dimensional disturbance can be obtained; (*c*) both transient and asymptotic behaviour of a disturbance can be analysed in detail once the specific initial disturbance is specified; (*d*) Lagrangian mechanics of material particles can be obtained.

Although the growth rates of the periodic disturbances rapidly increase in the early period, it has not been demonstrated whether or not they are the optimal disturbances that are most excited in the transient period. Optimal disturbances for the bounded shear flows using a similar approach have been investigated by Farrell (1988). The large-time behaviour of the disturbance for different wavenumbers has been analysed by looking at the exponentially growing term of the disturbance and the behaviour of the kinetic energy, but no formal asymptotic analysis is given. On the other hand, such behaviour is strongly suggested.

This work was supported by the Department of Energy under grant No. DE-FG06-88ER25061. The authors would also like to extend their appreciation to the Center for Turbulence Research at Stanford University and NASA while they were guests.

## REFERENCES

ASHURST, W. T. & MEIBURG, E. 1988 Three-dimensional shear layers via vortex dynamics. *J. Fluid Mech.* **189**, 87–116.

BALSA, T. F. 1987 On the spatial instability of piecewise linear free shear layers. *J. Fluid Mech.* **174**, 553–563.

BALSA, T. F. 1988 On the receptivity of free shear layers to two-dimensional external excitation. *J. Fluid Mech.* **187**, 155–177.

BATCHELOR, G. K. 1967 *An Introduction to Fluid Dynamics.* Cambridge University Press.

BENNEY, D. J. 1984 The evolution of disturbances in shear flows at high Reynolds numbers. *Stud. Appl. Maths* **70**, 1–19.

BENNEY, D. J. & GUSTAVSSON, C. H. 1981 A new mechanism for linear and nonlinear hydrodynamic stability. *Stud. Appl. Maths* **64**, 185–209.

BERNAL, L. P. & ROSHKO, A. 1986 Streamwise vortex structure in plane mixing layers. *J. Fluid Mech.* **170**, 499–525.

BETCHOV, R. & CRIMINALE, W. O. 1967 *Stability of Parallel Flows.* Academic.

BREIDENTHAL, R. 1981 Structure in turbulent mixing layers and wakes using a chemical reaction. *J. Fluid Mech.* **109**, 1–24.

BROWN, G. L. & ROSHKO, A. 1974 On density effects and large structures in turbulent mixing layers. *J. Fluid Mech.* **64**, 775–816.

CASE, K. M. 1960 Stability of inviscid plane Couette flow. *Phys. Fluids* **3**, 143–148.

CASE, K. M. 1961 Hydrodynamic stability and the inviscid limit. *J. Fluid Mech.* **10**, 420–430.

CRIMINALE, W. O. & DRAZIN, P. G. 1990 The evolution of linearized perturbations of parallel flows. *Stud. Appl. Maths* **83**, 123–157.

CRIMINALE, W. O., LONG, B. & ZHU, M. 1991 General three-dimensional disturbances to inviscid Couette flow. *Stud. Appl. Maths* **85**, 249–267.

DRAZIN, P. G. & REID, W. H. 1981 *Hydrodynamic Stability.* Cambridge University Press.

ELLINGSEN, T. & PALM, E. 1975 Stability of linear flow. *Phys. Fluids* **18**, 487–488.

ESCH, R. E. 1957 The instability of a shear layer between two parallel streams. *J. Fluid Mech.* **3**, 289–303.

FARRELL, B. F. 1982 The initial growth of disturbances in a baroclinic flow. *J. Atmos. Sci.* **39**, 1663–1686.

FARRELL, B. F. 1988 Optimal excitation of perturbations in viscous shear flow. *Phys. Fluids* **31**, 2093–2102.

HO, C. & HUANG, L. 1982 Subharmonics and vortex merging in mixing layers. *J. Fluid Mech.* **119**, 443–473.

HO, C. & HUERRE, P. 1984 Perturbed free shear layers. *Ann. Rev. Fluid Mech.* **119**, 365–424.

HUSSAIN, A. K. M. F. 1986 Coherent structures and turbulence. *J. Fluid Mech.* **173**, 303–356.

KELVIN, W. 1871 Hydrokinetic solutions and observations. *Phil. Mag.* **42**, 362–377.

KELVIN, W. 1887 Rectilinear motion of viscous fluid between two parallel plates. *Phil. Mag.* **24 (5)**, 188–196.

KONRAD, J. H. 1976 An experimental investigation of mixing in two-dimensional turbulent shear flows with application to diffusion limited chemical reaction. PhD thesis, California Institute of Technology.

LASHERAS, J. & CHOI, H. 1988 Three-dimensional instabilities of a plane free shear layer. *J. Fluid Mech.* **189**, 53–86.

LIN, C. C. 1955 *The theory of Hydrodynamic Stability*. Cambridge University Press.

LIN, C. C. 1961 Some mathematical problems in the theory of the stability of parallel flows. *J. Fluid Mech.* **10**, 430–438.

LIN, S. J. & CORCOS, G. M. 1984 The mixing layer: deterministic model of a turbulent flow. Part 3. *J. Fluid Mech.* **141**, 139–178.

LOCK, R. C. 1951 The velocity distribution in the laminar boundary layer between parallel streams. *Q. J. Mech. Appl. Maths* **4**, 41–63.

METCALFE, R. W., ORSZAG, S. A., BRACHET, M. E., MENON, S. & RILEY, J. J. 1987 Secondary instability of a temporally growing mixing layer. *J. Fluid Mech.* **184**, 207–243.

MICHALKE, A. 1964 On the inviscid instability of the hyperbolic tangent velocity profile. *J. Fluid Mech.* **19**, 543–556.

MICHALKE, A. 1965 Vortex formation in a free boundary layer according to stability theory. Part 2. *J. Fluid Mech.* **22**, 371–383.

ORR, W. M'F. 1907*a* The stability or instability of the steady motions of a perfect liquid and a viscous liquid. Part I. *Proc. R. Irish Acad.* A **27**, 9–68.

ORR, W. M'F. 1907*b* The stability or instability of the steady motions of a perfect liquid and a viscous liquid. Part II. *Proc. R. Irish Acad.* A **27**, 69–138.

OSTER, C. & WYGNANSKI, I. 1982 The forced mixing layer between parallel streams. *J. Fluid Mech.* **123**, 91–130.

PIERREHUMBERT, R. T. & WIDNALL, S. E. 1982 The two- and three-dimensional instabilities of a spatially periodic shear layer. *J. Fluid Mech.* **114**, 59–83.

RAYLEIGH, LORD 1894 *The Theory of Sound*, 2nd edn. Macmillan.

REDDY, S. C., SCHMID, P. J. & HENNINGSON, D. S. 1991 Pseudospectra of the Orr–Sommerfeld operator. *SIAM J. Appl. Maths* **53**, 15–45.

ROGERS, M. M. & MOSER, R. D. 1989 The development of three-dimensional temporally evolving mixing layer. *Seventh Symp. on Turbulent Shear Flows, Stanford, CA.*

TUNG, K. K. 1983 Initial-value problems for Rossby waves in a shear flow with critical level. *J. Fluid Mech.* **133**, 443–469.

VAN DYKE, M. 1982 *An Albumn of Fluid Motions*. The Parabolic Press.